

# Improving signal aspect awareness of a driver advisory system over the Dutch signalling system to increase capacity

Panagiotis Chatzis



*Cover image source: [bitnary.info](http://bitnary.info)*

# Improving signal aspect awareness of a driver advisory system over the Dutch signalling system to increase capacity

by

Panagiotis Chatzis

to obtain the degree of

**Master of Science**  
in Civil Engineering

at the faculty of Civil Engineering and Geosciences, department of Transport & Planning of Delft  
University of Technology,

to be defended publicly on Monday November 16<sup>th</sup>, 2020 at 15:00.

Student number: 4929071

Thesis committee: Prof. dr. R.M.P. Goverde, Delft University of Technology, Committee chairman  
Dr. ir. E. Quaglietta, Delft University of Technology, Daily Supervisor  
Ir. J.J.W. van Luijckeloo MBR, ProRail, Company supervisor  
Dr. ir. Y. Yuan, Delft University of Technology, External supervisor

An electronic version of this thesis is available at <http://repository.tudelft.nl/>.



This page was intentionally left blank.

# Preface

This thesis is the "last act" of my studies at the Delft University of Technology. By completing this thesis, I will successfully have obtained the title of MSc in Civil Engineering. During my search for a good graduation topic, Rob Goverde introduced me to Jelle van Luipen. The main concept of this study was an idea of Jelle. I was enthusiastic with the topic, so I had no second thoughts of going on with it. After having completed it, I am totally satisfied by my choice since I learned a lot regarding new technologies that can be used for the real-time train traffic control. Also, I grew skills that will be useful for my professional career.

At this point, I want to thank Rob Goverde for introducing me to the topic and for his feedback on critical points regarding the terminology of rail concepts and for drawing my attention into having a solid scientific approach. Also, I want to thank Egidio Quaglietta for always replying to my mails and giving valuable answers. Additionally, I want to thank Yufei Yuan for his help in the modelling approach and in data-fusion related topics of this thesis.

There is a number of colleagues within ProRail who I want to thank. First, I want to express my sincere gratitude for Jelle van Luipen for trusting this topic in me and for his daily coaching. Second, I want to thank Wilco Tielman for helping me understand the architecture and specifications of several data sources and systems provided by ProRail. Special thanks also go to Erik Theunissen who helped me with modelling the developed framework in the simulator NEO-DMI Suite with 3D viewer.

But most of all, I want to thank my parents and family for always standing by my side and for encouraging me whenever I faced challenging moments during my time at the Delft University of Technology. Finally, during my time in Delft, I made some intimate friends. Thanks for the priceless moments during the past two years and especially for the psychological support and the productive time we spent during these tough coronavirus times.

*Panagiotis Chatzis  
Plomari, October 2020*

This page was intentionally left blank.

# Summary

## Background and research objective

The increasing passenger demand for rail service in the Netherlands, urges the Dutch infrastructure manager (IM) ProRail to increase network capacity. Instead of building new infrastructure, ProRail promotes information and communications technology solutions which aim for a more efficient utilization of the existing infrastructure. One of the ways to achieve improved capacity utilization is through decreasing the variability of train runs, i.e. by attaining more uniform train driving profiles. A driver advisory system (DAS) constitutes such a solution and it serves as a support for the driver to perform the train driving tasks. Additionally, the roll-out of the European Train Control System Level 2 (ETCS L2) on the first part of the mainline Dutch network is planned for 2030. Developing a DAS compatible with ETCS L2 operation would yield high quality advice. Still, until the complete roll out of ETCS L2, ProRail aims to improve capacity on given bottlenecks using existing systems.

A DAS constitutes a non-safety critical, Grade of Automation 1 system. Under DAS operation, the driver adjusts the train controls and he/she is responsible for the safety of operations. A frequently arising problem when using a DAS, is that its advice usually leads to conflicts due to poor or no consideration of the actual traffic. An approach to handle this, is to provide the speed profile calculation module of a DAS with a dynamic speed profile that considers static and temporary speed restrictions as well as speed restrictions originating from the signalling system. The latter approach increases a DAS's awareness regarding the actual signal state. This study aims to tackle conflicts with the latter approach. This approach for coping with conflicts when using a DAS is mentioned by several publications or commercial DASs but none of them explicitly defines how this is achieved.

The main aim of this study is to increase the awareness of a conceptual C-DAS-On board regarding the actual signal state in order to minimise conflicts in disturbed operations. The proposed framework addresses the a C-DAS-On board operating on top of the Dutch signalling system NS'54 and the Class-B automatic train protection system ATB-EG. In order to increase the proposed model's effectiveness, this information must be provided in real time. Real-time signalling information is delivered on board by the maximum allowed speed data stream (Figure 1). It is proven that the only missing function from existing ProRail systems to provide this real-time information flow, is to determine the red signal in real time. Thus, the initial objective of this study can be scoped down to determining the red signal. It is also proven that the goal of determining the red signal is equivalent to the goal of locating the predecessor train. This information is planned to be fed to the on board equipment of a DAS via a novel data stream. Additionally, this section explained how this data stream fits to the train control architecture using a C-DAS-On board.

## Model development

The determination of the most relevant red signal is based on train positioning data. This thesis opted for a data-driven approach to investigate the potential of two train positioning systems – provided by ProRail – to deliver the red signal to the on board DAS equipment in real-time. The two systems are TPS and MTPS. TPS performs train positioning using real-time information from the Dutch train describer system TROTS. MTPS is a train positioning system that uses both TPS and GPS data.

Using TPS is regarded as the *baseline* approach to deliver the red signal, while it is assisted by *infill*, which constitutes a fusion of TPS with MTPS data. The *infill* approach is the main contribution of this study since MTPS data have never been used for the derivation of the actual signal state. *Baseline* data is easy to handle and yields the red signal when predecessor train is located on an interlocked area or when it is about to move to a downstream track-segment. In contrast, *infill* data require more preprocessing but they are able to yield the red signal when predecessor is located on the open track.

An assessment framework has been proposed to quantify the positioning solution quality of the

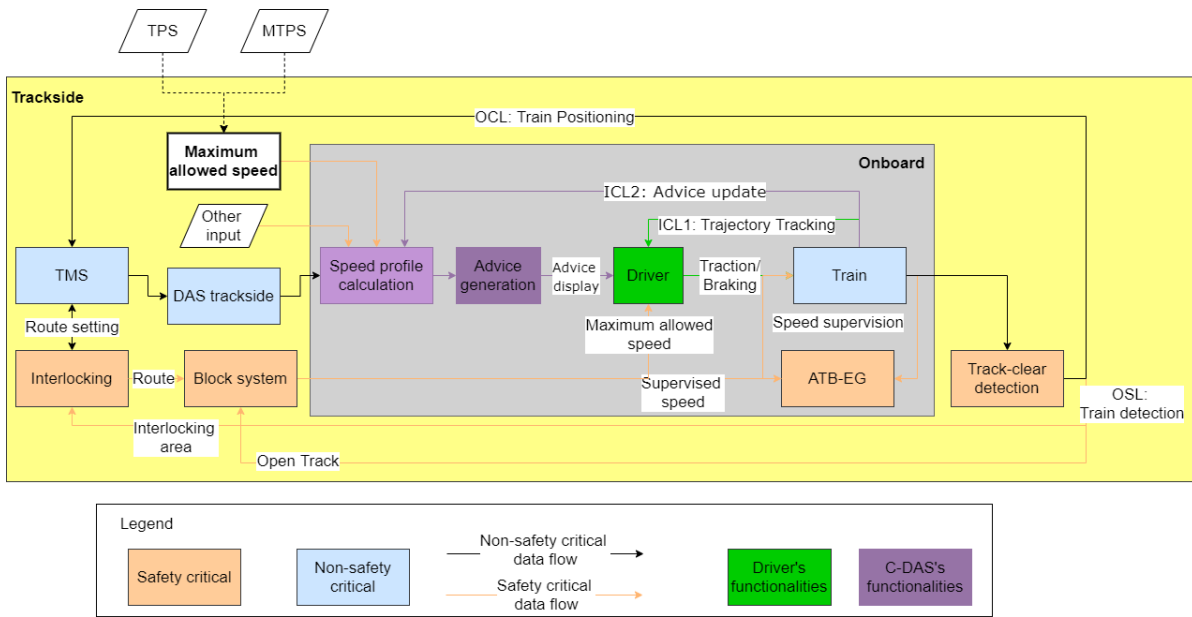


Figure 1: Generic train control architecture using a C-DAS-On board according to which the onboard DAS equipment receives—among other input—information regarding the maximum allowed speed of the track. The maximum allowed speed is determined using either TPS or MTPS data, adapted from Goverde and Theunissen, 2018

two data sources (Figure 2). The framework consists of four components: the definition of the required navigation performance (RNP) parameters, the translation of RNP into reliability–availability–maintainability–safety integrity (RAMS) parameters, the worsening performance of TPS + MTPS data and the contribution of GPS data in the reliability of determining the red signal. The attributes of the framework components are quantified by key performance indicators (KPIs). The RNP component regards the reliability and the RNP-availability. Reliability is calculated using the mean time between failures (MTBF) and the minimum observed discontinuity  $T$ . MTBF is an ideal parameter to capture both the total duration and the number of discontinuities of a data stream.  $T$  captures the criticality of a gap. RNP-availability is used to capture the non safety-critical part of the RAMS framework.

This study introduces two novel KPIs. Since MTPS data is used to assist TPS data in determining the red signal, this solution is expected to be more reliable than using solely TPS data. Yet, in practice this is not always the case. To that end, a KPI is proposed to capture the fraction of observations which are worse-off by the introduction of TPS + MTPS data. The other novel KPI addresses the reliability benefit stemming from GPS data. The proposed framework can also be used to assess the positioning quality of other non safety-critical applications of GNSS systems in the railway sector.

## Case study- Simulator experiments

It was selected to test the proposed red signal framework on Series 6300 since recently, the exact series were chosen by NS to perform ATO tests on top the legacy Dutch signalling system. The analysis is performed for the stretch between Haarlem (Hlm) and Leiden Centraal (Ldn) (direction Hlm-Ldn). This study uses only the *TpsMessageHandler* publication service of MTPS which shows some information gaps for the study area.

The NEO-DMI Suite with 3D Viewer simulator, developed and owned by ProRail, is used to assess the behaviour of the proposed red signal framework on a DAS. The hypothesis being tested states that the as the reliability of the input to a DAS increases, the reliability of the produced advice (DAS output), increases too. Using more reliable advice, the driver trusts the DAS more and keeps on using it. Given that the DAS optimizes for better capacity usage the hypothesis can be scoped down in this statement: increased DAS input reliability can potentially lead to operating more trains. This hypothesis is tested based on scenarios using sensitivity analysis.

NEO-DMI is an event-based simulator which performs micro-simulation using distance-formulated

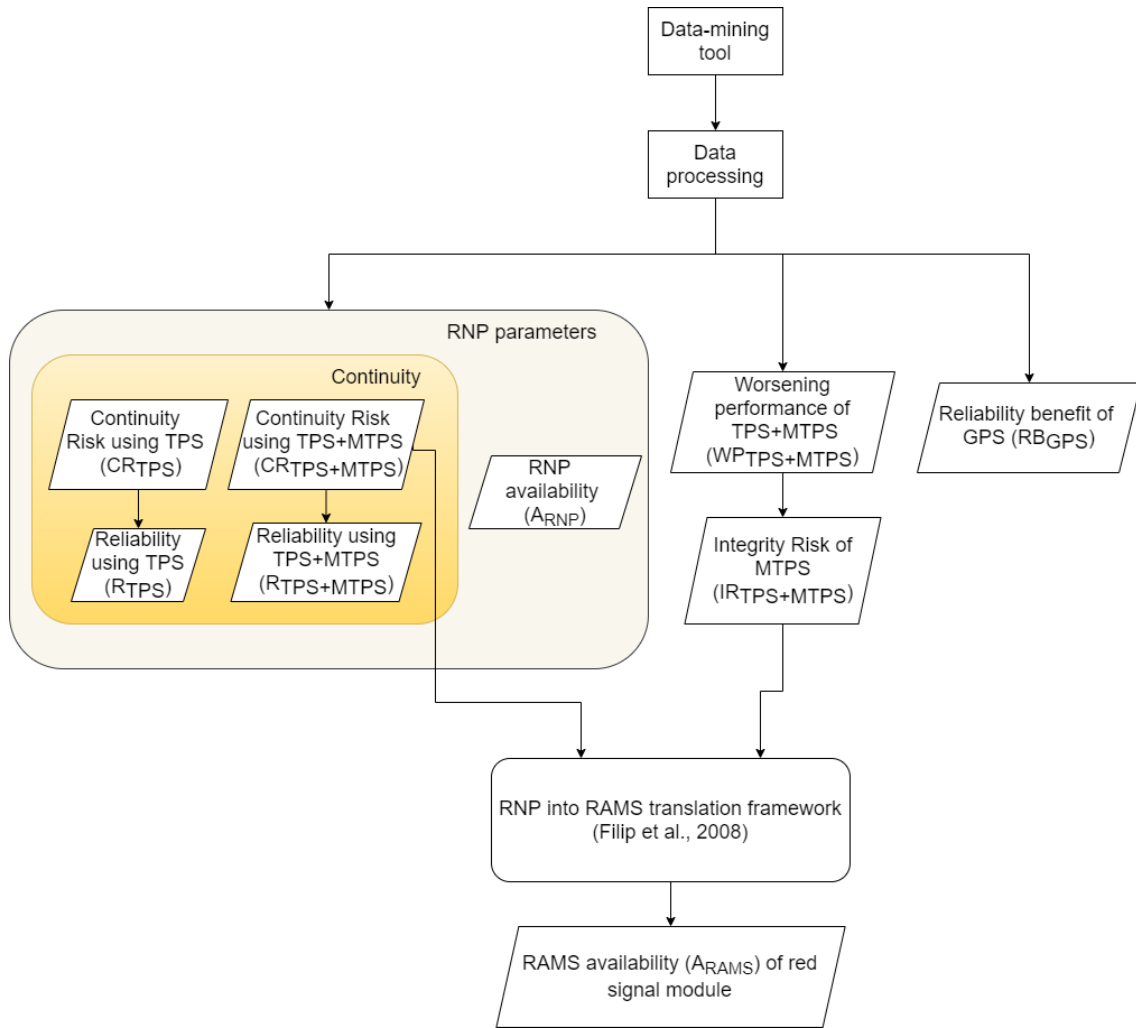


Figure 2: Assessment framework

scripts. NEO-DMI has three modules: train, DMI and 3 DV. NEO-DMI includes a model for all the on-board functions of the train control architecture. This study uses the S-DAS model included in NEO-DMI.

All input relevant to a simulation is scripted. Each feature is modelled by setting the attribute feature along with its location from the start of the simulation where it should occur. The basic calculation regards the speed advice which is available to the driver. Advice reliability is embedded in the available speed advice to the driver. This advice is calculated offline using an iterative process. The goal of this iterative process is to construct a speed advice which satisfies all the following attributes: reliability of the data stream with which the red signal is determined, speed limit stemming from the DSP and punctuality (if possible).

The simulations are performed per scenarios. Each scenario has three decision variables: aggregate delay of the predecessor, train type (peak or off-peak train) and advice reliability. The former two decision variables were retrieved from historical RouteLint observations. Then, the third decision variable was calculated by the data-mining tool using the former two decision variables as input.

Advice reliability is segmented into four variants: No DAS, DAS using baseline or infill data as well as a DAS having access to the flawless data feed of ETCS L2. The first three variants operate on top of ATB-EG, while the latter operates on top of ETCS L2. The variants are set in increasing order with respect to advice reliability. The hypothesis was tested against three scenarios; a peak train having zero delay (scenario 1), an off-peak having +3 min delay (scenario 2) and a peak train having +7 min delay (scenario 3). Thus, only scenario 3 regards a conflicting train.

## Conclusions

The numerical results derived from historical data prove that indeed *infill* data manage to yield a more continuous data stream of providing the DAS on board with the red signal in real-time. A qualitative proof backing up this statement is shown in Figure 3. *Infill* data entirely bridge the gap of *baseline* in determining the red signal between 100 and 200 s, 1500-1600 s and partially bridge the gap between 600 and 850 s (all approximate values). Quantitatively now, *infill* data manage to decrease by 43.5% the frequency with which the red signal knowledge is lost. This frequency is captured by the mean time between failures (MTBF). The median value of MTBF increased from 543.0 s with *baseline* data to 779.3 s with *infill* data. MTBF is the core component of the formula calculating reliability (the ability of a system to work without interruptions) as defined in the RAMS framework. The introduction of *infill* data increases the total system reliability by 1.9% (from 95.9% with *baseline* to 97.8% with *infill*). Still, the introduction of MTPS does not always lead to increased system reliability. Possible reason to this is the limited availability of MTPS data on the examined corridor.

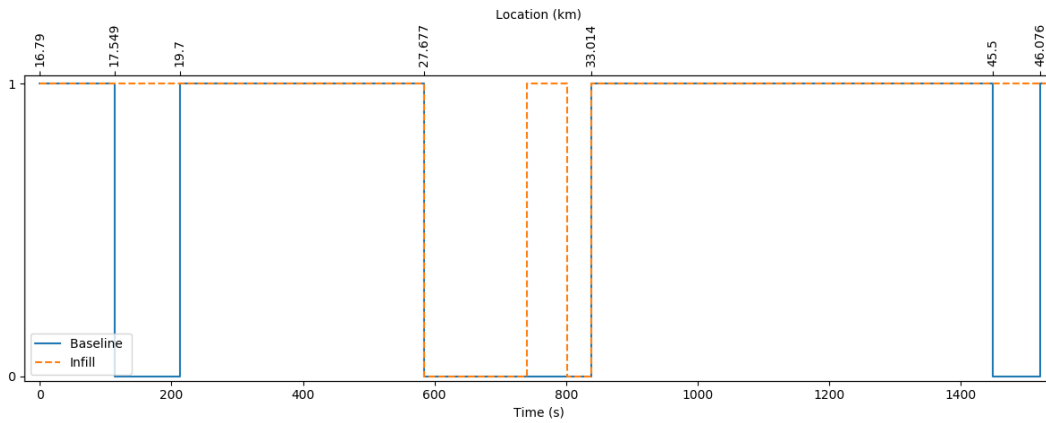


Figure 3: Continuity of *baseline* and *infill* data stream for Scenario 1. The graph expresses the continuity of each data stream with respect to time. X-primary-axis demonstrates the actual running time, while X-secondary-axis demonstrates the location along the track. Y-axis discloses the potential of a data source to yield the red signal expressed as a binary parameter. The data stream receives value 1, when the data source can yield the red signal while it receives value 0 in case of the opposite

Figure 4 summarizes the findings of the performed simulation. According to the Figure, the hypothesis of this study is well supported for scenarios 1 and 2. In other words, as input reliability increases, the advice reliability increases and infrastructure occupation decreases for nominal (i.e. non-conflicting) train runs. Nevertheless, this statement does not hold for the conflicting train run of scenario 3. In fact, baseline variant yields infrastructure occupation equal to that of infill, while driving without a DAS leads to better capacity usage than the afore mentioned variants.

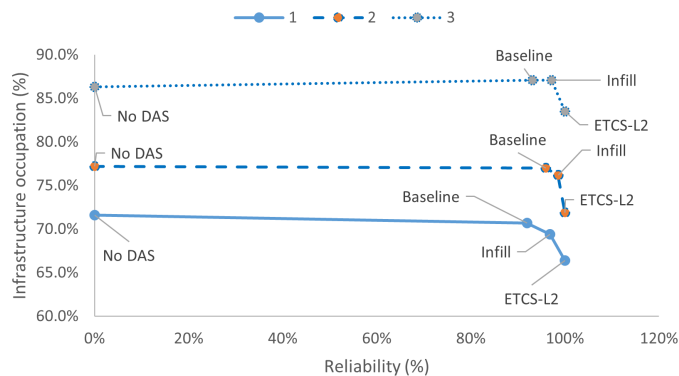


Figure 4: Simulation output regarding infrastructure occupation for the different scenarios and their reliability variants

# Glossary

AF	Automatic Functions Lötschberg
ARI	Automatische Rijweginstelling, Automatic route setting
ASTRIS	Aansturing en Statusmelding Rail Infra Structuur
ATB-EG	Automatische Treinbeïnvloeding-Eerste Generatie, Dutch ATP System
ATC	Automatic Train Control
ATP	Automatic Train Protection
ATO	Automatic Train Operation
C-DAS	Connected-Driver Advisory System
CDR	Conflict detection and resolution
DAS	Driver Advisory System
DIS	Driver Information System
DMI	Driver Machine Interface
DSP	Dynamic Speed Profile
EMS	Enterprise Message Service
ETCS	European Train Control System
GNSS	Global Navigation Satellite System
GoA	Grade of Automation
GPS	Global Positioning System
HMI	Human Machine Interface
ICL	Inner Control Loop
IM	Infrastructure Manager
LARS	Landelijke Actueel Plan Rijweg Server
MTBF	Mean Time Between Failures
MTPS	Materieel Trein Positie Service, Dutch train describer service using track occupation and GPS data
N-DAS	Network-Driver Advisory System
NS	Nederlandse Spoorwegen, Dutch railway undertaking
NS'54	Nederlandse seinstelsel 1954, the Dutch signalling system
OBE	Overzicht Baan en Emplacement, Track and Shunting Area Overview
PRL	Procesleiding, Dutch manual traffic management system
RAMS	Reliability, Availability, Maintainability, Safety Integrity
RITS	Rail Infra Toestand Service
RNP	Required Navigation Performance
RTS	Railway Transport Systems
RU	Railway Undertaking
SA	Situation Awareness
SASP	Signal Aspect Speed Profile
S-DAS	Standalone-Driver Advisory System
SPAD	Signal Passed at Danger
SSP	Static Speed Profile
TCC	Train Control Center
TMS	Traffic Management System
TNS	Train Number Step
TPE	Train Path Envelope
TPS	Trein Positie Servicer
TROTS	Trein Observatie & Tracking Systeem, Dutch train describer system
TSR	Temporary Speed Restrictions
UIS	Uitvoerings Informatie Server
VOS	Verkeersleiding Ondersteunend Systeem

This page was intentionally left blank.

# Contents

<b>List of Figures</b>	<b>xiii</b>
<b>List of Tables</b>	<b>xvi</b>
<b>1 Introduction</b>	<b>1</b>
1.1 Background . . . . .	1
1.2 Problem statement . . . . .	1
1.2.1 Research objective . . . . .	2
1.2.2 Research questions . . . . .	3
1.3 Scope . . . . .	3
1.4 Thesis structure. . . . .	4
<b>2 Literature review regarding train positioning and driver advisory systems</b>	<b>5</b>
2.1 Automation on the main line . . . . .	5
2.2 Driver Support Systems . . . . .	6
2.3 Driver Advisory Systems . . . . .	6
2.3.1 General characteristics. . . . .	7
2.3.2 DAS classifications . . . . .	7
2.4 Dealing with conflicts when using DAS . . . . .	8
2.4.1 Current research . . . . .	9
2.4.2 Practice . . . . .	10
2.5 Driver-related factors . . . . .	10
2.6 Commercial driver support systems providing a real time connection to the traffic management system . . . . .	11
2.7 Assessment of DAS . . . . .	14
2.7.1 Human factors . . . . .	14
2.7.2 Driver's acceptance regarding the advice . . . . .	14
2.7.3 Capacity gains using a DAS . . . . .	14
2.7.4 DAS assessment methods. . . . .	15
2.8 GNSS deployment in the railway industry. . . . .	15
2.8.1 GNSS - A novel data source for railways . . . . .	15
2.8.2 GNSS as a means for train positioning . . . . .	16
2.8.3 Fusion of GNSS with other sensors . . . . .	17
2.8.4 Performance evaluation of GNSS applications in railways . . . . .	17
2.9 Discussion . . . . .	18
<b>3 Background information</b>	<b>21</b>
3.1 The Dutch railway signalling system. . . . .	21
3.2 Dutch implementation of train positioning and driver support systems . . . . .	22
3.2.1 TROTS & TPS . . . . .	22
3.2.2 RouteLint . . . . .	23
3.2.3 MTPS . . . . .	26
3.3 Blocking time theory . . . . .	28
<b>4 Model development</b>	<b>30</b>
4.1 Problem description and research objective . . . . .	30
4.2 Conceptual framework . . . . .	32
4.2.1 Modelling approach for acquiring the actual signal state . . . . .	32
4.2.2 Train control architecture of a C-DAS-On board . . . . .	33
4.2.3 Input to the speed profile calculation module of the DAS. . . . .	34

4.3	A data mining tool to improve red signal state awareness of DAS . . . . .	34
4.3.1	Data format . . . . .	34
4.3.2	Data preparation routine . . . . .	37
4.3.3	Red signal routine using baseline data . . . . .	37
4.3.4	Red signal routine using infill data . . . . .	41
4.3.5	Blocking time diagram routine . . . . .	44
4.4	Assessment framework . . . . .	45
4.4.1	Framework architecture . . . . .	45
4.4.2	RNP parameters for the red signal determination. . . . .	47
4.4.3	Worsening performance of infill data . . . . .	48
4.4.4	Translation of RNP into RAMS parameters . . . . .	48
4.4.5	Contribution of GPS in determining the red signal . . . . .	49
4.5	Summary . . . . .	49
<b>5</b>	<b>Numerical results of the data-mining tool</b>	<b>51</b>
5.1	Case study . . . . .	51
5.1.1	Selection of study area . . . . .	51
5.1.2	Data set selection . . . . .	53
5.1.3	Availability of the train positioning systems for the examined corridor . . . . .	53
5.2	Comparison between baseline and infill data . . . . .	54
5.3	Calculation of key performance indicators . . . . .	56
5.4	Causality of the worsening performance of infill data . . . . .	57
5.5	Correspondence of data stream continuity and predecessor position . . . . .	57
5.6	Summary . . . . .	58
<b>6</b>	<b>Model assessment on a simulator</b>	<b>60</b>
6.1	Motivation of simulation . . . . .	60
6.2	NEO-DMI Suite with 3D Viewer . . . . .	60
6.2.1	Simulator general characteristics - Architecture . . . . .	61
6.2.2	Correlation between train control and simulator functions . . . . .	63
6.3	Experiment setup. . . . .	65
6.3.1	Adjustments to the original simulator architecture . . . . .	65
6.3.2	Development of general scripted input . . . . .	65
6.3.3	Scripted input regarding speed advice and aggregate delay. . . . .	67
6.3.4	Capacity analysis of the examined corridor . . . . .	69
6.3.5	Modelling operational rules in the simulation environment . . . . .	70
6.3.6	Assumptions-Limitations . . . . .	71
6.4	Scenario development . . . . .	72
6.5	Scenario analysis. . . . .	72
6.5.1	Input determination for the scenarios . . . . .	72
6.5.2	Simulation results. . . . .	74
6.6	Discussion . . . . .	75
<b>7</b>	<b>Conclusions and Recommendations</b>	<b>77</b>
7.1	Conclusions. . . . .	77
7.1.1	Discussion . . . . .	77
7.1.2	Answers to research questions . . . . .	78
7.2	Contributions . . . . .	79
7.3	Recommendations . . . . .	80
7.3.1	Recommendations for improvement of the current model . . . . .	80
7.3.2	Recommendations for future research . . . . .	81
	<b>References</b>	<b>83</b>
<b>A</b>	<b>Detailed tool results</b>	<b>87</b>
<b>B</b>	<b>Detailed related files</b>	<b>92</b>
<b>C</b>	<b>Statistical analysis</b>	<b>96</b>

---

<b>D</b>	<b>Technical drawings</b>	<b>101</b>
<b>E</b>	<b>Simulator-user interface</b>	<b>102</b>
<b>F</b>	<b>Blocking time diagrams of the simulator experiments</b>	<b>104</b>

# List of Figures

1	Generic train control architecture using a C-DAS-On board according to which the on-board DAS equipment receives—among other input—information regarding the maximum allowed speed of the track. The maximum allowed speed is determined using either TPS or MTPS data, adapted from Goverde and Theunissen, 2018 . . . . .	v
2	Assessment framework . . . . .	vi
3	Continuity of <i>baseline</i> and <i>infill</i> data stream for Scenario 1. The graph expresses the continuity of each data stream with respect to time. X-primary-axis demonstrates the actual running time, while X-secondary-axis demonstrates the location along the track. Y-axis discloses the potential of a data source to yield the red signal expressed as a binary parameter. The data stream receives value 1, when the data source can yield the red signal while it receives value 0 in case of the opposite . . . . .	vii
4	Simulation output regarding infrastructure occupation for the different scenarios and their reliability variants . . . . .	vii
1.1	Thesis structure . . . . .	4
2.1	RNP parameters into RAMS translation, source Beugin et al., 2010 . . . . .	19
3.1	Comparison between a train speed profile complying with the maximum allowed speed and the supervised speed profile by ATB-EG (adapted from marcpieters.nl) . . . . .	22
3.2	Example HMI of RouteLint integrated with TIMTIM . . . . .	24
3.4	Example of RouteLint’s driver interface . . . . .	26
3.5	MTPS architecture, Adjusted from MTPS Software Requirements Specification, ProRail . . . . .	27
3.6	Break down of blocking time components for a three-aspect signalling, adapted from Kecman, 2014 . . . . .	29
4.1	Generic train control architecture using a C-DAS-On board according to which the on-board DAS equipment receives—among other input—information regarding the maximum allowed speed of the track. The maximum allowed speed is determined using either TPS or MTPS data, adapted from Goverde and Theunissen, 2018 . . . . .	31
4.2	Example of the determination of the speed limit originating from the signalling using the method of reproducing the signal aspect speed profile starting from the red signal . . . . .	32
4.3	Data-mining tool architecture to investigate the potential of baseline and infill data to determine the most relevant red signal . . . . .	36
4.4	Schematic representation of elements/parameters included in the analysis of a RouteLint record . . . . .	37
4.5	Detailed description of the routines used to yield the most relevant red signal . . . . .	39
4.6	RouteLint HMI examples . . . . .	40
4.7	Most relevant red signal determination using the baseline data source. Correlation of RouteLint display with the actual signal state using a schematic representation of the track layout. Top: the most relevant red signal can be determined, while Bottom: it cannot . . . . .	41
4.8	Method for determining predecessor position from MTPS data . . . . .	43
4.9	Search technique to limit the search space within MTPS log files. The search is based on the MTPS timestamps . . . . .	43
4.10	Schematic representation of the RouteLint-record reading method by the data mining tool . . . . .	44
4.11	Assessment framework . . . . .	46
4.12	Continuity graph of the data stream used for red signal determination . . . . .	48
4.13	Illustration of the positioning solution using event theory . . . . .	49
5.1	6300 series shown on the map of the Dutch timetable 2020 . . . . .	52

5.2	Schematic representation of the timetable pattern for the considered railway corridor between Haarlem and Den Haag Centraal . . . . .	52
5.3	Track layout between Haarlem and Leiden Centraal, source: sporenplan.nl . . . . .	53
5.4	Histogram of MTPS records along the considered corridor . . . . .	54
5.5	Box plot of MTBF for the two data sources. The orange line illustrates the median value of the sample. The box indicates the inner quartile range (IQR), i.e. the range where values between the 25 <sup>th</sup> percentile (lower box edge, 1 <sup>st</sup> quartile: Q1) and the 75 <sup>th</sup> percentile (upper box edge, 3 <sup>rd</sup> quartile: Q3) percentile lie within. Box-plot whiskers illustrate the minimum (Q1-1.5*IQR) and maximum (Q3+1.5*IQR) value of the sample which are not considered outliers. . . . .	55
5.6	Contribution of GPS in determining the red signal when using infill data per type. General: all train types, Peak: peak hour trains, Off-peak: off-peak hour trains, . . . . .	55
5.7	Percentages of peak and off-peak trains which are positively or negatively affected after the introduction of the <i>infill</i> data source. <i>Positively</i> : infill yields higher MTBF compared to baseline, <i>Negatively</i> : infill yields lower MTBF compared to baseline. X-axis: train type, Y-axis: positive/negative effect of infill . . . . .	56
5.8	Schematic representation of the correlations $\text{delay} - \text{MTBF}_{\text{baseline}}$ and $\text{delay} - \text{MTBF}_{\text{infill}} - \text{MTBF}_{\text{baseline}}$ for trains that are negatively affected by the introduction of infill data source.	57
5.9	Correlation of the continuity of the data stream and the realised time-distance diagram . . . . .	58
6.1	Architecture of the NEO-DMI Suite with 3D Viewer simulator . . . . .	62
6.2	Correlation of modules between train control architecture using a C-DAS-On board and a maximum allowed speed module and NEO-DMI architecture . . . . .	64
6.3	Construction of the dynamic speed profile (DSP) by merging the static speed profile (SSP) with the signal aspect speed profile (SASP) . . . . .	66
6.4	Interface between the data-mining tool and NEO-DMI simulator . . . . .	67
6.5	Advised speed profile (ASP) and dynamic speed profile (DSP) stemming from NS'54 along the route for a scenario . . . . .	68
6.6	Procedure of developing the speed advice profile available to the driver for a scenario using baseline data. Upper: Continuity of data stream, Mid: Scheduled speed advice, Bottom: Speed advice available to the driver . . . . .	69
6.7	Continuity of <i>baseline</i> and <i>infill</i> data stream for Scenario 1. The graph expresses the continuity of each data stream with respect to time. The landmark locations of the discontinuities are determined via interpolation using the realised time-distance profile . . . . .	73
6.8	Compressed blocking time diagram of Scenario 1 using <i>Baseline</i> data. Red dots indicate the critical blocks. . . . .	74
6.9	Simulation output regarding infrastructure occupation for the different scenarios and their reliability variants . . . . .	75
A.1	RouteLint display of all the TPS records that capture the passage of train 6335 through open track <i>LJ</i> . . . . .	88
A.2	Example where it is (a) feasible and (b) unfeasible to determine the position of train 2222 (predecessor of train 6335) and thus, red signal using infill data. Figures are not in scale.	89
A.3	The average and standard deviation of critical parameters . . . . .	91
B.1	Example of RouteLint interface . . . . .	92
B.2	Examples of movements of trains on the vicinity with respect to (proper) train's position as they appear on the description of TNS-status . . . . .	94
C.1	MTBF histogram for both baseline and infill data source . . . . .	97
D.1	Simplified track layout . . . . .	101
E.1	Display of the NEO-DMI Suite with 3D Viewer simulator . . . . .	103
F.1	Scenario 1 - No DAS - Compressed . . . . .	104
F.2	Scenario 1 - Baseline - Compressed . . . . .	104

---

F.3	Scenario 1 - Infill - Compressed . . . . .	105
F.4	Scenario 1 - ETCS L2 - Compressed . . . . .	105
F.5	Scenario 2 - No DAS - Uncompressed . . . . .	105
F.6	Scenario 2 - No DAS - Compressed . . . . .	106
F.7	Scenario 2 - Baseline - Uncompressed . . . . .	106
F.8	Scenario 2 - Baseline - Compressed . . . . .	106
F.9	Scenario 2 - Infill - Uncompressed . . . . .	107
F.10	Scenario 2 - Infill - Compressed . . . . .	107
F.11	Scenario 2 - ETCS L2 - Compressed . . . . .	107
F.12	Scenario 3 - No DAS - Compressed . . . . .	108
F.13	Scenario 3 - Baseline - Compressed . . . . .	108
F.14	Scenario 3 - Infill - Compressed . . . . .	108
F.15	Scenario 3 - ETCS L2 - Compressed . . . . .	109

# List of Tables

2.1	Effect of DMI designs on the human factors of a DAS and approaches to tackle them according to relevant literature . . . . .	11
2.2	Commercial DSS connected to a TMS in real-time . . . . .	13
2.3	RNP requirements for non-safety critical operations . . . . .	18
3.2	Performance characteristics of MTPS subsystems . . . . .	28
4.1	Necessary information to reproduce the signal aspect speed profile . . . . .	33
4.2	Input for the speed profile calculation module of the DAS . . . . .	34
4.3	RouteLint log file format . . . . .	35
4.4	Format of MTPS record published by the <i>TpsMessageHandler</i> service . . . . .	42
5.1	Key performance indicators . . . . .	56
6.1	Matching of simulator functions to the functions of the train control architecture using a conceptual N-DAS-On board. The labels stem from Figure6.2 . . . . .	63
6.2	Simulated timetable of the series 6300 departing from Haarlem at 0:00 and heading to Leiden Centraal. The case study area stations are selected as explained in Subsection 5.1.1 . . . . .	65
6.3	Blocking time components used in this thesis . . . . .	70
6.4	Scenario setup . . . . .	73
6.5	The advised speed profile available to the driver according to different advice variants of Scenario 1 . . . . .	74
6.6	Scenario results . . . . .	75
7.1	Necessary information to reproduce the signal aspect speed profile . . . . .	78
A.1	Tool results for simple and MTPS-infill algorithm, Train: 6335, Date: 13/12/2019 . . . . .	87
A.2	Tool results for simple and MTPS-infill algorithm, Train: 6337, Date: 13/12/2019 . . . . .	90
B.1	Detailed example of RouteLint record. The record corresponds to a line of the RouteLint log file . . . . .	93
B.2	Correlation of TNS-status with colour and description . . . . .	95
C.1	Descriptive statistics regarding the reliability of the two algorithms . . . . .	99
C.2	Comparison of baseline, infill data as well as their difference with respect to delay . . . . .	100

This page was intentionally left blank.

# Introduction

## 1.1. Background

The increasing passenger demand for rail service in the Netherlands, urges the Dutch infrastructure manager (IM) ProRail to increase network capacity. Instead of building new infrastructure, ProRail promotes information and communications technology (ICT) solutions which aim for a more efficient utilization of the existing infrastructure. One of the ways to achieve improved capacity utilization is through decreasing the variability of train runs, i.e. by attaining more uniform train driving profiles. A driver advisory system (DAS) constitutes such an ICT solution and it serves as a support tool for drivers aiming to improve efficiency in nominal and disturbed operations. Additionally, the roll-out of the European Train Control System Level 2 (ETCS L2) on the first part of the mainline Dutch network is planned for 2030. Developing a DAS compatible with ETCS L2 operation would yield high quality advice. Still, until the complete roll out of ETCS L2, ProRail aims to improve capacity on given bottlenecks using existing systems. Today, no DAS operating on the Dutch railway network gives explicit speed advice.

DAS's objectives include energy efficiency, decrease in the number of SPADs (Signal Passed at Danger) and punctuality. A DAS receives both static and transient (i.e. updated on coarse intervals) input such as timetable, infrastructure description and train characteristics as well as dynamic input regarding current train status (time, position and speed). Then, the DAS calculates an optimal speed profile, generates adequate advice and presents the advice via a Human Machine Interface (HMI). A DAS constitutes a non safety critical system which is regarded as a Grade of Automation (GoA) 1 system. The driver is always responsible for the (manual) control of the train as well as the safety of operations and he/she must disregard advice that conflicts with information coming from safety critical systems.

The most important DAS classification focuses on the frequency with which input data are updated. DAS variants that facilitate no or limited input data updates, can be used for nominal operations. Yet, in case of disturbed operations, a dynamic solution is required. A Connected-DAS (C-DAS) receives dynamic information regarding the route plan (i.e. scheduled routes and target times for all trains), while a Standalone-DAS (S-DAS) receives static input prior to train's departure. The route plan is published for a short-term horizon. A C-DAS can contribute to improved efficiency in case of disturbed operations. Although a DAS may receive information regarding the actual route plan, it is not guaranteed that the resulting advice does not pose conflicts with the installed safety system. In case of advice leading to conflicts, driver's acceptance towards it may be challenged. Then, the driver is unlikely to consult on the DAS next time and thus, DAS's goals will not be achieved.

## 1.2. Problem statement

One of the calculation tasks of a DAS includes the determination of the Train Path envelope (TPE), i.e. target windows at a microscopic level aiming for energy efficiency. Based on the TPE, a speed profile is generated which is not guaranteed to be conflict-free. There are several approaches to minimize conflicts stemming from the speed profile calculation. One alternative is to calculate an initial speed

profile and adjust the speed profile by comparing current traffic status with the timetable. Also, the solution of having a DAS connected to a TMS that performs automatic conflict resolution can be selected. Another approach is to provide the speed profile calculation module of a DAS with a dynamic speed profile that considers static and temporary speed restrictions as well as speed restrictions originating from the signalling system. The latter approach increases a DAS's awareness regarding the actual signal state. This study aims to tackle conflicts with the latter approach. This method of coping with conflicts when using a DAS is mentioned by several publications or commercial DASs but no study explicitly defines how this is achieved.

Still, ProRail possesses data sources and systems which, if adequately combined, can be used to develop a C-DAS. Aiming to develop a DAS based on existing ProRail systems and aiming for a solution that improves the DAS's awareness regarding the actual signal state, a dedicated component of this DAS which provides the actual signal state, is still missing. The DAS contemplated in this study is at a conceptual level since there is no actual DAS or a model of it available within ProRail. For simplicity, it is called conceptual DAS on the remainder.

The Dutch Automatic Train Protection (ATP) system ATB-EG (Automatische Treinbeïnvloeding-Eerste Generatie) does not accommodate real time knowledge about signalling status onboard. The only ATB-EG information available on board regards a continuous data stream that provides the current supervised speed which does not always coincide with the maximum allowed speed of the track. In fact, ATB-EG supervises five speed values (40, 60, 80, 130, 140 km/h) but the signal status can impose different speed restrictions from the afore mentioned values. Hence, the actual signal aspects are not available to the on board equipment of the train. A solution to this is real time to reproduce the speed profile originating from the signalling system and infer the aspect of the signal the train is approaching. Required input for this solution is the train's position, the ID of the signal showing a red aspect and configuration files containing the signalling logic and topology of signals. Determining the red signal serves as a reference point for the reproduction of the speed profile stemming from the signalling system. Existing ProRail systems can deliver all the necessary input data except from a system that delivers red signal-ID in real time.

Among ProRail systems, the red signal can occasionally be inferred from the Dutch train describer system TROTS (Trein Observatie & Tracking Systeem). RouteLint — the Driver Information System (DIS) deployed by NS and DB Cargo trains — makes use of real time TROTS data. RouteLint demonstrates the actual rail traffic status in a train's vicinity. RouteLint's level of detail (which is inherited from TROTS) is at track-segment level. In interlocking areas, a RouteLint track-segment corresponds to a single block-section, while in open tracks a RouteLint track-segment aggregates several (automatic) block-sections. The basic logic for inferring signalling from RouteLint is that in case a track-segment is occupied, its entry signal must show a red aspect. In practice, in interlocking area, the red signal can be determined using RouteLint since at that area, the red signal is determined by the interlocking system based on route setting and locked switches and routes. Using RouteLint, the red signal can be determined also when the predecessor is about to exit an open track and move to the downstream track. Yet, in case the predecessor is within the open track, determining the signal that shows a red aspect becomes challenging. Therefore, the existence of open tracks makes it impossible to determine red signal's location using only TROTS data. To that end, another data source must be found and a method to analyse this data source must be determined so as to make a conceptual DAS aware of the actual signal state also in open tracks using existing ProRail systems. MTPS (Materieel Trein Positie Service) is a train positioning service provided by ProRail. It uses both TROTS and GPS data and can potentially locate the predecessor train on an open track and thus, deliver the red signal.

### 1.2.1. Research objective

This study aims to bridge the awareness gap of existing ProRail systems with respect to the actual signal state on open tracks. This is the missing function which combined with existing ProRail systems can lead to the development of a DAS that minimizes conflicts with the signalling system. The objective of this study is to develop a data-driven algorithm that improves the awareness of signal aspect information on open track of a DAS over ATB-EG and therefore, enhances its advice reliability towards an increased corridor capacity utilization.

## 1.2.2. Research questions

The research objective can be expressed in the following main research question:

*What are the actions that must be taken towards improving the awareness of a conceptual DAS regarding the actual signal state on open tracks equipped with ATB-EG aiming for better capacity usage on Dutch railway corridors?*

The main research question can be divided into the following sub-questions:

- Which data sources are available to improve the awareness level of a DAS regarding actual signalling status on open tracks equipped with ATB-EG?
- Which architecture allows an effective interface of DAS to additional data sources to increase reliability on signal aspect information?
- Which mathematical algorithm can efficiently support the combination of multiple data sources to improve awareness of DAS over ATB-EG?
- How does the advice reliability of a DAS — whose awareness of the actual signal state on open tracks has been improved with a data-driven method — affect a corridor's capacity when compared to DAS/ETCS L2 operation?

## 1.3. Scope

This study is meant to deliver an algorithm that increases the awareness of a conceptual C-DAS regarding the actual signalling status. No other parts of that conceptual DAS are developed, for example the speed profile or the advice calculation module. Also, this thesis aims to develop a non-safety function. Hence, safety related analysis lies outside the scope of this study. Additionally, the assessment of the effectiveness of the developed model is limited at a corridor of the Dutch railway network. Thus, possible network-wide effects cannot be captured.

It is important to give the definitions of important terms used in the following. First, it is explained the sense in which the term *reliability* is used. The data used as input for the data-driven algorithm for increasing DAS's awareness regarding actual signal state, originate from ProRail systems. These systems are not meant to be used for the purpose they do in this study. As a consequence, the data show a certain level of latency on delivering the desired function when used to yield the red signal. It is important to capture that latency since it directly affects the quality of the produced advice. It was decided to quantify the quality of the data through its *continuity*, a term borrowed from Required Navigation Performance (RNP) parameters, which is ideal to capture the desired latency in data. Actually, continuity quantifies the ability of a system to provide the required function when it is really needed and it approximates the reliability of that system to work within specifications (Filip, Beugin, Marais, & Mocek, 2008). Thus, data quality is assessed via its reliability, with continuity being the measurable parameter.

Next, the term *awareness* is used in the sense of constituting a DAS aware of the actual signal state. It must not be confused with *situation awareness* (SA) which is a human factors related term. According to Endsley (1995), SA reflects a person's overall performance on a dynamic environment namely his/her ability to acquire information, interpret it based on operational requirements and predict future states. Increased SA leads to increased probability of conducting the correct actions.

This study is based on some assumptions. First, it is assumed that the reliability of the conceptual DAS's advice is equal to the reliability of the data stream that delivers the red signal on board. Other input to the DAS such as the route plan, other speed restrictions as well as the algorithm itself, are considered totally reliable. Based on that, in the following, when mentioning reliability it will refer to that of the advice. Yet, only the input's reliability is measured. So, although the data reliability will explicitly be discussed, advice reliability will be implied. By doing so, possible capacity gains from the operation of the conceptual DAS that is characterized by increased awareness of actual signal state on open track can directly be compared to DAS's advice reliability.

Second, it is assumed that driver's acceptance for DAS's advice is positively correlated with the advice reliability. Other factors that affect the driver's acceptance are not examined. Third, it is assumed that the driver will follow exactly the advice in case he/she considers it reliable. The latter assumption helps defend the line of reasoning which suggests that given a reliable advice, driver's acceptance towards DAS operation increases and in turn, better capacity utilization is achieved.

Finally, a DAS with a certain level of connection to the TMS is considered in this study. Yet, the proposed model is tested on a simulator that does not facilitate a model of real time data connection between the TMS and the on board equipment of the DAS. Yet, this limitation does not interfere with the proposed red signal framework. That is why the conceptual DAS mentioned earlier, is in fact a C-DAS.

## 1.4. Thesis structure

Chapter 2 presents related work and the current research towards train positioning and driver advisory systems. Chapter 3 discusses all relevant ProRail systems used in this study as well as presents the blocking time theory. Chapter 4 describes the development of a data-driven algorithm that aims to increase the actual signal state awareness on open track as well as a data-mining tool that is used to assess the developed function against historical data. In Chapter 5, the performance of the developed model is analysed using historical data. Chapter 6 introduces a case study of a Dutch railway corridor in which the developed model is tested. It is explained how the problem was modelled on a simulator and then, its results are demonstrated. Finally, in Chapter 7, the findings of this study are discussed and recommendations for further model improvement and future research are given. The thesis structure is included in Figure 1.1. In the same Figure, arrows illustrate dependencies between different chapters wherever they exist.

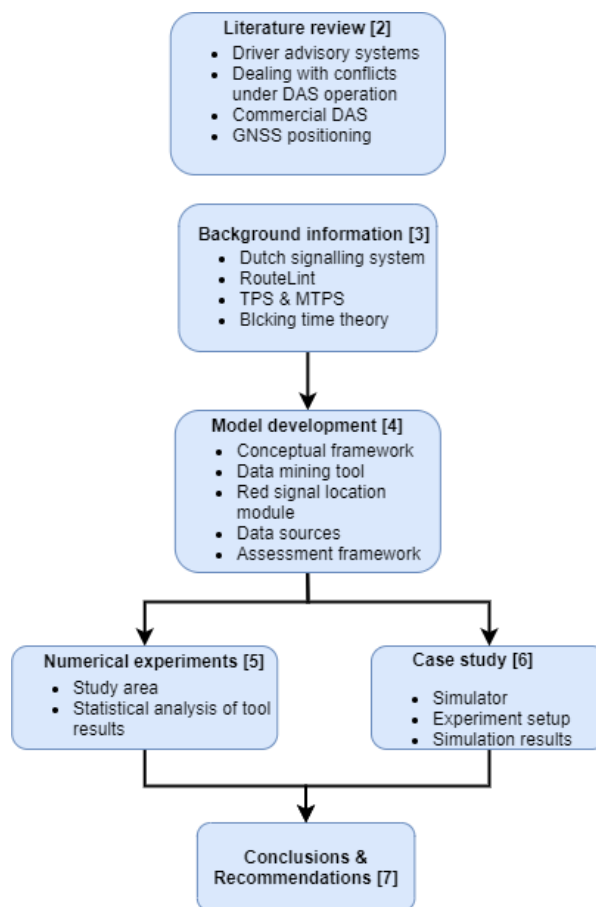


Figure 1.1: Thesis structure

# 2

## Literature review regarding train positioning and driver advisory systems

In this chapter, information regarding systems that are relevant to this study is presented. The information concerns driver support systems with a special focus on driver advisory systems. Also, this chapter provides an overview of the ongoing research regarding DAS dealing with conflicts. Moreover, a section of this chapter presents important information related to the DAS-driver interaction. Additionally, representative examples of DAS available to the market are discussed. Methods to assess different aspects of a DAS are presented. A section is dedicated to GNSS and especially, for their use in non-safety critical applications on the railway sector.

### 2.1. Automation on the main line

Yin et al. (2017) mention that automatic train operation (ATO) aims for improved efficiency in railway operations and decreased energy consumption by applying optimized train driving commands (acceleration, cruising, coasting and braking). Rao, Montigel, and Weidmann (2016) adds to this that ATO can lead to better capacity usage compared to manual driving. The functions of ATO include automated train speed control, stopping at stations and open/closure of doors. According to UITP (2011), apart from GoA 0 where no ATP is installed (driving on-sight), four GoAs – each with a certain level of automation – can be distinguished. First, under GoA 1 (manual driving) operation, ATP is installed and manual driving is performed. Second, in GoA 2 (Semi-automated Train Operation) train speed control and stopping are performed automatically, while the driver is responsible for train departure, the safety of operations, while he/she takes over in case of disruptions. Third, in GoA 3 all on board staff is replaced by an attendant (Driverless Train Operation). Finally, under GoA 4 (Unattended Train Operation), no staff is on board.

The first fully operational ATO system has been installed on a metro line in the late 1960's (Nicholson, 2010), while ATO has enabled subway operators to achieve almost 100 % punctuality (Yin et al., 2017). Today, while the introduction of ATO is common in urban railways, its implementation on the main line is considered rather challenging due to the inherent complexity of the main line (Yin et al., 2017). The authors consider characteristics of the main line such as heterogeneous traffic and network size as the major obstacle to the rapid deployment of ATO on the main line. Moreover, to date there is no roadmap of ATO functions deployment. Venkateswaran, Nicholson, Roberts, and Stone (2015) add to that other characteristics of the main line that make its automation challenging such as the effect of external factors (e.g. weather) and the existence of several Train Control Centres (TCC).

To date, there are only a few examples of fully operational ATO on the main line. Such systems include the one installed on Thameslink and which was inaugurated in 2018 as well as that of the Czech republic (LZA) which is in operation already since the 90's (Poulus, R., Kempen, E. van, & Meijeren, J. van, 2018). The freight line of Rio Tinto in Australia is the first fully automated main railway line (Smith, 2019). The entire stretch of 1500 km of the line became fully operational under GoA 4 on June, 2019.

ProRail is investigating the application of ATO GoA2 over ATB-NG (Automatische Treinbeïnvloeding-Nieuwe Generatie). ATB-NG is the Dutch intermittent ATP system which supervises the dynamic speed profile of a train. ATB-NG is able to yield the braking curve of a train using the rolling stock characteristics which are manually set by the driver. To that end, a preliminary set of formal requirements has been defined addressing the interface of ATO with both the TMS and the installed signalling system (Buurmans, 2019).

## 2.2. Driver Support Systems

Driver Support Systems (DSS) have principally been developed to assist the train driver in achieving energy-efficient and punctual driving (Albrecht, 2014). Note that energy efficiency can be achieved through the intelligent use of the allocated running time supplement along the route on nominal operations. Moreover, energy-efficiency can be achieved in disturbed operations, too. More precisely, conflicts can lead to unplanned stops which among other negative effects, can lead to increased energy consumption. Re-acceleration after an unplanned stop leads to unnecessary energy-consumption (Albrecht, Goverde, Weeda, & van Luipen, 2006).

Anticipating train control constitutes a solution to minimize conflicts and in turn, decrease energy consumption. In order for the anticipating train control to be effective, an accurate prediction of train trajectories is required which in turn requires good knowledge of the current traffic state. The necessity for the latter demands for a dynamic network-related DSS (Albrecht, 2014). The author provides a categorization of DSS depending on the time character of their input data. The following variants can be distinguished:

- *Static* DSS. They receive input prior to train departure. These systems are mainly paper-based and give advice based on some empirical rules, e.g. when to start applying coasting after having reached a certain speed and provided that there is no delay. The output of these systems is highly sensitive to deviations compared to the timetable.
- *Dynamic train-related* DSS. Input is delivered on board prior to departure and on-board sensors determine the level at which the realised speed profile matches the planned one in real-time. Then, adequate advice is displayed.
- *Dynamic network-related* DSS. These systems allow for a real-time data transfer between on board and the train control centre.

Dynamic network-related DSS exchange data between onboard and the dispatching system of the traffic control centre (Albrecht, 2014). The GSM-R protocol is mainly used for this data exchange. The traffic control centre sends onboard information such as the time windows that a train should target in order to use a specific piece of infrastructure, an overview of the current traffic state as well as predictions of it (e.g. train positions and signal aspects).

According to Albrecht (2014), there are two variants of DSS with respect to the type of support they provide. The two alternatives are driver information systems (DIS) and driver advisory systems (DAS). DIS supply the driver with unprocessed information, while DAS calculate and display control variables based on that unprocessed information. As control variables are regarded speed, timekeeping, traction, braking or coasting.

Energy-efficient driving achieved using DSS, can yield collateral benefits. Such a gain applies to the railway capacity. A DSS is able to decrease the variations in the realized running time and the driving style. Since the operations become more predictable, buffer times can be shrunk, increasing, in turn, capacity. The buffer time is set between successive train runs to prevent a delay being transmitted to other trains and as a consequence, it reduces capacity (Pachl, 2014).

## 2.3. Driver Advisory Systems

This section gives an overview regarding DAS. Basic technological components of a DAS are discussed. Also, several classifications of DAS are contemplated.

### 2.3.1. General characteristics

A DAS comprises of two parts: the DAS onboard, which is mounted on the train and the DAS trackside. The two components communicate between each other. According to Albrecht (2014), the entire DAS configuration requires the following technological components:

1. A positioning or speed module,
2. A clock at each sub-module of the DAS. The clocks should be synchronized,
3. A database containing information regarding:
  - timetable data
  - speed limits: SSP, TSR
  - infrastructure: curve radii, slopes
  - rolling stock attributes: acceleration and braking capacity, resistances, mass and length
4. A HMI offering driver interface

Regarding the time character of the data, the majority of the units deals with dynamic data with the only static data being those regarding the rolling stock and the infrastructure.

Additionally, units 1-3 provide input while 4 mainly output, but also input. HMI presents visual or audible notifications concerning the advice, while it can receive manual input from the driver regarding the rolling stock type used for the specific trip. The output that can be given through a HMI regards speed advice, timekeeping advice and advice for adjusting the train controls (traction/braking).

When driving under DAS, driver has full responsibility of moving the train between stations and the underlying safety of the operations. Additionally, modern railway systems are equipped with an ATP system. Train operations both under ATP and DAS are categorized as GoA 1. According to Yin et al. (2017), a DAS does not belong to ATO systems. In fact, the function that makes ATO distinct from DAS is that of traction/braking command generation. In case a system integrates also the latter function, it is considered as a GoA 2 system.

### 2.3.2. DAS classifications

Several categorizations of a DAS can be distinguished. First, according to Goverde and Theunissen (2018), the major distinction between DAS regards the time character of the data exchange between the DAS trackside and the onboard equipment. According to this categorization, the following variants can be distinguished:

- Standalone-DAS (*S-DAS*). A static variant with respect to input data. The on board DAS equipment receives all relevant input prior to train's departure.
- Network-DAS (*N-DAS*). A partially dynamic variant. The on board DAS equipment receives updates regarding timetable or route setting, but usually not in real-time.
- Connected-DAS (*C-DAS*). A dynamic variant. There is a real-time data transmission between the trackside and the onboard segment of the DAS. Also, a two-way communication is possible. The trackside DAS equipment sends onboard updates regarding changes in the timetable, the route and the speed limit in real-time. The onboard DAS equipment sends to the trackside the train's actual status (e.g. delay, position).

Combining the afore mentioned classification and the categorization regarding the time character of data exchange of a DSS, it can be argued that a S-DAS embeds both static and dynamic train-related DSS, while N- and C-DAS can be characterized as dynamic network-related DSS.

The trackside equipment of a DAS is connected to a traffic management system (TMS) which is embedded in the traffic control centre (TCC). A TCC includes interlocking systems, the TMS and the automatic route setting (ARS). According to Lochman (2009) TMS integrates all the required functions for safe and efficient train operations. All relevant information of a DAS system is exchanged between the TMS and DAS trackside.

According to Panou, Tzieropoulos, and Emery (2013), the following tasks are performed within the TCC: tracking of train movements, train run forecasting and conflict detection and resolution (CDR). Today, the former two functions are performed automatically within TCC systems. In case of disturbances it is proposed to apply real-time replanning (Quaglietta et al., 2016). In that case, the CDR updates the route plan. The route plan contains the scheduled routes and target times for all trains. The CDR module resolve conflicts by applying control measures, i.e. reordering, retiming and rerouting of trains. In practice, CDR is realised manually by a human dispatcher, thus it cannot be ensured that the realised route plan is the optimal with respect to minimising delays. In order to improve this non-optimality of the route plan, several studies have promoted the automation of CDR (i.e. decision and application of control measures). Before the CDR publishes a route plan, a train path envelope (TPE) can be computed based on the route plan which improves the energy efficiency of the constructed speed profiles. A TPE provides target windows. In practice, IM are cautious in introducing automatic CDR because they are unaware of the effect that these systems will have on the actual traffic (Quaglietta et al., 2016).

When using a DAS, the TCC functions explained earlier are considered to be performed by the TMS. Panou et al. (2013) refer to DAS which accommodate a real-time connection to the TMS, as systems that provide advice according to the route plan. These DASs can further be categorized based on how the calculation tasks are distributed between the DAS onboard and the DAS trackside equipment. The authors call this distribution *intelligence balance*. The calculation tasks considered in the intelligence balance are: train movement tracking, train movement prediction, conflict detection and resolution, TPE (i.e. target points or windows) determination, speed profile calculation, advice definition and advice display. Following, the tasks performed by each DAS component are presented:

- TMS: train movement tracking, train movement prediction, conflict detection and resolution
- DAS trackside: TPE (i.e. target points or windows) determination. Note that a TPE is used, i.e. a route plan catering for energy efficiency within train paths.

It can be concluded that the aforementioned calculation task distribution is constant for all the DAS variants presented in the following. Below, the three variants differ only according to which part of the DAS, the speed profile calculation and advice definition tasks are performed. Then, the variants according to the intelligence balance are:

- *DAS-Central*. The DAS trackside calculates the optimal speed profile, defines the advice and sends it to the train. Then, DAS onboard displays the advice.
- *DAS-Distributed*. The DAS trackside calculates the optimal speed profile and sends it on board. Afterwards, the DAS onboard defines the advice and displays it.
- *DAS-On board*. The DAS onboard receives the TPE from the DAS trackside. Next, it performs optimal speed profile calculation, advice definition and displays the advice on board.

Panou et al. (2013) examine the design of the driver interface of DAS. The authors recognize two aspects of the driver integration with a DAS; the context, i.e. the conditions under which the advice is updated, and the form of the advice, i.e. the information presented to the driver. The advice of a DAS is usually communicated to the driver via a human machine interface (HMI) (mentioned as driver machine interface: *DMI* on the ERTMS/ETCS context). A variant of the context of the advice is to update it at fixed time or distance intervals. In case of the latter, a positioning module is required, e.g. balise-odometer combination or GPS. Also, there is the option of event-based advice update. The *updated speed profile* solution is favourable when real-time update of the advice based on current status is required. The *contextual advice* alternative resembles a DIS. Hence, the driver performs the driving tasks according to real-time information regarding track, timetable and traffic status. As regards the form of advice, the analogy of the current operations to the timetable can be presented but also speed advice or adjustments of the train control stick. Usually, the two latter are preceded by a timely notice.

## 2.4. Dealing with conflicts when using DAS

This section presents approaches proposed by the ongoing research towards tackling the problem of DAS advice leading to conflicts. Also, this section discusses the current practice towards dealing with

conflicts in general, when using DSS systems. The sub-section contemplating the current practice uses the working principle of a number of commercial DSS as approaches to tackle conflicts.

### 2.4.1. Current research

DAS models have been proposed in literature that do not cater for conflicts but they deem it important. Li, Chen, Roberts, and Zhao (2018) have developed a model for the calculation of an optimized trajectory aiming for reduced energy consumption and punctuality. This model is planned to be included in a DAS. First, an optimal train trajectory is calculated offline. Then, at an online phase, the model updates the trajectory (and therefore, the advice) by comparing the current train status with the planned optimized trajectory. The authors examine only nominal operations. As a consequence, the offline optimal trajectory is conflict-free and in turn, adjustments to it are also conflict-free. Nevertheless, the authors acknowledge that the current framework will not be effective in case of disturbances. As a solution and direction for further research, the authors suggest either the incorporation of a model of the signalling system so as to constraint the train driver to drive to the maximum allowed speed imposed by the signalling, or the calculation of a new route plan by a high level TMS.

Some publications focus on the role of TMS in resolving conflicts. Rao et al. (2016) emphasize on the effect that the combination of TMS with train automation will have on real-time conflict resolution. The authors provide two solutions. The first solution addresses an existing conflict in the traffic. In this case, a decision support system aids the dispatcher to apply control actions (rerouting, rescheduling, retiming) so as to produce a new conflict-free plan. The other variant focuses on new targets to avoid conflicts after a new TMS solution. In this case, optimized speed profiles are calculated by a DAS-Central which are presented to the train driver.

Current research on DAS acknowledge the importance of integrating signalling in the advice generation. Wang and Goverde (2017) developed a C-DAS model that caters for energy-efficiency. The authors report conflicts of the advised speed profile with the current Dutch signalling system. As a result, the authors suggest the integration of a model of the signalling system as a further development of their model.

The same research team, on a latter publication of them, try to deal with conflicts through anticipating train control. A model has been proposed which aims to smoothly merge a freight train between passenger services, i.e. establish a green wave for the merged train (Wang, Goverde, & van Luipen, 2019). The framework intends a real-time application therefore it considers a C-DAS which allows for real-time communication with the TMS. Core part of the framework is the buffer stairway prediction which includes the prediction of blocking times and thus red signals. The blocking times are predicted by forecasting the traffic state using the Dutch train describer system TROTS.

Part of the ongoing literature investigates the potential of new data sources in acquiring the actual signal state. Zhu, Sun, Chen, Gao, and Dong (2016) propose a low-cost implementation of C-DAS where a PC emulates the trackside, while a smartphone mimics the onboard equipment, aiming for energy efficiency. In this publication, it is mentioned (also shown on image) that the signal aspects of the two downstream signals are shown on the driver interface. Yet, no further clarification is given on how this is achieved. According to later work of the team, it is revealed that through the positioning function of the smartphone (using a dedicated GNSS antenna), train position can be assigned to the correct track (by a map-matching technique) and thus, the signalling status can be inferred (Zhu, Gao, & Dong, 2018).

de Fabris, Longo, and Medeossi (2008) propose a technique to derive signalling information in real-time although their main intention is not to tackle conflicts. The authors develop a software that aims to improve micro-simulation models. The objective is to develop a software that constitutes a calibration tool that analyses observed rail operations based on train event recorder data. The trains examined are equipped with a DIS (jointly coupled with on board ATC module). The onboard-DIS collects information from other onboard sensors such as GPS, odometer, and event recorder via wireless communication. Also, the module is able to collect signal-aspect information through balise messages. A case study has been performed for nominal operations. The authors propose an extension of the software to facilitate disturbed operations so as to observe driving behaviour on restrictive speed signals.

### 2.4.2. Practice

Albrecht (2014) recognizes three alternatives so as to make the support from a DSS be in accordance with the signalling constraints:

- A DAS that compares planned with actual operations. The system constantly compares the realized operations with the timetable such as the EBULa-ESF and adjusts the advice adequately (see also 2.6).
- Real-time display of the track status (and thus the signal status) on a DIS such as in RouteLint (see also 3.2.2 and 2.6).

The variant that is mostly compliant with the signalling system regards a C-DAS that has access to vital information in order to perform its non-vital functions. The onboard module of the installed ATP provides this vital information which includes: actual train position and speed, SSP, movement authority, braking curves and temporary speed restrictions. Note that train positioning information is collected from the vital data stream used in the ATP systems. For these systems, train positioning is based on continuously determining the location offset from installed balises and communicate it between the onboard and trackside equipment of the DAS (Rahn, Bode, & Albrecht, 2013). Also, note that whatever the level of signalling constraints used in a DSS, these systems remain non-safety critical. Two sub-categories can be distinguished based on the level of automation of the conflict detection and resolution function of TMS:

- C-DASs that are connected to an automatic TMS. Such systems are Automatic Functions Lötschberg (AF); a C-DAS installed on a main line equipped with ETCS L2 (see also 2.6) and Trainguard MT; a C-DAS over CBTC (Communications Based Train Control) applied in urban lines. Both systems receive route plans which are conflict-free and thus, the calculated speed profile is conflict-free, too.
- C-DAS with frequent automatic conflict detection and manual conflict resolution such as Adaptive Lenkung (ADL).

## 2.5. Driver-related factors

Driver's acceptance towards a DAS is highly affected by both the reliability of input data (Albrecht, 2014) as well as the drivability of the advice. Drivability of the advice means that the changes in driving advice must be sufficiently separated in time in order for the driver to be able to interpret and apply them (Albrecht, Binder, & Gassel, 2013). Drivability of the advice is related to the human factors of a DAS. On the one hand, human factors stem from the design of the HMI and are related to the workload and confusion originating from using a DAS. On the other hand, advice reliability is affected by the quality of input data and in turn affects driver acceptance.

As regards reliability, Albrecht (2014) deem important to look into the level at which DAS incorporate the constraints imposed by safety critical systems such as the signalling system. If signalling information is used as input to a DAS, the reliability of the signalling information directly affects the reliability of the produced advice. The signalling system provides constraints to the TPE. Main aim of the author is not to assess the level of safe advice the system can provide, but to appraise the reliability of the support and therefore, driver's acceptance towards it.

As regards the workload originating from the advice, attention must be drawn to the amount of information communicated so as not to overwhelm the driver (Yang, Liden, & Leander, 2013; Albrecht, 2013). Additionally, the advice should not be confused with the information coming from safety related systems. For example, colours and numerals of the DAS-HMI should not be frustrated with these of safety related systems.

In Table 2.1 there is an attempt to break down the approach with which a selected number of publications tried to address the disputes that the selection of driver integration aspect (advice context/form) have on human factors (workload/confusion). Each problem is followed by the workaround proposed in the publication. For instance, at the early releases of CATO, DMI colours were mistakenly interpreted by the drivers as information related to the signalling. For that reason, it was selected neither to use

colours in the DMI which are originally used by the signalling system (i.e. green, yellow, red) nor to show the current speed on the DAS's DMI (Yang et al., 2013). According to Table 2.1, both the form and the context of advice can violate the design criteria of the DMI.

Table 2.1: Effect of DMI designs on the human factors of a DAS and approaches to tackle them according to relevant literature

Publication	Problem	Driver integration	Human factors	Workaround
<i>Yang et al. (2013)</i>	Advice misinterpreted as information coming from signalling	Form	Confusion	Neither "signalling" colours nor current speed displayed on DMI
		Form	Workload	Speed profile on Y axis; info about surroundings
	Frequently updated optimized speed profile	Context	Workload	Change in profile shown when close to target point (< 5 km)
<i>Albrecht (2013)</i>	Insufficient speed restrictions	Form	Confusion	No speed
<i>Rahn et al. (2013)</i>	Speed profile calculated for entire route	Context	Workload	Only current regime

Some studies propose DMI design strategies based on experience. Panou et al. (2013) mention the optimal combination for driver integration being event-based advice update (context) presented as speed suggestion (form). The context of advice is in accordance with that proposed by Jin and Kadhim (2011). According to this study, the advised speed profile is calculated between timetable points is updated only when new points are received (event-based update). Then, DAS defines the advice according to driver's behaviour compared to the calculated advice speed profile. In contrast to Panou et al. (2013), the advice should be presented on the DMI in the form of deviation seconds compared to the timetable. By doing so, the driver is motivated to keep up with the schedule. The alternative of time deviation advice is adopted over that of speed as the latter may be confused with information from the signalling.

## 2.6. Commercial driver support systems providing a real time connection to the traffic management system

In the following lines, commercial DSS are presented. The considered systems may be fully operational or limited to some pilot studies. This section includes only DSS that allow for real-time data exchange between the TMS and the onboard equipment of the DSS via the trackside equipment of the DSS.

ADL is a C-DAS operating on a part of the Swiss network by SBB (Schweizerische Bundesbahnen) aiming to decrease the number of unplanned stops (Weidmann, Bruckmann, Fumasoli, Herrigel, & Schranil, 2015). Energy efficiency is a latent benefit of ADL (Luijt, van den Berge, Willeboordse, & Hoogenraad, 2017). The current traffic state is updated every 3 s and conflicts are detected automatically. Train path envelopes are manually computed and are sent onboard by the TMS. Then, the speed profiles are calculated by the on board ADL equipment. Also, ADL displays the advice in the form of speed (Schumann, 2014).

AF is a C-DAS operating on mixed rail traffic at a tunnel in Switzerland (Mehta, Rößiger, & Montigel, 2010). The tunnel is equipped with ETCS L2. The special layout of the tunnel (double-track merging into single-track within the tunnel) imposes conflicts. To that end, main responsibility of AF is to predict and resolve conflicts. AF is the only existing traffic control system equipped with an automated conflict detection and resolution module. Despite the benefit on capacity, energy savings has been proven a latent benefit of the system as a consequence of the minimization of unplanned stops. According to Rao et al. (2016), AF constitutes the only C-DAS in operation on a mainline today. Albrecht (2014) points out that under its current configuration, AF neither facilitates a standardized communication channel between the trackside and onboard part of the DAS nor has proper HMI. Instead, speed advice is

communicated via text messages. Nevertheless, the author points out that a C-DAS based on ETCS has all the requisites to provide advice totally compliant with the railway safety systems.

Computer Aided Train Operation (CATO) is a C-DAS which was initially developed to be deployed in the iron ore line, a line mainly operated by freight trains at northern Scandinavia (Yang et al., 2013). Its main goal is energy efficiency and to a smaller extent coordination of trains (Tschirner, Andersson, & Sandblad, 2013). The latter becomes relevant since the biggest part of the network comprises of single track and the trains usually do not follow the timetable, due to often delayed loading procedures of the freight wagons. In order to tackle this, TMS sends new route plans on board and each train builds its own speed profile, defines and displays the optimal traction advice. The calculated speed profile is constrained by the Static Speed Profile (SSP) as well as Temporal Speed Restrictions (TSR).

Driver Style Manager (DSM) (also referred to as EBI Driver 50) is a C-DAS developed by Bombardier and it has been deployed on a small number of pilot studies around Europe. It displays speed and traction advice (Bombardier-Transportation, 2008). An improved version of DSM can accommodate dynamic speed and signalling information (Kent, 2009). Yet, the author does not give details into how this is achieved.

GreenSpeed is a DAS developed by Cubris and it is installed in all the trains of the Danish Railways since 2012 (Thales, 2019). It displays speed advice (Luijt et al., 2017) and contains track signal status information (Dong, Zhu, & Gao, 2018). The latter publication does not provide details into how signal status knowledge is achieved. GreenSpeed is available at four levels (Schumann, 2014). Level 0: constitutes a S-DAS, Level 1: provides data connection with the trackside equipment, Level 2: constitutes a DAS coupled with other train systems and timetable adjustments and Level 2+: is a DAS coupled with ETCS. Also, GreenSpeed is the first C-DAS introduced in the UK and it has been deployed by the South Western Railway (Railway-News, 2015).

Ketech has developed a C-DAS that aims for energy efficiency and smooth train operation (Darlington, 2019). The system is currently at a test phase in the UK. Ketech C-DAS offers a real-time connection to the TMS and Darwin, a service used throughout the UK that provides real-time arrival and departure predictions, platform numbers, delay estimates, schedule changes and cancellations. Ketech facilitates train positioning from GNSS but only as a backup source. This is due to the limited availability of GNSS and the need for a map-matching technique to match a point to the correct track. Also, the author considers it as the only situationally aware (i.e. aware of the actual signal state) C-DAS of the market to date. Yet, the author neither clarifies the way that the C-DAS receives input from the signalling system nor the ATP systems that it supports. What is more, it can perform as a S-DAS in case of degraded communication. The presented advice includes traction and speed.

RouteLint is a DIS developed by the Dutch IM ProRail aiming for a decrease in the number of conflicts and unplanned stops (Albrecht, 2014). RouteLint provides real time information regarding the position and delay of the train as well as of the surrounding traffic. Train positioning is provided by a train describer system and it is the same information delivered to the TMS. Using train positioning information, RouteLint can give a notion of the downstream actual signalling state (see also Subsection 3.2.2). Its information is communicated to the driver via a dedicated HMI. RouteLint became fully operational in 2016 and it is currently used by NS and DB-Cargo trains. Based on a simulator experiment, RouteLint was proven to successfully reduce the number of SPADs and decrease the duration of stops before a red signal (Albrecht & van Luipen, 2006). Additionally, RouteLint is believed to improve riding comfort, energy efficiency and punctuality (Albrecht, van Luipen, Hansen, & Weeda, 2007).

Zuglaufregelung (ZLR) is a C-DAS that operates on all ICE lines of the German railway operator DB (Deutsche Bahn) (Albrecht, 2014). ZLR constitutes a dynamic network-related DAS and it is an improvement of its predecessor EBU-La-ESF which was a dynamic train-related DAS that provided advice regarding when to start applying coasting. The current configuration of ZLR provides speed advice, too. ZLR aims for reduced energy consumption and it supports temporary speed restrictions. It comes in both DAS-Central and DAS-On board configurations. ZLR also includes restrictions from the signalling system by comparing the realised with the planned speed profile (Hoffmann & Böttcher, 2018).

Table 2.2: Commercial DSS connected to a TMS in real-time

System	DSS Type	Task distribution	Signalling <sup>2</sup>	Real time data exchange			ATP <sup>6</sup>
				TtD <sup>4</sup>	DtT <sup>5</sup>	Train positioning	
ADL	C-DAS	Central	Standalone	TPE <sup>8</sup>	No	ATP	ETCS L2 <sup>7</sup>
AF	C-DAS	Central	Full	TPE	Position	ATP	ETCS L2
CATO	C-DAS	On-board	Standalone	TPE	Position, speed, performance	GNSS, ATP	Class-B, ETCS L2
DSM	C-DAS	On-board	Partial	TPE	No	GNSS, on-board sensors	Class B
GreenSpeed <sup>1</sup>	C-DAS	On-board	Partial	TPE	Position, track-signal-train status	GNSS	Class-B, ETCS
Ketech	C-DAS	On-board	Partial	TPE	No	GNSS, TDD <sup>3</sup>	Class-B
RouteLint	DIS	N/A	Only on interlocking areas	Surrounding traffic state	No	TDD	Class-B, ETCS
ZLR	C-DAS	Distributed	Partial	TPE	No	GNSS, ETCS, odometry	Class-B, ETCS

<sup>1</sup> Level 2 which constitutes a C-DAS;

<sup>2</sup> In case of a DAS, signalling constrains the solution, while in case of DIS, signalling is given as information;

<sup>3</sup> Train Descriptor Data;

<sup>4</sup> TtD: TMS to DAS trackside equipment;

<sup>5</sup> DtT: DAS trackside equipment to TMS;

<sup>6</sup> In case the installed ATP system is not explicitly mentioned in a publication, this information was inferred by the location it operates and consulting on Vincze and Tarnai (2006);

<sup>7</sup> SBB (2017);

<sup>8</sup> Train Path Envelope, i.e. route plan catering for energy efficiency

## 2.7. Assessment of DAS

This section discusses the different scopes in which a DAS can be assessed. A DAS can potentially be assessed according to its human factors, the acceptance of the driver using it and the effect it has on capacity. Also, the means to assess a DAS are presented. This section includes DAS that have been tested on a simulation environment only.

### 2.7.1. Human factors

D. Large, Golightly, and Taylor (2014) have attempted to answer the question "speed or timekeeping" over the form of advice by researching the effect that these forms have on driver's workload with the use of a simulator. The alternatives considered were speed advice, timekeeping advice and driving without advice. The scenarios are extended by two operational conditions; *low* referring to nominal operations with stops only at major stations and *high* referring to disturbed operations with intermediate stops. The findings can be summarized as that the workload of the timetable solution being higher than that of the speed alternative which in turn is higher than the option of not consulting a DAS. Nevertheless, the speed advice led to a smaller number over speeds compared to the timetable solution for all participants.

Additionally, the participants perceived that they have performed better when using the timetable DAS. According to the authors, the timetable solution can be used by the driver as a means of assessing own performance. In contrast, the speed alternative should be considered as a rather short-term solution.

The authors state that the use of DAS, and consequently a marginal increase in the workload, is desirable since it can decrease driver's passivity, thus increase situation awareness. Using a DAS may result in the unforeseen benefit of keeping the driver more *in-the-loop* which may result in capacity gains. Yet, this requires further investigation. This statement is conflicting with the goal-setting of Yang et al. (2013) who aim to induce the minimum possible workload.

### 2.7.2. Driver's acceptance regarding the advice

The more conflicting the advice of a DAS is, the less likely is for the driver to keep on consulting it. Mitchell (2009) is concerned about the driver's over-reliance to the DAS and the misconception that the speed advice coincides with the allowed speed originating from signalling and speed signs. Nevertheless, the author appraises that the safety risk can be compensated by a system that provides full supervision of the movement authorities. DAS performs a non-safety-critical function of the railway signalling system (EGNSSA, 2019). Although, it may be fully constrained by the signalling, there is always an independent ATP module (Albrecht, 2014).

Albrecht (2014) suggests that the reliability of DAS is directly affected by the quality of input data. In that direction, Albrecht, Lüddecke, and Zimmermann (2013), examine the relation between driver's acceptance and positioning quality. The study examines the use of GPS as the positioning module of a conceptual DAS. Its low accuracy with respect to speed and location, may lead to wrong advice regarding change of driving regimes. In case these errors result in delayed operations, it is likely that the driver challenges the advice, thus leading to decreased effectiveness of the system.

### 2.7.3. Capacity gains using a DAS

One way to improve capacity is to use DAS (Wang & Goverde, 2017). Venkateswaran et al. (2015) propose a framework to assess the impact of the use of automated subsystems on the capacity of main railway lines. The study considers several automation levels; from S-DAS to GoA 4 under ETCS. The main contribution of the study pertains to the delivery of a framework that directly relates different automation alternatives on the main line with their expected impact on capacity. The derivation of a framework specially for the main line is imperative since for metro lines such frameworks already exist. Recall the inherent differences between urban and main lines which can be summarised in the discrepancy in homogeneity, network size, effect by external factors e.g. weather and the existence of several TCCs on the main line. The authors suggest that by increasing the automation on the main line,

the variability of the service will decrease since the probability of failure on the subsystems will shrink and its consequences will be more controllable. Powell, Fraszczyk, Cheong, and Yeung (2016) adds to that the better train speed control that comes with increasing GoA. Then, as variability of subsystems decreases, reliability of the whole service will increase. Finally, as a service turns more reliable, the probability of secondary delays decreases. The formula considered is an exponential expression of capacity consumption and amount of secondary delays. A regression analysis yields the parameters which capture the reliability of the subsystems.

#### 2.7.4. DAS assessment methods

It is usual to assess commercial DAS by collecting empirical data (Yang et al., 2013; Mehta et al., 2010). Yet, the most prominent way to assess a DAS at its design phase is via a simulator. Especially when the human factors of the system are of interest, simulators allow for capturing human interaction by adjusting the interface design (Abril et al., 2008). D. Large et al. (2014) assess the human factors of their DAS in that way. Advice is manually constructed and presented real-time to the driver via a monitor. This practice follows the "Wizard of Oz" methodology according to which the subject ("Oz") perceives to be in an automated simulation environment, while the machine (simulator) is partially or totally manipulated by the experimenter ("Wizard") (Steinfeld, Jenkins, & Scassellati, 2009). A similar practice with an experimenter adjusting the advice according to the simulated operations was followed in (Albrecht, Binder, & Gassel, 2013). Wang and Goverde (2017) assessed their model with respect to energy savings on a simulator.

In literature, there are attempts to model operational constraints such as temporary speed restrictions. Dong et al. (2018) assess their DAS on a simulator with respect to energy efficiency and punctuality. For the punctuality scenario, a temporary speed restriction is introduced and the manoeuvres to recover the delay are recorded. HMI announces the speed restriction 5 kilometres upstream the location it occurs. Albrecht, Gassel, Binder, and Luipen (2010) discuss a trajectory calculation model of a DAS that caters for operational constraints such as bottlenecks and the driving limitations imposed by ATB-EG. The simulator, under the current configuration can provide time, position and speed. Delay information is presented externally.

The inability to recruit a number of experienced drivers that will lead to the minimum required sample size for an experiment, has led the authors to enrol inexperienced driver's (D. R. Large, Golightly, & Taylor, 2017). D. Large et al. (2014) measure the performance of the subject by counting the number of SPADs and speed limit overshoot. The findings show no significant difference of the performance between experienced and inexperienced drivers. Yet, a later study of the authors demonstrates that this same performance is not achieved in the same way (D. R. Large et al., 2017). In fact, experienced drivers conduct a smooth ride while the speed profile of inexperienced users is rather oscillating. This suggests that experienced drivers achieve better energy efficiency and passenger comfort compared to inexperienced ones.

## 2.8. GNSS deployment in the railway industry

Global Navigation Satellite System (GNSS) is a system that slowly enters the railway industry. At the beginning GNSS train positioning data was used only for recording train operations. Yet, today's research focuses on using GNSS for safety-critical functions. This section introduces GNSS and specifies the different uses it can have in the railway industry. Special attention is given to the use of GNSS as train positioning source for non-safety critical applications. Moreover, methods to increase GNSS accuracy are presented. Finally, an approach to assess GNSS applications on railways is discussed.

### 2.8.1. GNSS - A novel data source for railways

Data has been used widely in railway transport systems (Ghofrani, He, Goverde, & Liu, 2018). The authors distinguish four layers according to which studies that follow a data-oriented approach (big or small) on railways can be categorized. The first layer pertains to the domain of the RTS, namely operations, safety and maintenance. The second layer regards the classification of big data analytics (BDA) studies. These studies can be categorized at a descriptive, predictive or prescriptive level. The

third layer contains models used for BDA such as (limited to some indicative examples): classification, simulation, statistical analysis, association and optimization. The fourth layer includes techniques of implementing BDA.

At a descriptive level and in order to analyse train operations, statistical analysis is performed on data originating from train describer systems (Yuan & Medeossi, 2014). Such a process can yield statistical measures regarding delays, running and dwell times. Train describer data have also been used in studies addressing the reproduction of realized blocking time diagrams (Kecman & Goverde, 2012).

GNSS is a positioning system that uses satellites (Marais, Beugin, & Berbineau, 2017). In order to determine a point's position, distances must be measured from that point to at least four satellites. Then the position is calculated using triangulation. GNSS data are computationally more demanding compared to the afore mentioned data sources (Yuan & Medeossi, 2014). In railways, GNSS data can be used to determine the realized speed profile as well as departure and arrival times. GNSS devices has been introduced in railways later than road transport since train describer devices already provided real-time train localization. Yet, the need of RUs to locate their fleet independently from IMs, has currently led RUs to install GNSS to their rolling stock.

GNSS data has been used in literature for the calibration of the performance parameters used in the equation of train motion (de Fabris et al., 2008; de Fabris, Longo, & Medeossi, 2011). These studies aimed for improving micro-simulation models. Additionally, GNSS data have been deployed in developing a timetable based on stochastic blocking times (Medeossi, Longo, & de Fabris, 2011). On the ensuing, studies that focus only on the use of GNSS for train positioning are presented.

Beugin, Filip, Marais, and Berbineau (2010) present several reasons of promoting the introduction of GNSS in railways. First, improved rolling stock positioning can result in better energy-tolling schemes. Also, GNSS can be used in safety-critical manner on secondary lines and pose a more cost-effective solution compared to installing a traditional signalling system. Finally, GNSS can be fused with ERTMS/ETCS and further promote the interoperability on cross-border European railways.

### 2.8.2. GNSS as a means for train positioning

Train separation is essential for safe train operation (Pachl, 2014). Railway lines that are based on fixed block signalling, are divided into block sections. At every time instant, a block section can be occupied by a single train. Dedicated track-clear devices such as track circuits or axle counters determine track occupation/release (also mentioned as train-detection) and thus, yield whether a block is occupied or not. According to Lüthi (2009), track-clear detection is a safety-critical function. Following, train describer systems couple the information from train detection systems with train numbers and deliver discrete train positioning (Kecman, 2014). Train describer systems are used for traffic management, traffic supervision, automatic train routing and passenger information (Yuan & Medeossi, 2014). The previously mentioned applications suggest that train describer systems are not safety-critical.

GNSS can be used for train positioning and it has been widely used for non-safety related functions (Marais et al., 2017). Still, GNSS deployment for safety-related functions is developing slowly due to its inability to meet the railway safety requirements (Beugin et al., 2010). Yet, GNSS constitutes a low-cost solution which potentially can be deployed for safety critical functions as it requires minimal investments only from the RU's side since it replaces expensive and maintenance-demanding trackside equipment which is required to meet the railway safety requirements (Albrecht, Lüddecke, & Zimmermann, 2013). To that aim, current research is focusing on increasing GNSS performance to meet railway signalling standards (Zheng & Cross, 2012; Neri, Capua, & Salvatori, 2018).

Safety critical functions are those functions related to railway signalling. Marais et al. (2017) present a thorough overview of the state-of-the-art research addressing the use of GNSS systems for safety critical railway functions. In EGNSSA (2019), non-safety relevant applications are further categorized with respect to the use of GNSS into liability and non-liability relevant ones. On the former category belong systems such as DAS and fleet management systems (e.g. tracking and tracing), while on the latter belong applications providing passenger information (e.g. delays). Some indicative examples from literature that use GNSS for DAS application include the work of Wang and Goverde (2017), Zhu et al. (2018) and from commercial C-DAS systems CATO, DSM, Greenspeed, Ketech and ZLR (see also subsection 2.6)

### 2.8.3. Fusion of GNSS with other sensors

Train movement is laterally constrained by the railway track. Therefore, after having acquired a train's position in world coordinates (GNSS), a map matching technique is required in order to transform it into track coordinates. In fact, map matching achieves both positioning accuracy and coordinate transformation (Albrecht, Lüddecke, & Zimmermann, 2013). Fundamental input of map-matching is a digital map of the railway network at a micro level. The authors recognize two map-matching alternatives. On the one hand, a map-matching technique used in safety critical operations assumes prior knowledge of the route the train is planned to traverse. Then a simple algorithm is used to overlay GNSS position on the actual route. On the other hand, in most of the cases the actual route is not known. Therefore, a reactive technique is used to estimate which track the train is heading to. This technique is realised in two consecutive stages. First, the search space is limited into railway tracks. Then, the coordinates are transformed from a three-dimensional into a one-dimensional reference system (Albrecht, Lüddecke, & Zimmermann, 2013). Hänsel, Ganzelmeier, Becker, and Schnieder (2004) mention that 1 meter of lateral accuracy is considered enough for that purpose.

Albrecht, Lüddecke, and Zimmermann (2013) deploy map-matching to fuse GNSS measurements with data from IMU (Inertial Measuring Unit), laser scanner, odometer, optical speed sensor. The GNSS accuracy is increased by using a differential technique. The proposed model can address both safety critical applications such as ATP, but also non-safety critical applications aiming for the improvement of railway operations such as ATO. Additionally, Becker, Hänsel, May, Poliak, and Schnieder (2006) propose an onboard positioning unit that has both a non- and a safety critical character. The safety critical application constitutes a cost-effective solution for secondary lines that are not equipped with an ATP. A map matching technique is used to combine GNSS and Eddy current measurements on top of a digital map.

Zheng and Cross (2012) perform a sensitivity analysis to assess the effect that the accuracy of the digital map has on the final position estimation. The authors use a stochastic approach to correlate a GNSS measurement with a track.

### 2.8.4. Performance evaluation of GNSS applications in railways

The infiltration of GNSS in railways has drawn the attention of researchers towards developing a framework to assess their performance. The research team of professor Filip has contributed significantly in delivering the specifications for the application of the European GNSS (Galileo) in safety critical railway functions. According to Filip et al. (2008), a similar determination of specifications for GNSS applications has been realized for aviation since the 90's. The authors aim to translate that methodology into the European railways standards.

Among others, the required navigation performance (RNP) was a solution for capacity and safety increase in aviation that became apparent in the late 90's (Kelly & Davis, 1994). RNP intends the airspace management. At the beginning, it addressed only en-route operations, but later it was broadened by the GNSS quality measures so as to be used in approach, departure and landing procedures (Filip et al., 2008). According to Langley (1999) the four GNSS quality measures are:

- **Accuracy:** The difference between the measured and a reference value. If known, this reference value is the true value. In other case, it is an pre-defined value. For GNSS, the reference value may be the published coordinates of a geodetic reference mark.
- **Availability:** The ability of the system to deliver the required function and performance for a given area at the beginning of the process.
- **Continuity:** The ability of a total navigation system to function without interruption during an intended period of operation. Continuity demonstrates the probability that the system will maintain its specified performance level for the duration of an operation, assuming system availability.
- **Integrity:** The trustworthiness of a system. Although the system may be available at the start of an intended operation and its continuity may be able to be predicted, it might be that the system does not deliver the proclaimed accuracy due to some unexpected latency. Still, the system must be able to detect this kind of failures. In other words, integrity refers to the system's ability to automatically provide timely warnings when accuracy criteria are not met.

Filip et al. (2008) give a slightly different meaning to the continuity parameter of the RNP. According to the authors, continuity emphasizes on the segment of the entire operation where the function is more needed than other segments. Also, the purpose of continuity is to guarantee, that a navigation or position determination system will not be interrupted when it is really needed. Therefore, the continuity requirement is defined for the most critical phase (very short time interval) of a safety operation. Continuity approximates reliability, i.e. the fact that a system works within specifications (desired accuracy and integrity is provided) and within a stated period of time. The authors refer to the reliability within the RAMS (reliability, availability, maintainability, safety integrity) context. RAMS is a framework addressing the quality of railway equipment as defined by the EN 50126 standard. RAMS is calculated by a dependability analysis (Filip et al., 2008). The RAMS definition given by CENELEC (2001) is:

- Reliability: The likelihood that the system can deliver the required function for a given period of time
- Availability: System's ability to perform its function at given moment or a predefined time period.
- Maintainability: The probability that a maintenance function can be realised according to predefined maintenance conditions. In other words, it is the ability of a system to return to normal function after having been maintained.
- Safety Integrity: The system's ability to perform all safety related functions within given time period.

Beugin et al. (2010) claim that certification of safety critical functions using GNSS is complicated. The authors base their argument on the fact that RNP parameters are mainly aviation-oriented. Aviation differs from railways in the sense that the former aims for high dependability, while the latter aim for increased safety. In turn, aviation's dependability is affected by the aircraft, while railway safety is associated with the signalling system (Filip et al., 2008). Beugin et al. (2010) continue arguing that railway-related systems are traditionally built and monitored by the railway industry. Increasingly, introducing an external system challenges user acceptance. Based on the inherent differences between aviation and railway, the authors suggest three discrete steps towards the further integration of GNSS in railways; translation of GNSS performance parameters into RAMS, construction of an adequate assessment framework and finally, quantification of these parameters.

Filip et al. (2008) propose a framework to translate RNP parameters into RAMS (Figure 2.1). Continuity approximates reliability and it indicates whether a system is working within the predefined specifications (accuracy and integrity) for a short period of time. Also, according to EN 50126, availability is a function of reliability and maintainability. Then, availability can directly be translated into dependability which encloses the non-safety critical part of the analysis. In short, the non-safety critical part of the specification is the dependability which equals  $1 - (\text{Continuity Risk (CR)} + \text{Integrity Risk (IR)})$ . The safety critical part is the combination of CR and IR. Progressively, merging the safety-critical with the non-safety critical part yields the integral RAMS specifications of GNSS applications on the railway domain.

Table 2.3 summarizes the RNP for non safety critical requirements as considered in different publications

Table 2.3: RNP requirements for non-safety critical operations

Publication	Accuracy	Availability	Integrity <sup>1</sup>	Continuity
Becker et al. (2006)	1 km	> 99.2 %	10s	-
EGNSSA (2019)	>10 m	High	30s	-
Barbu (2000)	50m	-	10s/125m	> 99.9 %

<sup>1</sup> Measured as Time or Distance to Alert

## 2.9. Discussion

DSS can improve the railway operations in several ways. Yet, in order for DSS to be effective in disturbed operations, they should facilitate a real-time data connection to the TMS. That is why a C-DAS is the most prominent alternative to the automation on the main line. This is because it can yield

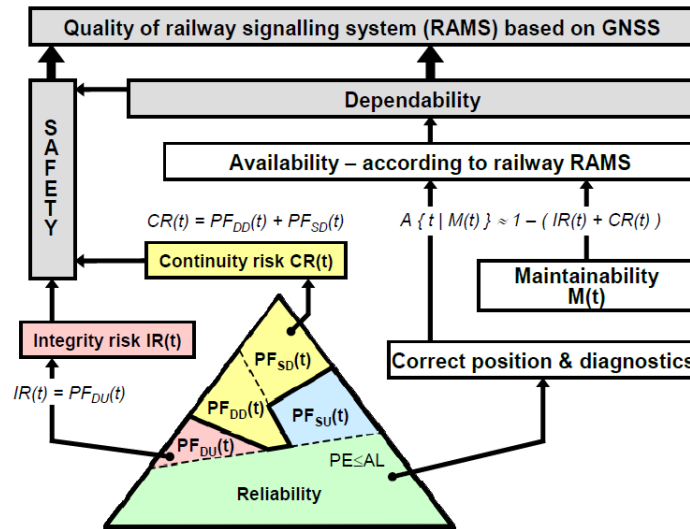


Figure 2.1: RNP parameters into RAMS translation, source Beugin et al., 2010

several benefits, while no special attention is required for its safety-related characteristics since it is a non-safety critical system.

Several DAS classifications can be distinguished. DAS vary per the frequency of data exchange between the trackside and the onboard DAS equipment, the distribution of calculation tasks between trackside and onboard, the level of incorporating constraints from the signalling system and the context and the form of the advice. Different alternatives of the calculation task distribution focus on optimizing traffic at network or train level. Regarding the form of the advice, developers of DAS usually opt for the speed-advice solution since it is more comprehensive for the driver.

Many publications advocate the introduction of the signalling constraints to a DAS. In fact, many commercial C-DAS (e.g. DSM, GreenSpeed and Ketech) claim to incorporate the signalling constraints but they do not define how this is achieved. A possible reason to that is the market confidentiality which enhances the competition between the developers of DAS. According to the literature review and the common practice regarding the ways to deal with conflicts when using DSS systems, the following strategies can be recognized. The strategies are shown in decreasing order of probability of the alternative leading to conflicts.

- Alt.1: The C-DAS has access to vital train positioning information of ETCS L2 (continuous positioning) and it is connected to a TMS that facilitates automatic conflict detection. Two sub-alternatives are possible.
  - Alt.1-1: Conflict-free advice stemming from an automatic conflict resolution system (e.g. ADL).
  - Alt.1-2: Frequent monitoring of the actual traffic state and manual computation of new route plans (e.g. ADL).
- Alt.2: The C-DAS is provided with a prediction of the signal status. This is achieved by predicting the blocking times using the real-time input from a train describer system, such as Wang et al. (2019).
- Alt.3: Using a DIS that receives information regarding the actual track status. The overview of the actual traffic is provided by train describer data (e.g. RouteLint).
- Alt.4: Advice partially compatible with the signalling system. Actual operations are compared to the timetable and the advice is adjusted adequately (e.g. EBULa-ESF).

Another point to address in the design of a DAS relates to the driver's acceptance. It is important to look into the level a DAS considers the constraints of the signalling system. In case of conflicting advice,

the driver is discouraged in consulting the DAS next time. Therefore, the effectiveness of the system decreases. Increasing the quality of the DAS input can be the solution to improve the trustworthiness of the output and thus, increase driver's acceptance.

Another strategy to prevent the driver from confusing the DAS's advice with information coming from safety-critical systems (e.g. signalling system) is to carefully select the form of advice. The most popular form of advice is speed advice.

A DAS's design must be in line with human-factors requirements. It is common to test a DAS on a simulator. Additionally, it is acceptable to test a DAS on simulator where the simulator is operated by inexperienced drivers. The only cases in which it is not advisable to use inexperienced drivers is when answering research questions related to energy efficiency and riding comfort.

GNSS is a novel data source which currently gains ground on the railway industry. In its early days of deployment GNSS was used for non safety-critical applications such as rolling stock positioning to inform passengers. Recently, academia has focused on the extent that GNSS train positioning can be used for safety-critical applications. Special attention has been given to improve GNSS positioning solution so as to meet RAMS criteria. While the performance of GNSS in safety-critical applications has been quantified, this is not the case for non safety-critical functions such as DAS.

# 3

## Background information

This chapter includes necessary information that serves as the background for this thesis. The information regards the Dutch railway signalling system, the ProRail systems that are used in this thesis as well as the blocking time theory which is necessary for the railway capacity assessment.

### 3.1. The Dutch railway signalling system

According to Theeg and Vlasenko (2009), a railway signalling system has four components:

- Track-clear detection: determines whether a track-segment is occupied or not,
- Interlocking: a setting of switches and signals. Changing that setting can be done in a unique order which ensures safe train movement,
- Block system: transmitting movement authorities via railway signals,
- ATP: protecting against driver errors

In the following, the latter two components are elaborated since they differentiate the Dutch safety system from the signalling systems installed in other countries. The Dutch signalling system (*Nederlandse seinstelel* 1954: NS'54) is a three-aspect two-block signalling system used at the majority of the Dutch railway network. NS'54 supports several signal configurations (combination of aspect, not-/flashing and numeral) each of which constraints train's speed. According to *Seinenboek* (2005) the different configurations are:

- Green light: Proceed with the maximum allowed speed of the track
- Flashing green light with white numeral : Proceed with speed not exceeding the speed indicated by the white numeral
- Flashing green light: Proceed with maximum allowed speed being 40 km/h
- Yellow light with flashing white numeral: Reduce speed to that indicated by the white numeral and keep applying braking since next signal orders a further speed reduction
- Yellow light with white numeral: Reduce speed to that indicated by the white numeral before next signal
- Yellow light: Reduce speed to 40 km/h and prepare to stop before next signal
- Yellow flashing light: Proceed with speed not exceeding 40 km/h and prepare to stop before any obstacle (running on site)
- Red light: Stop before the signal

ATB-EG is a continuous ATP system that supervises five speed steps (codes) (40, 60, 80, 130, 140 km/h) which are transmitted to the cab via coded track circuits (Albrecht et al., 2010). Each ATB-code has a corresponding light in the driver's cabin. The supervised speed is the minimum of the speed limit

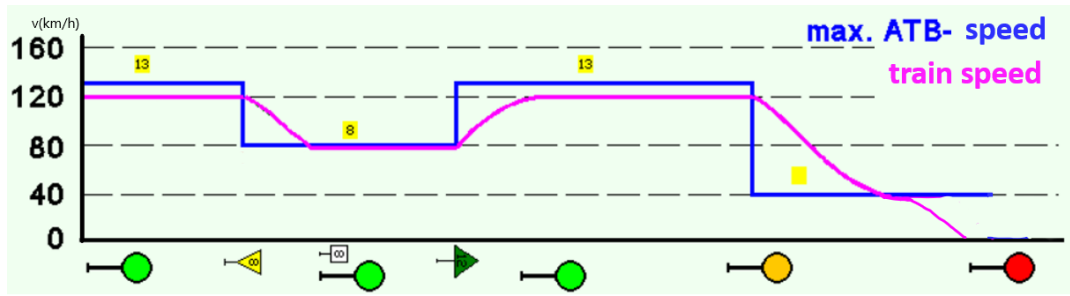


Figure 3.1: Comparison between a train speed profile complying with the maximum allowed speed and the supervised speed profile by ATB-EG (adapted from marcpieters.nl)

originating from: the current track circuit, the signalling system as well as the speed limit imposed by an upcoming speed sign. Under ATB-EG operation, the maximum allowed speed does not always coincide with the supervised speed (Goverde, Corman, & D'Ariano, 2013). In case the maximum allowed speed is not included in the five speed steps, the next higher speed step is supervised. For example, in Figure 3.1 for part of the route, 120 km/h is the maximum allowed speed, yet the supervised speed is 130 km/h.

A change in the supervised speed is marked by a change in the ATB code. This event is followed by a single bell sound. Since ATB-EG constitutes a continuous ATP system, in case of a signal aspect improvement, the ATB-code change is instantaneously transmitted to the cabin allowing the driver to accelerate immediately and not to wait to reach sight distance from the signal. In contrast, in the event of a down speed, ATB-EG checks whether the driver applies at least two of the seven in total, braking steps. This check is called braking criterium (*rem criterium* in Dutch) and the driver has 4 sec to react to it. In case the braking criterium is not met, a continuous bell ring is initiated until the driver starts applying brakes. Speeds below 40 km/h are not supervised. Hence, avoiding a signal passed at danger (SPAD) incident when driving below 40 km/h lies within driver's responsibility. Aiming to some extent alleviate that pitfall of the system, ATB-vv (Verbeterde Versie: improved version) has been introduced in some parts of the Dutch railway network. What is more, ATB-EG checks periodically the alertness of the driver by ringing a bell. The driver confirms his/her alertness by pressing the "dead man's" pedal. In case, he/she fails to do so, emergency braking is applied.

Figure 3.1 includes a representation of a train's speed profile that follows the maximum allowed speed as well as the supervised speed profile imposed by ATB-EG. On the X-axis, railway signals as well as speed signs along the route can be observed. The yellow boxes containing a number demonstrate the supervised speed by ATB-EG.

## 3.2. Dutch implementation of train positioning and driver support systems

This chapter presents information regarding the systems used in this study which are provided by ProRail and other organisations. First, the ProRail train positioning systems are elaborated. Next, a DIS developed by ProRail is presented and its deployment by the Dutch railways is demonstrated. Also, this chapter briefly discusses several sub-systems that are used by the the main ProRail systems. In case the source of information included in this chapter is not cited, knowledge has been collected from ProRail corporate documents.

### 3.2.1. TROTS & TPS

TROTS is the train describer system operating in the Netherlands (Kecman, 2014). TROTS consists of two modules. One module records messages originating from the infrastructure such as track occupation, signalling status as well as interlocking events such as switch position changes. As track is intended the TROTS *track-segment* which is the piece of track that is operated by a signaller. Then, another module couples track-segment occupation with train numbers. The traffic controller assigns train numbers manually. The coupling of train numbers with infrastructure is stored in train number

steps (TNS). Note that only events of controlled signals are recorded and thus, blocks of an automatic (also mentioned as *open*) track constitute a "dark" area for the system. Note that block sections that are located on an open track are aggregated on a single track-segment as defined in TROTS.

TPS (Trein Positie Service) provides real-time train position information of trains from the 13 local TROTS source systems operating in the Netherlands. ProRail subsystems do not have to retrieve train positioning information directly from TROTS, but can receive the same information via TPS. TPS periodically updates all train positions, enabling subsystems to quickly build up a complete and up-to-date picture of all train positions.

### 3.2.2. RouteLint

RouteLint is a DIS built and maintained by ProRail and it is currently deployed by NS passenger trains and DB-cargo freight trains. RouteLint displays the actual traffic status in the vicinity of a train. RouteLint became fully operational in 2016 after almost a decade of development. RouteLint aims for the decrease in the number of conflicts and the reduction of the time spent before red signals (Albrecht & van Luipen, 2006). Albrecht et al. (2007) mention that RouteLint is expected to increase punctuality and improve energy efficiency as well as riding comfort.

RouteLint displays information regarding train positions at track-segment level as well as train delays. Delay presented in RouteLint refers to the total delay of a train. RouteLint manages to improve the communication between train drivers and traffic controllers mainly to enable drivers to use their skills to the maximum for punctuality and energy efficiency. In other words, the information provided enhances the driver's situational awareness (Tschirner et al., 2013).

The following example tries to illustrate the sense in which RouteLint is used in practice. Assume that the train experiences zero delay while the predecessor train is considerably delayed and it is on the adjacent downstream track-segment. Hence, the two trains are closely following. As a consequence, the train is more likely to come across restrictive signal aspects. Based on this, the driver shall cut out traction early enough to avoid possible conflicts.

For NS trains, RouteLint is integrated with TIMTIM and driver interface is achieved through a tablet device. TIMTIM-RouteLint configuration is for simplicity, called TIMTIM on the remainder. TIMTIM data are transmitted onboard via a 4G mobile data connection that is facilitated by the tablet. Figure 3.2 includes an example of TIMTIM interface implemented by a tablet. The TIMTIM configuration displays information regarding:

- Start coasting advice
- Distance to next station
- Actual time
- Local speed limit
- Temporary speed restrictions
- Information provided by RouteLint:
  - Scheduled arrival and departure time
  - Delay of considered train and of trains in the vicinity
  - Track occupation status
  - Arrival platform at station

TIMTIM makes use of the train positioning data originating from the built-in GPS antenna of NS trains to determine a train's location referenced on the track. Given the location of the next stop, a simple train dynamics module calculates the distance to the next station. Based on the actual speed, the arrival time to that station can be estimated. Consulting on the arrival time estimation and the actual time, the available time slack can be computed. If there is sufficient slack time, the system advises the driver on when to start applying coasting. This start-coasting function is called Roltijd-app and constitutes a simple DAS system.

Figure 3.3 depicts an overview of RouteLint's architecture. Original data sources provide input to ProRail systems and these, through an interface layer (EMS) provide input to RouteLint. The data sources as well as the ProRail systems are briefly presented in the following lines.

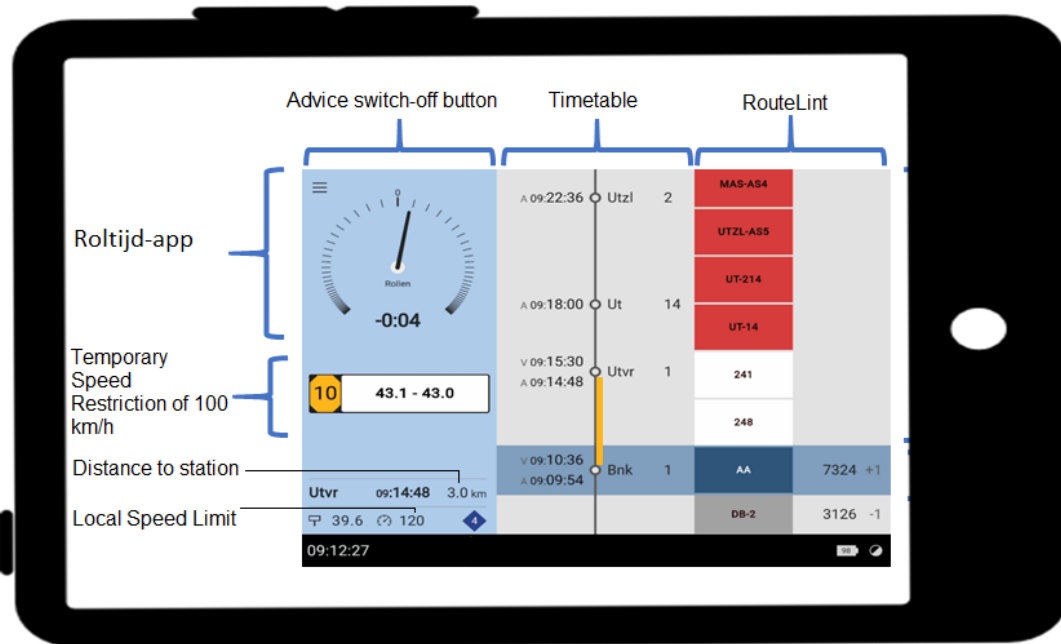


Figure 3.2: Example HMI of RouteLint integrated with TIMTIM

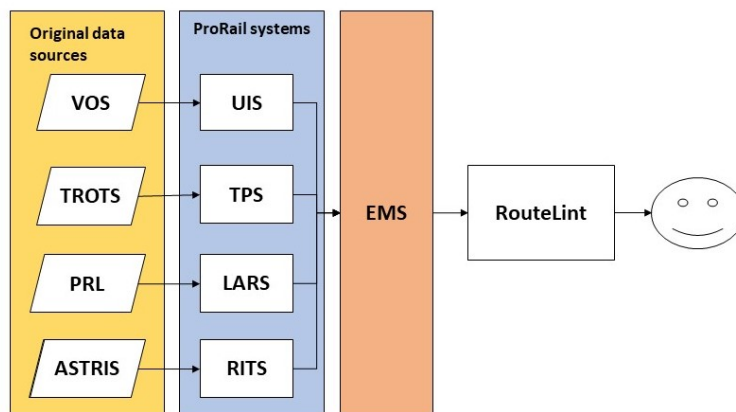


Figure 3.3: RouteLint system architecture

- VOS (*Verkeersleiding Ondersteunend Systeem*: Traffic Control Support System). The tool used by the dispatcher. The functions of VOS include: accept orders, check in freight trains, handle disruptions, monitor operations, reschedule train paths and maintenance slots as well as communication with other dispatching centres.
- TROTS: The Dutch train describer system that comprises the source of the train positioning data for RouteLint (see also Chapter 3.2.1).
- ASTRIS (*Aansturing en Statusmelding Rail Infra Structuur*: Control and Status Report Rail In-

frastructure Structure). The aim of the ASTRIS project is to develop and deliver a new, uniform train control system in the Netherlands. This system, in cooperation with ATP adapters, levels the differences of the various ATP systems used in the Netherlands. This allows all train traffic controllers to use one uniform process control system to perform route setting, regardless of the underlying ATP.

- PRL (*Procesleiding*: Process management). It is the Dutch implementation of a TMS supporting manual conflict detection and resolution. It is the tool used by signallers. PRL supports signallers in checking the plan, executing orders, handling disruptions, authorizing infrastructure, monitoring operations and communicating with other local traffic control centres. It contains the planned train and shunting activities with associated planned route settings.
- UIS (*Uitvoerings Informatie Server*: Implementation Information Service). UIS combines the train positioning data received from TROTS/TPS with other configuration data, compares it with the scheduled track occupation according to the timetable and translates this into the adjusted route plan (PLN) (including delays and train position information) for publication to customers.
- TPS: Train positioning service using TROTS data (see also Chapter 3.2.1)
- LARS (*Landelijke Actueel Plan Rijweg Server*: National Current Route Plan Service). LARS provides the real-time route plan from PRL into a format that is usable from other ProRail systems.
- RITS (*Rail Infra Toestand Service*: Rail infrastructure condition service). RITS aims to decouple PRL from the various subsystems providing rail infrastructure data. That is why it uses the novel data source ASTRIS. In case ASTRIS is not available, RITS uses PRL data.
- EMS (*Enterprise Message Service*). Constitutes the interface among ProRail systems shown on Figure 3.3 and between those systems and Routelint.

RouteLint displays information regarding the surrounding traffic status downstream of the train. The information regards the occupation of tracks or route setting for following trains. The granularity of the information is at track-segment level which is inherited from TPS (See also 3.2.1). Adjacent segments are separated by controlled signals. Automatic signals are not recorded. The information is updated each time a new event (e.g. delay, route setting etc.) is published (event-based update).

Figure 3.4 demonstrates an example of RouteLint's HMI display. The display comprises of three columns and can show up to ten rows. The left column displays the train number. For rows without a train number, the first train number shown on a row below the considered row is implied (e.g. the orange block with track name "LIS-302" corresponds to train "2226"). The middle column displays the labels of the track segments which comprise the train's planned route. In TROTS (and thus RouteLint), automatic tracks are distinguished from controlled tracks by the former being named with two letters (e.g. "LH" in Figure 3.4), while the latter are named with more than two characters (e.g. "ZSPL-LJ"). The right column shows the amount of delay for each train which is rounded to the whole minute with the positive sign indicating the train being behind the schedule.

Each row depicts a TNS (as expressed in TROTS). The colour of a TNS (middle column) reflects the segment's status. More specifically, the train in which the HMI is mounted on is depicted in a blue colour (train "6339", located in segment "ZSPL-LJ" and it is behind the schedule for one minute). Also, the HMI includes up to two successor trains which are depicted in black colour ("2139" and "2228"). The colours of TNS downstream the train stem from TNS-status. More information regarding TNS-status can be found in Appendix B. The colours can be decoded as follows:

- White: Track segment authorised for the under consideration train. Thus, the entry signal of the segment shows at least a yellow aspect.
- Grey: Applicable only for open track. The entry signal of that track does not show a red aspect for the considered train. Nevertheless, there is already, at least one more train on the same open track.
- Orange: Currently unoccupied track segment but already set for the train number shown on the left column, i.e. entry signal of the segment shows at least a yellow aspect. In other words, that train has triggered the Dutch automatic route setting system ARI (Automatische Rijweginstelling).

Treinnr	09:57:02	Vertraging
2137	LF	-1
726	LEDN-510B	+0
2226	LEDN-9A	+1
	LG	
	LIS-302	
2226	LH	+1
	LH	
6339	ZSPL-LJ	+1
2139	SJ	+1
2228	ASD-2A	

Figure 3.4: Example of RouteLint's driver interface

The trigger point of the ARI is located at an insulated joint and a dedicated mechanism performs automatic route setting for the downstream track of an open track. According to D'Ariano, Corman, and Pacciarelli (2014), ARI is capable of detecting and resolving small conflicts.

- Red: Currently occupied track, i.e. entry signal shows a red aspect.

Table 3.1 presents the quality of the data sources used in RouteLint as well as that of the information provided by it as reported by ProRail. All systems mentioned in this chapter are of SIL-0 (Safety Integrity Level) since they are intended for non safety-critical operations.

Table 3.1: RouteLint data performance

	Availability	Integrity
Original data sources	High	High
ProRail systems	High	Medium
RouteLint	High (99.98% per month )	-

### 3.2.3. MTPS

MTPS (Materieel Trein Positie Service) is an application that aims to provide real-time positioning information regarding trains and track equipment. This service is owned by ProRail. In general, MTPS uses TPS and GPS (Global Positioning System) which is the most widely used GNSS. TPS data are provided by ProRail, while GPS data are provided by railway undertakings. Under its current configuration, MTPS contains information only from NS (Nederlandse Spoorwegen) trains.

According to (Kecman, 2014), there are train-based (e.g. GPS) and track-based (e.g. train describer) train positioning systems. Given this, it can be argued that MTPS is a fusion of train- and track-based positioning systems. By combining these two data sources, MTPS achieves better coverage and positioning accuracy compared to the two data sources being used independently. This is achieved by combining the advantages of both; the global coverage (almost 100% availability) of TPS, and the increased accuracy of GPS (10 m for absolute positioning).

MTPS uses information from data sources each using a dedicated reference system. To that end, a module provides the necessary transformations in order to combine those data sources. The process followed by the MTPS module is comprised of two legs. First, TPS measurements are transformed into a geographical format so as to be comparable with GPS measurements. Then, TPS is enriched with GPS in case the adequate measurements are available.

At this point, the various reference systems of the ProRail subsystems used for positioning purposes are presented. First, TROTS data are expressed in the OKT reference system, a format that has been developed for train traffic control purposes. Second, GPS provides the world coordinates ( $\phi$ ,  $\lambda$ ) of a point at WGS '84 (World Geodetic System 1984) reference frame. Third, IA (Infra Atlas) is an information system that manages data regarding the railway network. IA contains information about the topology as well as the characteristics of track elements and it is the reference system used in technical drawings (OBE, Overzicht Baan en Emplacement-bladen: Track and Shunting Area Overview

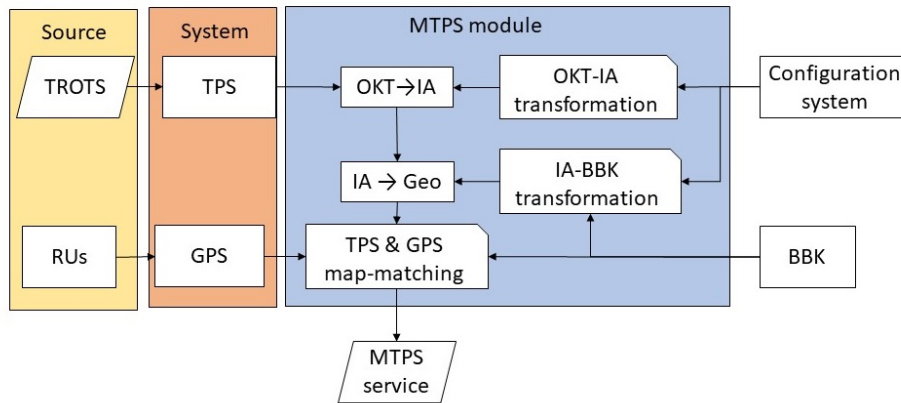


Figure 3.5: MTPS architecture, Adjusted from MTPS Software Requirements Specification, ProRail

Sheets). The reference system used by IA is based on route ribbons. Route ribbons (*km-linten* in Dutch) constitute the 1D reference system used by ProRail to identify locations along the track. Each position expressed in route ribbon has two components. First, it has a unique name usually indicating its end point stations (e.g. route ribbon "Asa-Zvg" stands for Amsterdam Amstel - Zevenaar grens). Second, it discloses distance along the ribbon which is measured from the ribbon's start with an accuracy of 1m. Finally, BBK (Basisbeheerkaart) is a topographic map of the track and its surroundings. The geographical information in BBK is expressed in both the Dutch geodetic reference system RD (Rijksdriehoeksstelsel), world coordinates as well as route ribbon coordinates.

Hereby are explained the processes taking place within the MTPS module. First, the MTPS module transforms a TPS measurement into a geographical point with the following procedure:  $OKT \rightarrow IA \rightarrow BBK \rightarrow Geographical\ point$ . Direct transformation from TPS to BBK and vice versa, is not feasible. Instead, two distinct transformation modules exist: OKT to IA and IA to BBK, both using configuration data. Therefore, IA provides a vital link between the fundamental data sources (Figure 3.5).

Next, TPS and GPS measurements are combined. Train movement is laterally constrained by the track. By default, TPS geo-position refers to the railway track since it is offered in the route-ribbon reference system. Yet, this is not the case for GPS points. Consequently, the coordinates must be transformed from 3D into 1D. This is realised by a map-matching technique with BBK constituting the reference surface. A GPS point is perpendicularly extrapolated to the nearest point of the last known track occupation entry. Note that the route the train has traversed is known in advance. The records from the two sources should be close time-wise otherwise extrapolation falls outside the predefined accuracy margins. MTPS supports output in three different reference systems, namely world coordinates (WGS 84), national grid projection coordinates (RD) as well as the name and the location on route ribbons.

MTPS publishes its information in two major services. *TpsMessageHandler* is considered as the default MTPS publishing service. This service provides the train head's location at the beginning of a track branch. Note that track branches are separated by insulated joints. This architecture makes possible to construct track circuits which are used for the vital function of track-clear detection. The procedure of adjusting a GPS measurement to match the location of an insulated joint is as follows. First, a GPS measurement is projected to the correct track. Then, the measurement is correlated to a specific track branch using BBK. Then position is moved towards the start of this track branch (offset to the insulated joint) and the timestamp is adjusted accordingly. The required speed knowledge to perform this adjustment is deduced from upstream GPS measurements. It is selected to present train's position as its passage through an insulated joint since this track element constitutes a reference point of the infrastructure. Train position is given in route-ribbon coordinates. Yet, *TpsMessageHandler* is not globally available. Possible information gaps of *TpsMessageHandler* can be filled with the *GpsGenericMessageHandler* service. This service performs all the functions of *TpsMessageHandler* except for transforming the coordinates from GPS into route-ribbon format. Therefore, the output of this service is a GPS position corrected for the track. Finally, this service provides the position for both the head (marked as 1) and the tail (marked as 2) of a train.

Table 3.2 quantifies the performance of the data sources used in MTPS. The horizontal accuracy of absolute GPS positioning ranges between 0 and 10 m, while GPS shows availability higher than 95 % with respect to time of use. TPS shows time deviations of the recorded events which range between 0 and 5 seconds for both systematic and random.

Table 3.2: Performance characteristics of MTPS subsystems

Component	Accuracy (m)	Availability	Time deviation (s)
GPS <sup>1</sup>	0-10	> 95 %	N/A
TPS	N/A	N/A	0-5 (systematic) & 0-5 (random)

<sup>1</sup> The standard positioning service, i.e. absolute positioning with single Frequency C/A-Code, source: European Space Agency (2015)

### 3.3. Blocking time theory

The calculation of blocking times is essential for any capacity assessment study for fixed-block signalling systems. Note that in fixed-block systems a block-section can be occupied by a train only. The blocking time represents the time reserved for a single train for a specific block.

The methodology for calculating blocking times was derived from Brünger and Dahlhaus (2014). An example of the blocking time components for the block between signals S2 and S3 is shown in Figure 3.6. S1 is considered as the distant signal for that block. Figure 3.6 considers a three-aspect two-block signalling system. Hence, a signal aspect discloses information regarding two downstream block-sections. In the example of Figure 3.6, the aspect of signal S1 contains information for both block S1-S2 and block S2-S3. Each blocking time component has duration  $dt$  and it refers to:

- Setup time  $dt_{setup}$ . It is the time to setup (clear) signal S2. It is a constant value and its value depends on the interlocking system.
- Sight and reaction time  $dt_{sight}$ . The time needed for the driver to react. The train must have reached at sight distance from signal S1. It is a constant value.
- Approach time  $dt_{approach}$ . It equals the travel time between signal S1 and S2.
- Running time  $dt_{run}$ . The actual running time between signals S2 and S3.
- Clearing time  $dt_{clear}$ . Depends on the train speed at the exit of the block.
- Release time  $dt_{release}$ . It is a constant value that depends on the interlocking system.

In order to calculate the time edges of a block, it is essential to determine the passage time  $t_{S_i}$  from every signal  $S_i$ . Once these times are known, block start and end times can be calculated for the example of Figure 3.6 using the following equations.

$$t_{block\ start} = t_{S2} - dt_{approach} - dt_{sight} - dt_{setup} \quad (3.1)$$

$$t_{block\ end} = t_{S3} + dt_{clear} + dt_{release} \quad (3.2)$$

where  $t_{block\ start}$  is the start time of the blocking time, while  $t_{block\ end}$  is the end time of it.

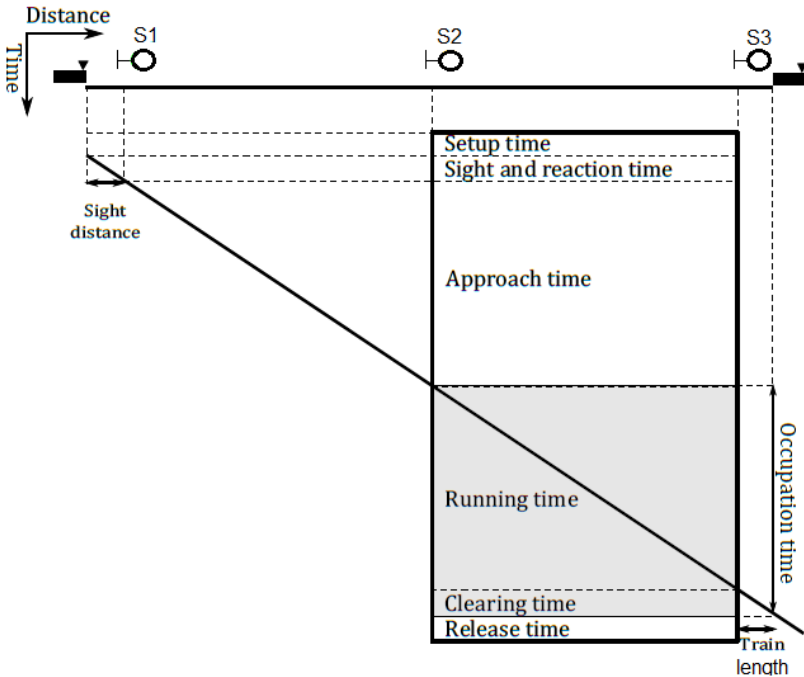


Figure 3.6: Break down of blocking time components for a three-aspect signalling, adapted from Kecman, 2014

# 4

## Model development

The chapter includes the development of the model that increases a DAS's awareness regarding the actual signal state on open tracks. The improvement of the signalling state awareness of the DAS is done by having the DAS provide driving advice based on more reliable positions of trains on the track, thereby increasing capacity. Better capacity usage could be obtained especially in those open track areas where the information on the actual track occupation and signal aspect of downstream block sections is limited or totally unknown. The section is structured as follows. First, the problem and the research objective of this study are defined. Then, the conceptual framework of the developed model is discussed. Also, the architecture of the considered conceptual DAS is presented which is integrated with the model developed in this thesis. Also, this chapter elaborates on the developed data-mining tool. This tool captures the potential of two positioning data sources to determine the red signal which is located downstream the train. The data sources contemplated in this study are TPS and MTPS. All the routines of the data-mining tool are thoroughly explained. Finally, a framework is proposed to assess the quality of the considered data sources with respect to their ability to improve the actual signal state awareness.

### 4.1. Problem description and research objective

This study addresses the problem of DAS advice leading to conflicts operating over the Dutch railway safety system. A reason to this is the fact that the DAS does not take or partially takes into account the actual traffic status when calculating the optimal speed profile. Several approaches to minimize the conflicts originating from DAS advice have been revealed from the literature review performed in this study. Such a solution is having C-DAS have access to the vital information from ETCS L2 to perform its non-vital function. Yet, this study aims to introduce the intended DAS on tracks equipped with a Class-B safety system. For this case, the number of conflicts caused by DAS's advice can be minimised, if the signalling information is directed to the on board equipment of a DAS in real-time. The speed limits originating from the signalling system will constrain the calculated speed profile and in turn, the advice will respect the signalling information. In short, the objective of this study is to improve the awareness of a DAS regarding the actual signal state by providing the onboard DAS equipment with the speed constraints stemming from it in real-time.

At this point, the method in which the actual signalling state information is directed to the onboard DAS equipment is defined. The novelty of the approach pertains to introducing a data channel which provides the speed profile calculation module of the DAS with the  $v_{max}$ , where the  $v_{max}$  is the maximum allowed speed for a given part of the track. The speed limit stemming from the signalling is embedded in  $v_{max}$ . The data flow proposed in this study is depicted in bold in Figure 4.1. By doing so, the on board DAS equipment becomes aware of the actual signal state. Note that  $v_{max}$  coincides with the speed limit considered by the driver and it is given by:

$$v_{max} = \min(v_{SSP}, v_{TSR}, v_{RS}, v_S) \quad (4.1)$$

where:

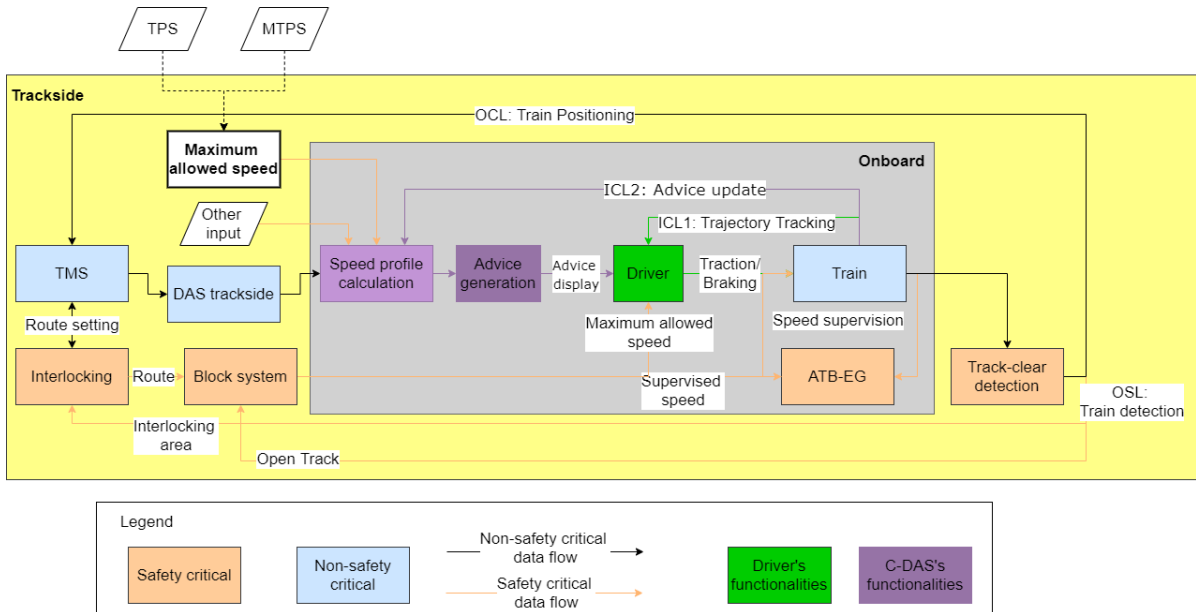


Figure 4.1: Generic train control architecture using a C-DAS-On board according to which the onboard DAS equipment receives—among other input—information regarding the maximum allowed speed of the track. The maximum allowed speed is determined using either TPS or MTPS data, adapted from Goverde and Theunissen, 2018

- $v_{SSP}$ : the speed limit imposed by the static speed profile (SSP)
- $v_{TSR}$ : the speed limit originating from temporary speed restrictions (TSR)
- $v_{RS}$ : the maximum speed of the rolling stock and,
- $v_S$ : the speed constraints imposed by the signalling system. Along the track, these constraints change dynamically and form the signal aspect speed profile (SASP).

Information regarding  $v_{SSP}$ ,  $v_{TSR}$ ,  $v_{RS}$  can be delivered by existing ProRail systems. Also, all the required functions/information to determine  $v_S$  can be delivered by existing ProRail and NS (TIMTIM) systems, except for a red signal determination module.

Therefore, the objective of this study can be scaled down in defining a red signal determination framework. Key element to the problem is the most relevant red signal which is the signal closer to the train which shows a red aspect. The red signal is used as a reference point to reproduce the SASP. It constitutes a reference point since the red aspect is the only aspect that is singularly correlated with a speed restriction (i.e. 0 km/h). In order to derive the most relevant red signal, the first downstream occupied block must be discovered. Therefore, the position of the predecessor train must be known at block level. If information regarding the first downstream occupied block is available, it can be deduced that its entry signal shows a red aspect.

To determine predecessor's actual position along the track, there is the need for a data source which can real-time deliver train positioning information. Such a data source is TROTS and more specifically, TPS; the publication service of TROTS. TPS defines train position at TPS track-segment level. Note that a TPS track-segment aggregates several blocks in case of open track, while it is one-to-one correlated with blocks in interlocking area (see also Section 3.2.1). In case the predecessor is located on an interlocking area, the block that it is located is shown as an occupied track-segment in TPS. As a general rule, the most relevant red signal can always be determined using TPS when predecessor is on a block-section of an interlocking area (mentioned in the remainder as *controlled track-segment*). Recall that RouteLint – which uses TPS data – is used in practice for inferring signalling as suggested by Albrecht and van Luipen (2006); Tschirner et al. (2013) (see also Section 3.2.2).

Still, TPS cannot deliver the red signal when predecessor is on open track. The events of automatic block sections are not recorded by TROTS since they are aggregated into a single TPS track-segment (see also Section 3.2.1). This thesis fuses TPS with MTPS in order to identify predecessor's position

at block level when it is on an open track and thus, infer the (automatic) signal showing a red aspect. TPS and MTPS serve as input for the  $v_{max}$  function as demonstrated in Figure 4.1.

To sum up, it can be argued that the main objective of constituting a DAS aware of the actual signal state can be scaled down to the goal of inferring the most relevant red signal in real-time. This goal can be reformulated as the goal of determining predecessor's position in real-time. If the predecessor's position is determined at block-section level, the red signal can be determined, too. Having that said, although the two goals are not in principal the same, they are used interchangeably in the upcoming analysis. The contribution of this study pertains to the novel method of determining the red signal when predecessor is located on an open track by fusing TPS with MTPS data.

## 4.2. Conceptual framework

The section discusses the conceptual framework of the proposed model. The section starts by presenting the modelling approach for obtaining signalling information in real-time. Following, it is explained how the proposed framework can be combined with existing ProRail systems and how does it fit into the general train control architecture under a C-DAS-On board operation. Furthermore, the necessary input to the maximum allowed speed data stream is defined.

### 4.2.1. Modelling approach for acquiring the actual signal state

This subsection illustrates the way in which  $v_S$  (see also Section 4.1) can be determined by reproducing the speed profile starting from the red signal up to the actual train position. The process is demonstrated employing the example of Figure 4.2.

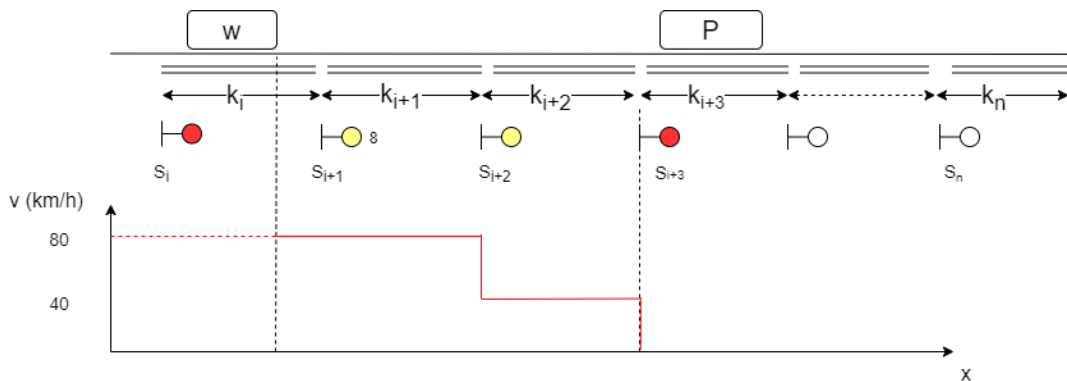


Figure 4.2: Example of the determination of the speed limit originating from the signalling using the method of reproducing the signal aspect speed profile starting from the red signal

The infrastructure elements included in Figure 4.2 are:

- $k_i$ : ID of block-section  $i$ , for  $1 \leq i \leq n$
- $S_i$ : ID of the entry signal of block section  $k_i$ , for  $1 \leq i \leq n$

Initially, RouteLint provides the actual route plan (PLN) for a train in real-time (see also Subsection 3.2.2). The planned route included in RouteLint is a list of track-segments. Using the *signal/block topology* file, each track-segment is translated into a single block-section or a list of block-sections (in case of open track)  $k_i$  ( $i=1, \dots, n$ ) of the planned route. The *signal/block topology* file both pairs a block-section to its entry signal and provides all the possible movements between adjacent signals (or blocks). Using this file, the list of block-sections  $k_i$  of the planned route is translated into a list of signals  $S_i$  ( $i=1, \dots, n$ ). Using the *signal location* file, each signal  $S_i$  is associated with its location along the route.

Now, suppose that train  $w$  is located at block  $k_i$  according to positioning information derived from TIMTIM (Figure 4.2). Also, assume that a data source informs that predecessor  $P$  is located at block-section  $k_{i+3}$ . Thus, it is signal  $S_{i+3}$  the one that shows a red aspect. Given this, the signal most relevant to  $w$  is  $S_{i+1}$ . So, the SASP will be reproduced until  $S_{i+1}$ . The *aspect correlation* file declares that when

$S_{i+3}$  shows a *red* aspect,  $S_{i+2}$  shows a *yellow* aspect. Likewise, when  $S_{i+2}$  shows a *yellow* aspect,  $S_{i+2}$  shows a *yellow-8* aspect. Therefore, the most applicable speed limit originating from the signalling equals 80 km/h. Table 4.1 summarizes the required input for determining the speed limit stemming from the signalling system.

Table 4.1: Necessary information to reproduce the signal aspect speed profile

Attribute	Source	Content	Time-dimension
Signal/block topology	Configuration file	Signal/block-IDs adjacent to each signal/block-ID	Static
Signal Location	"	Signal coordinates [in route-ribbon]	Static
Aspect correlation	"	Aspect correlation of adjacent signal-IDs	Static
Train position	TIMTIM	Train coordinates [in route-ribbon]	Dynamic
Planned route	RouteLint	Planned downstream track-segments	Dynamic
Red signal	This study	signal-ID	Dynamic

### 4.2.2. Train control architecture of a C-DAS-On board

It is important to discuss the train control architecture using the DAS considered in this study. To begin with, it is assumed that the proposed red signal determination framework addresses a Connected-DAS (C-DAS)-On board. It is assumed that this C-DAS-On board can be developed at a conceptual level using existing ProRail systems. The *C-DAS-On board* configuration allows for real-time data communication between the DAS onboard equipment and other systems. On the one hand, the DAS on board equipment receives the route plan from TMS via the trackside DAS equipment in real-time. On the remainder, this function is assumed to be available from existing ProRail systems and it is not further elaborated. On the other hand, the DAS on board equipment receives the maximum allowed speed ( $v_{max}$ ) in real-time. The remainder of this chapter focuses on the latter data stream. Note that a degraded – with respect to the update frequency of the route plan – mode of DAS can be used (e.g. N-DAS) without this affecting the applicability of the proposed framework.

Since a *C-DAS-On board* configuration is considered, the on board equipment of the DAS comprises of the following modules: optimal speed profile calculation, advice determination and advice display module. The speed profile calculation module calculates a new optimal speed profile based on the route plan and using the constraints imposed by the  $v_{max}$  data stream. Note that the suggested data stream is non-safety critical. Next, the optimal speed profile is directed to the advice generation module. Finally, a dedicated DAS module displays the advice via a HMI. The driver performs the driving tasks consulting the advice, always considering the  $v_{max}$  and in any case being responsible for the safety of the operations. Note that in some cases,  $v_{max}$  is different (lower) than the supervised speed by the ATB-onboard (see also Section 3.1). The considered C-DAS-On board architecture is shown in Figure 4.1. In the Figure, modules that perform a function are connected with arrows. Additionally, the content of each arrow is explained by its label.

In Figure 4.1, track side functions are included in the outer frame (in yellow colour), while onboard functions lay on the inner frame (in grey colour). Several feedback loops can be distinguished. The outer safety loop (OSL) constitutes a safety-critical information flow that serves for train detection. In case the train is located on an interlocking area, the information is directed to the interlocking system. In other case, this information is directed to the automatic route setting of the open track. Moreover, the outer control loop (OCL) is a non-safety critical data flow that serves for train positioning. TMS needs this train positioning information to monitor the traffic state and predict conflicts. Hence, this information flow facilitates the necessary onboard-to-trackside data channel of the conceptual DAS.

Additionally, the driver constantly monitors the speed of the train and adjusts traction or braking (inner control loop 1: *ICL1*). Finally, in case the driver does not cope with the advice, the realised operations will considerably deviate from the planned speed profile. A time threshold for this deviation can be set as suggested in Wang and Goverde (2017). In that case, a new optimized speed profile is calculated for based on the updated route plan and the advice generation module defines the new advice (inner control loop 2: *ICL2*).

### 4.2.3. Input to the speed profile calculation module of the DAS

This study considers the speed restrictions coming from the signalling system as an information source to the onboard equipment of the DAS. Also, since the conceptual DAS is a C-DAS, dynamic adjustments of the route plan constitute another data input. The updates occur at frequent time intervals, the magnitude of which lies outside the scope of this study. All the other input data considered in this study were discussed in Subsection 2.3.1. The remaining data sources regard the original timetable, technical characteristics of the rolling stock, infrastructure data, train positioning information as well as the static speed profile and temporary speed restrictions. The input sources considered in this study are included in Table 4.2. The novel information source is marked in bold in Table 4.2. In Figure 4.1, the maximum allowed speed input has a dedicated box, while all the other input sources are embedded in the *Other input* box. Note that both the aforementioned inputs are non-safety critical.

Table 4.2: Input for the speed profile calculation module of the DAS

Input category	Attribute	Time character	Source
Timetable	Original timetable	Static	TIMTIM
	Route plan adjustments	Dynamic	TMS
Rolling stock	Acceleration /braking capacity, length, mass	Static	Driver
Infrastructure	Curve radii, slope	Static	ProRail service
Position	Train positioning	Dynamic	TIMTIM
	SSP	Static	TIMTIM
Max allowed speed	TSR	Dynamic	TIMTIM
	<b>Signalling</b>	Dynamic	TPS+MTPS

At this point, the source of each data input is discussed. The study assumes the TIMTIM-RouteLint configuration deployed by NS trains (see also Section 3.2.2). Through TIMTIM, the following are available onboard: SSP, TSR, original schedule and actual train position. Also, it is assumed that the driver manually sets the rolling stock's characteristics. Additionally, the transient timetable adjustments are provided by the TMS-DAS. It is assumed that a ProRail service can send a database containing the infrastructure characteristics to the on board equipment of the DAS.

## 4.3. A data mining tool to improve red signal state awareness of DAS

The proposed module of providing the on board equipment of a DAS with the red signal in real-time is tested against real-world data. Two train positioning systems, TPS and MTPS, are used for that purpose. The potential of the two data sources to deliver the red signal is examined. In case TPS data fail to yield a result, the tool investigates the ability of TPS + MTPS data to derive the desirable outcome. The historical data are analysed using a data-driven approach. A dedicated data-mining tool has been developed to that end. This chapter is structured as follows: the data format which the data-mining tool is based on is discussed and then, the three routines that build up the tool are presented. The routines are: data preparation, red signal determination and blocking time diagram routine. All routines were developed in the Python programming language.

### 4.3.1. Data format

The data-mining tool is structured in such a way that follows the format of RouteLint log files. Thus, this study follows a data-driven approach. The tool uses historical TPS and MTPS data. This study

assumes that TPS and MTPS are available in real-time with the same format. Then, it is assumed that a real-time version of the historical data contemplated in this study achieve the same potential as the historical data on delivering the red signal. Thereupon, the red signal determination routine can be used with real-time data.

RouteLint data is stored in comma-separated log files where each file includes the records of all trains that have operated on the Dutch network on a specific day. Each RouteLint record corresponds to a line of the log file. The generalised format of a RouteLint record is included in Table 4.3. Each RouteLint record has a unique timestamp (field No. 1). Fields 2, 4-9 contain information regarding the train this RouteLint record refers to. The train is located at a track-segment the start (field 6,7) and end (field 8,9) of which are described in route-ribbon coordinates.

Table 4.3: RouteLint log file format

No. field	Field content	Format
1	Timestamp	YYYY-MM-DD-HH:MM:SS.SSS Prefix (1- 2digits): Train series, Suffix (2 digits):Train number from the start of the day
2	Train number	
3	Time	HH:MM:SS.SSS
4	Delay	+/- min
5	Track segment	String
6	Start route-ribbon	String
7	Start route-ribbon's location	Integer expressed in metres
8	End route-ribbon	same as 6
9	End route-ribbon's location	same as 7
10	TNS- <sup>1</sup> <i>i</i> -status	String
11	TNS- <i>i</i> -track	same as 5
12	TNS- <i>i</i> -route-ribbon	same as 6
13	TNS- <i>i</i> -route-ribbon-location	same as 7
14	TNS- <i>i</i> -train-number	same as 2
15	TNS- <i>i</i> -delay	same as 4

<sup>1</sup> ranging from 0 to 6

Fields starting with the label *TNS* display information regarding the traffic downstream of a train (see also Chapter 3.2.1). For each TNS, five fields are mentioned. In Table 4.3, fields 10-15 refer to a group of TNS for track segment *i*. Information regarding the occupation of the track-segment *TNS-*i*-track* and by which train is captured in fields *TNS-*i*-status* *TNS-*i*-train number*, respectively. The combination of these three fields encloses the train positioning information and it is fundamental for this study. Track status is explained in detail in Appendix B. Up to 7 TNS can be included in a timestamp, i.e. 7 groups of *TNS-*i*-field*. Therefore, a RouteLint record can have at minimum 15 fields (in case only the first TNS is available), while it can have up to 45 fields (in case all 7 TNS are available). More information regarding the format of RouteLint log files can be found in Appendix B. Timestamps are not updated at regular intervals. Instead, timestamps are linked to events. As TPS events (followed by a change in the RouteLint HMI display) are considered the following:

- Train merging/dispersing from the route planned for the train that is being examined.
- Update on delay of the displayed trains
- Change in track status. This signifies a train movement.

The tool reads line by line the whole subset of a RouteLint log file for a train and thus, comes across all these events. Yet, events of the latter type only can potentially affect the tool's result since it is the only event among the three related to train positioning. The fact that the tool reads records that do not contribute to its goal, suggests that the time efficiency of the tool can be increased if these events are omitted from the process.

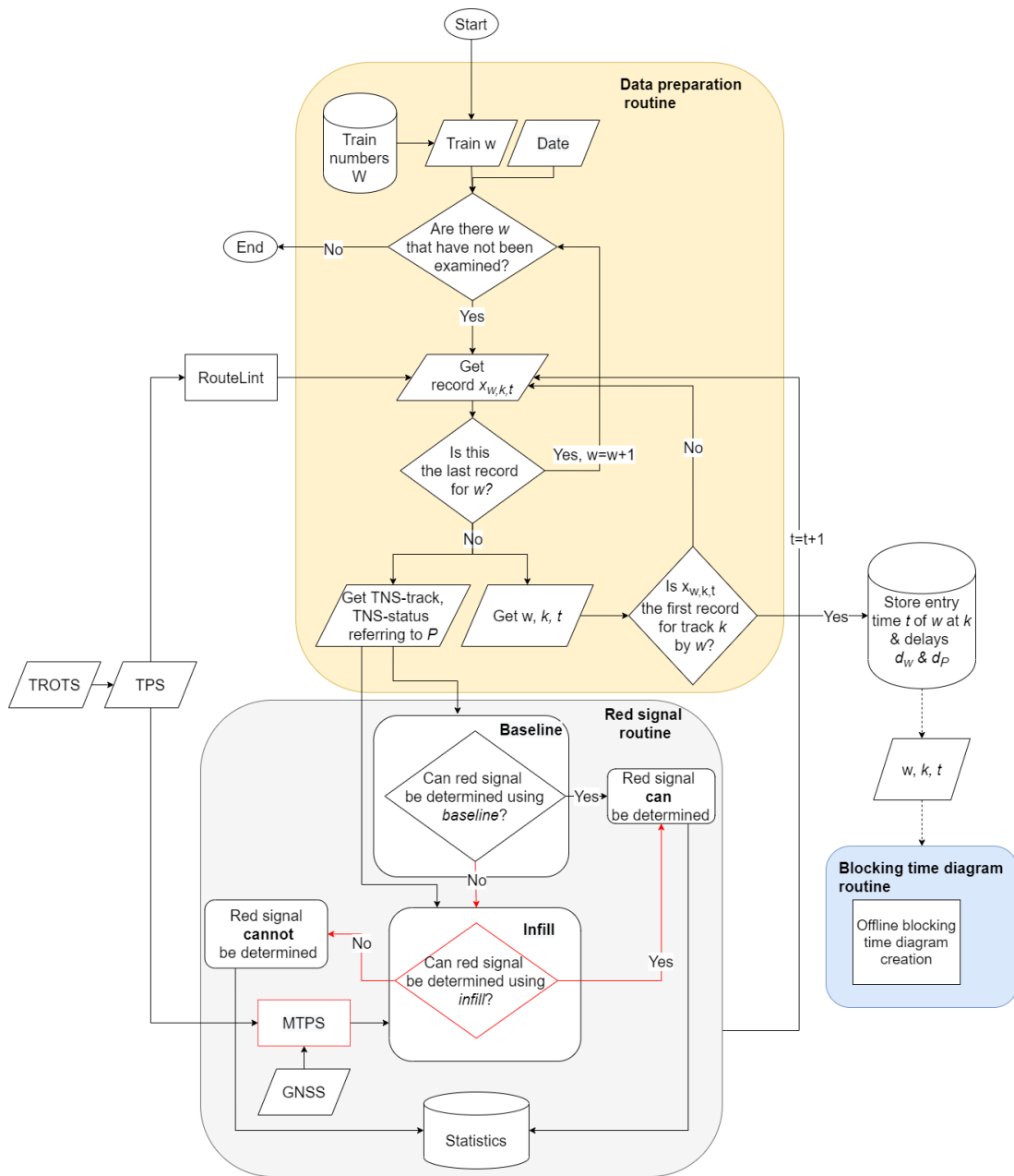


Figure 4.3: Data-mining tool architecture to investigate the potential of baseline and infill data to determine the most relevant red signal

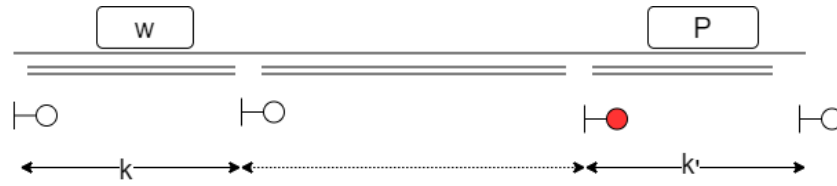


Figure 4.4: Schematic representation of elements/parameters included in the analysis of a RouteLint record

### 4.3.2. Data preparation routine

First, the data-preparation routine is triggered. The routine is run online for a pool of train runs. The process starts by having the user introduce a desired date as well as provide a list of train numbers  $W$  (Figure 4.3). The tool searches in a repository for the RouteLint file referring to that day. The analysis is performed for each train  $w$  out of the set  $W$ . All records referring to train number  $w$  are collected by setting a query on the file. The records of a RouteLint log file are sorted in chronological order and thus, the query returns a subset of records of that train in chronological order. Each line of the log file corresponds to a unique RouteLint (TPS) record  $x_{w,k,t}$ , where  $k$  refers to the track-segment-ID in which train  $w$  is located and  $t$  is the timestamp. The following information disclosed in the  $x_{w,k,t}$  record is necessary for the data-mining tool:

- Information referring to train  $w$ : train number  $w$ , TPS track-segment  $k$  and time  $t$  of entrance of  $w$  at track  $k$ ,
- $d_w$ : delay of train  $w$ ,
- $d_P$ : delay of train  $P$ ,
- TNS fields that refer to train  $w$ ,
- TNS fields that refer to predecessor train  $P$

The previously mentioned delays regard the aggregate published delay of a train. This delay cannot be distinguished into primary or secondary delay. Also, only the TNS fields necessary for train positioning (i.e. NS-track and TNS-status) are used (see also 3.2.1). Train number  $P$  is identified by being the first number assigned to a downstream TNS that is different from train number  $w$ .

If the record  $x_{w,k,t}$  is the first of train  $w$  for track-segment  $k$ , the  $w$ ,  $k$  and  $t$  information of the record is stored on a database. The blocking time diagram routine receives information from this database. The TNS fields that refer to both train  $w$  and predecessor  $P$  are forwarded to the red signal routine.

The process is repeated until the last timestamp for train  $w$  is reached, i.e.  $x_{w,k,t}$  is the last record for the route of train  $w$ . Once the whole train route has been analysed, the process is repeated for a new train number. Finally, once all train numbers have been analysed, the data-mining tool stops running. A schematic representation of parameters  $w$ ,  $P$ ,  $k$  as included in a  $x_{w,k,t}$  record can be found in Figure 4.4. Appendix A includes an example of the records of the data-mining tool.

### 4.3.3. Red signal routine using baseline data

The red signal routine is the core routine of the data-mining tool. This routine is comprised of two sub-routines each one analysing a data source. One sub-routine analyses solely TPS data, while another routine analyses the fusion of TPS with MTPS data. This routine is triggered after the data preparation routine. Same as the data preparation routine, it is performed online for the same pool of trains. The red signal routine receives input from the data preparation routine which includes TNS-status and TNS-track referring to the train  $w$  and predecessor  $P$ .

The basic idea of the red signal determination routine is the following: the red signal can be concluded if the predecessor's location can be determined at block level. It is important to note that the tool only investigates the potential of a data source to yield the red signal for a specific  $x_{w,k,t}$  record. In practice, the tool results only the basis of this concept, i.e. whether the predecessor's position can be determined. No routine has been developed that defines the actual *signal-ID* of the most relevant signal that shows a red aspect. Given this, the output of the routine is a binary parameter indicating whether the red signal can or cannot be determined for a  $x_{w,k,t}$  record depending on whether the predecessor's

position can be determined at block level. The binary output of the red signal routine is depicted in the two round-edge boxes of Figure 4.3. The output is stored in the database icon of Figure 4.3 which is used to perform the statistical assessment in Chapter 5.

As *baseline* is considered the approach using TPS data for the determination of the red signal. Input to this sub-routine are the TNSs of the record  $x_{w,k,t}$  concerning the predecessor train  $P$ . The procedure explained in the following lines uses domain-based knowledge since it is based on the logic according to which professional train drivers use the RouteLint HMI to infer signalling. In Figure 4.3, the sub-routine analysing *baseline* data is included in the diamond (decision point) drawn in black line.

Figure 4.5 describes in detail the procedure followed for determining the red signal using *baseline*. All blocks on the uncoloured background of Figure 4.5 regard the *baseline*. Note that all blocks of Figure 4.5 contemplate TNS between train and predecessor. Initially, TNS data that refer to train  $w$  are examined. Train  $w$  may be authorised to more than one downstream track-segments for a RouteLint record  $x_{w,k,t}$ . In case of several adjacent authorised track-segments for train  $w$ , only the further downstream track (called *last authorised track-segment* in Figure 4.5) is examined since the red signal is most likely to be placed downstream of that track. Moreover, *TNS-status* is the field which discloses information regarding a train's authorisation to move into a track-segment. TNS-status is explained in detail in Appendix B. This study assumes that when predecessor is *authorised* for a track-segment, the entry signal of the track-segment shows at least a yellow aspect. The term *at least* is used to point out that this aspect is the most restrictive the train can face. In contrast, an unauthorised track-segment means that the entry signal of corresponding segment shows a red aspect.

In case there are no authorised track-segments for train  $w$ , it is moving towards a red signal i.e., the red signal can be determined. Progressively, in the event of authorised track-segments, it must be examined whether the last authorised TNS-track refers to an open track. If this is not the case (i.e. TNS-track refers to a block-section which is guarded by an controlled signal) the exit signal of the last authorised track-segment shows a red aspect. Now, in case the last authorised track-segment is an open track, further analysis is necessary.

In detail, in case the last authorised track-segment (open track) is followed by an unauthorized one (irrespective of the type of track), the exit signal of the last authorised track-segment shows a red aspect (Figure 4.6a). The opposite regards the train being authorised on the same open track as the predecessor. Since the status of signals within the open track cannot be recorded, predecessor's position must be inferred by the signalling logic. There are some cases that stem from the signalling logic. One such case examines the case of the ARI being triggered. Recall that ARI is the automatic route setting and it indicates the TPS track-segments that have been set for a train. ARI can be captured by TPS in the TPS-status of a record (see also Section 3.2.2).

Now, given that train  $w$  is authorised to the same open track as predecessor  $P$  and the ARI has been triggered, the train that triggered the ARI must be found. If it is the predecessor train  $P$  the one that triggered the ARI, this means that  $P$  has been authorized to the downstream track-segment from the open track it is currently in. Thus, the predecessor has passed the last automatic signal of the last authorised open track for train  $w$  and thus, the last block of the open track is occupied by the predecessor. Consequently, this block's entry signal shows a red aspect (Figure 4.6b). In case it is not the predecessor the train that triggered the ARI, this means that it is not authorised to a downstream track-segment (Figure 4.6c). Thereupon, the red signal cannot be determined using the *baseline* data. Moreover, the red signal is not available in case the ARI has not yet been triggered while the examined train is authorised to the same open track as predecessor (Figure 4.6d). The two latter cases are directed to the *infill* routine. *Infill* routine is further discussed in the following section. For all other scenarios that have not been discussed previously, the red signal can be determined using *baseline* data. To sum up, *baseline* can determine the red signal position when predecessor is on an interlocking area or when it is about to move from an open track to a downstream TPS track-segment. It makes no difference whether the downstream track-segment is an open track or an interlocking area since both are recorded by TPS.

Figure 4.7 demonstrates two cases in which it is or it is not feasible to determine the red signal using *baseline* data. In the top sub graph of Figure 4.7, train 520 is located at the open track MA. Predecessor 1820 is located on the downstream from MA open track FA. For train 520, FA is depicted in red, i.e. the entry signal of FA shows a red aspect. Yet, for the bottom sub graph of Figure 4.7, the ARI has been triggered by train 3824 which merges into the route already planned for 520. Thus, the most relevant red signal cannot be determined.

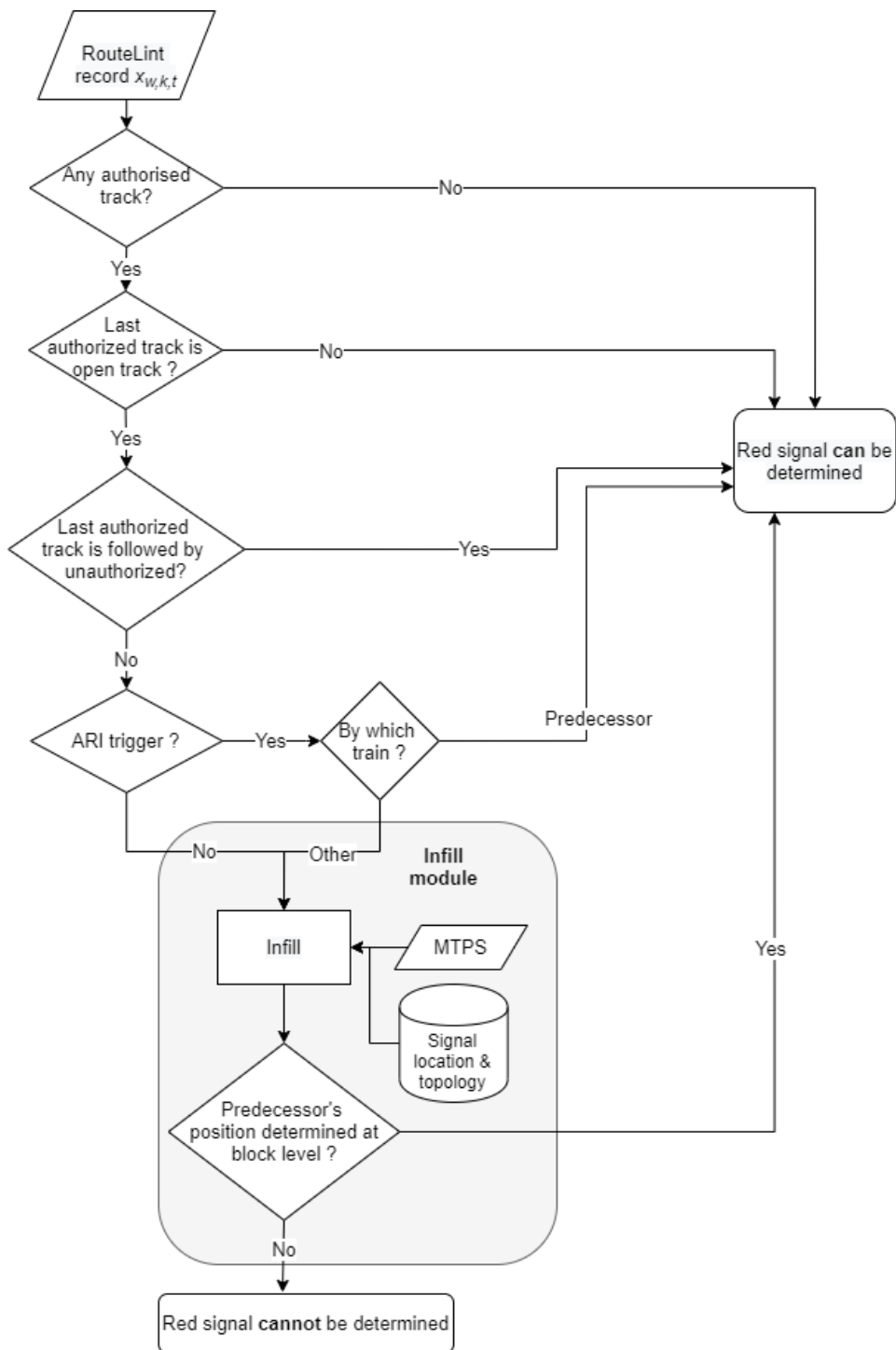


Figure 4.5: Detailed description of the routines used to yield the most relevant red signal

Treinnr	08:57:15	Vertraging
2133	LEDN-510B	+1
99971	LEDN-9A	+4
	LG	
	LIS-302	
99971	LH	+4
2222	LH	+5
	LJ	
6335	ZSPL-122	+2
4818	HLM-126	+0
3435	BO	+0

(a)  
Last authorised track is controlled track—Red signal available

Treinnr	10:06:33	Vertraging
4622	LF	+0
726	LF	-1
726	LEDN-510B	-1
2226	LEDN-9A	+1
2226	LG	+1
	LG	
	LIS-302	
6339	LH	+1
2139	HLM-6B	+0
2228	ASD-21	+2

(b)  
Train authorised to the same open track as predecessor & ARI triggered by predecessor—Red signal available

Treinnr	07:03:29	Vertraging
	ZLRA-301	
5615	101A	+3
14620	ZL-5	
	ZLGEA-201	
3824	BA	+0
1820	FA	+1
	FA	
520	MA	+2
8122	HGV-2	+0
622	HR-3	+1

(c)  
No authorised track—Red signal available

Treinnr	10:06:23	Vertraging
4622	LF	+0
726	LF	-1
726	LEDN-510B	-1
2226	LEDN-9A	+1
2226	LG	+1
	LG	
	LIS-302	
6339	LH	+1
2139	HLM-6B	+0
2228	ASD-2AW	

(d)  
Train authorised to the same open track as predecessor and ARI not triggered—Red signal unavailable

Figure 4.6: RouteLint HMI examples

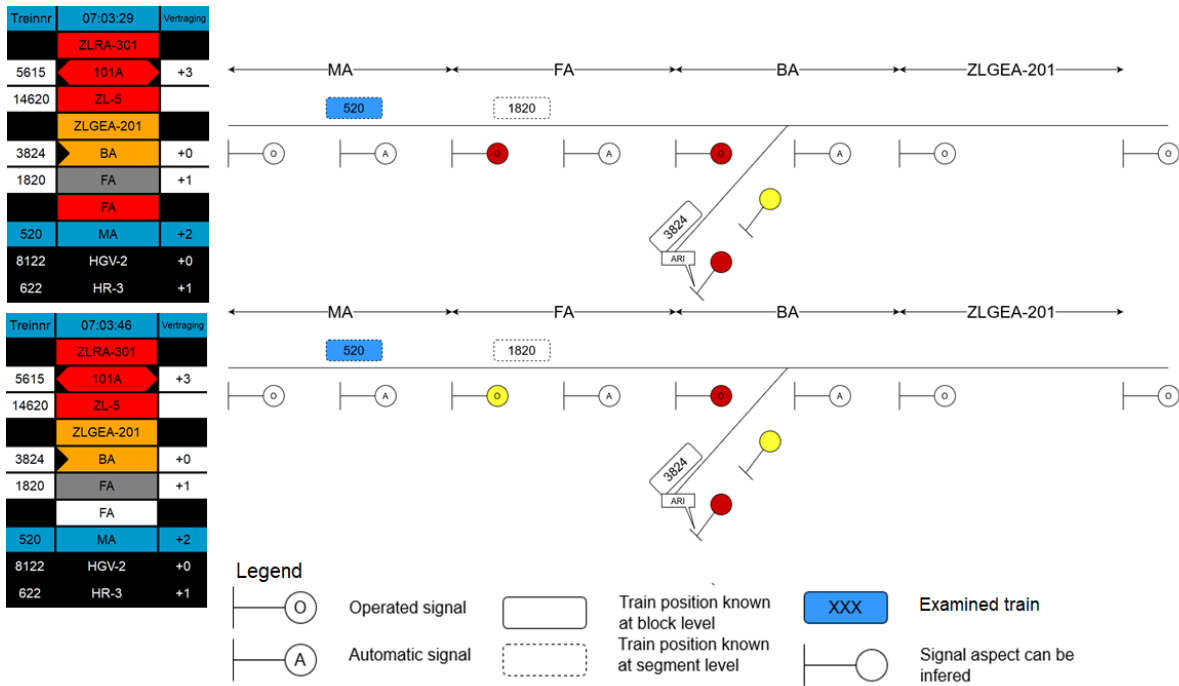


Figure 4.7: Most relevant red signal determination using the baseline data source. Correlation of RouteLint display with the actual signal state using a schematic representation of the track layout. Top: the most relevant red signal can be determined, while Bottom: it cannot

### 4.3.4. Red signal routine using infill data

As *infill* is intended the approach of using MTPS in conjunction with TPS data to yield predecessor’s position in real-time. *Infill* data (TPS + MTPS) is used to assist the *baseline* in cases when the latter is unable to determine red signal’s location. These cases are mostly observed when predecessor is located within an open track. These cases were discussed in detail in Subsection 4.3.3 (see also Figure 4.5). The GPS component of MTPS makes it feasible to locate the predecessor train within the open track. The way the *infill* data source is used is the main contribution of this thesis and is depicted in red lines in Figure 4.3 and it is supplementary to the *baseline* for deriving the red signal as it can be seen in Figure 4.3 and 4.5. The tool allows for switching-on/off the *infill* module. When this option is switched off, the output comes solely from *baseline*, while in case the option is on, the output comes from *infill*.

MTPS data is collected in log files which are stored in folders. Each MTPS folder contains the log files of a specific day arranged in chronological order. On average, a folder contains 1300 log files and has a size of 13 GB. Each file contains MTPS records of a time period around one minute. Predecessor’s position is searched in the MTPS log files of a day based on train name and timestamp.

Additionally, the *infill* approach requires a configuration file containing signal topology along with their location on route ribbons (See also Figure 4.5). Train’s position is determined between the closest to it, with respect to timestamp, available MTPS records. Finally, MTPS provides its output at block level which is the necessary level of detail in order to infer signalling at “dark areas” such as the open track.

Figure 4.8 explains the methodology followed for acquiring train’s position from MTPS. This methodology is the process included in the decision point at the grey font of Figure 4.5. In the example of Figure 4.8, the considered level of detail of the railway track is at block level.

The position-related elements included in Figure 4.8 are:

- $x_i$ : location of signal  $i$  for  $1 \leq i < n$ ;
- $y_j$ : predecessor’s position for MTPS record  $j$  for  $1 \leq j < m$

Table 4.4: Format of MTPS record published by the *TpsMessageHandler* service

Attribute	Format
Timestamp	Date, Time
Train number	String
Position	Route-ribbon Name and Location

where  $n$  is the total number of signals along the route, and  $m$  total number of MTPS records for predecessor train for a specific day. Positions and locations along the track are expressed in route-ribbon coordinates. The term *position* is selected for a train to illustrate its dynamic character, while the term *location* is used for signals since it is static. Parameter  $x_i$  is collected from signal topology and location files while  $y_i$  is retrieved from MTPS log files.

The search for MTPS records is time-based. The time character of the routine is given in the form of timestamps  $t$  (time axis in Figure 4.8). These represent:

- $t_{MTPS,j}$  is the timestamp of the MTPS measurement  $j$ . Marked as black dots in Figure 4.8
- $t_{R,k}$  is the timestamp of the RouteLint measurement  $k$ . Marked as coloured dots in Figure 4.8

Suppose that predecessor's position is searched for timestamp  $t_{R,k}$  (depicted with a blue dot in Figure 4.8). A search is initiated within the MTPS folder of that specific day in order to yield the closest record earlier ( $t_{MTPS,j}$ ) as well as the record later ( $t_{MTPS,j+1}$ ) than  $t_{R,k}$ . The search will end by the time the tool has encountered both  $t_{MTPS,j}$  and  $t_{MTPS,j+1}$ . Note that  $MTPS,j$  and  $MTPS,j+1$  are consecutive measurements. Therefore the *infill* routine traverses through MTPS files to find records  $MTPS,j$  and  $MTPS,j+1$  such that:

$$t_{MTPS,j} \leq t_{R,k} \leq t_{MTPS,j+1} \ \& \ (x_i \leq y_j \leq x_{i+1} \ \& \ x_i \leq y_{j+1} \leq x_{i+1}) \quad (4.2)$$

If these records are not found, an error message is stored. For the depicted case,  $t_{R,k}$  lays between  $t_{MTPS,j}$  and  $t_{MTPS,j+1}$ . As illustrated in Figure 4.8, MTPS measurements are located on the same block section ( $y_1, y_2$  are within the block section that starts at location  $x_1$  and ends at  $x_2$ ). Given that two consecutive MTPS measurements for predecessor train are on the same block and since the timestamp that is being searched is within these positions, it can be concluded that signal at location  $x_i$  shows a red aspect. Appendix A contains two numerical examples; one for a case in which *infill* data is able to determine predecessor's position at block level and for another case for which it is not able to do so.

At this point, the search technique within MTPS files to minimize the search time is discussed. To start with, the *infill* sub-routine searches in the MTPS log files for a certain date of records referring to the predecessor, i.e. for a certain *train-ID*. Each line includes a MTPS record. This study uses only the *TpsMessageHandler* publishing service of MTPS (see also Section 3.2.3). This is achieved by searching for a specific format of lines. The fact that the developed *infill* routine limits its search space into only the basic publishing MTPS service suggests that not all available positioning records for that *train-ID* are taken into consideration in the consecutive steps.

Given that predecessor's position must be found for  $t_{R,k}$ , the data-mining tool must find  $MTPS,j$  and  $MTPS,j+1$  records based on their timestamps  $t_{MTPS,j}$  and  $t_{MTPS,j+1}$ , respectively. Each timestamp  $t_{R,k}$  has the format *hh:mm:ss.ssss*. Aiming to limit the search space and thus, speed up the process, a technique was developed that examines log files whose information is close (time-wise) to the *hh* of the timestamp. The technique is shown in Figure 4.9. In case, the minutes (mm) of the timestamp are earlier than the first minutes of the hour (05), it might be the case that ( $t_{MTPS1}$ ) is in the files of the previous hour of *hh*. For that reason, all files that have a timestamp starting with both *hh-1* and *hh* are considered. Likewise, in case the timestamp's *mm* is higher than 55', it might be the case that ( $t_{MTPS2}$ ) is in the files of the next hour of *hh*. Therefore, the search is limited to the files that have timestamp *hh* and *hh+1*. In the opposite case, only files referring to *hh* are considered. The search technique results in a subset of files of all MTPS log files of a specific day. The process shown in Figure 4.9 is embedded in the white box at the grey font of Figure 4.5.

The process explained earlier is based on some assumptions. First, the TPS time inaccuracy is not taken into consideration (See also 3.2.3). Second, TPS's time is assumed perfectly coordinated with that of MTPS so as to make the comparison plausible.

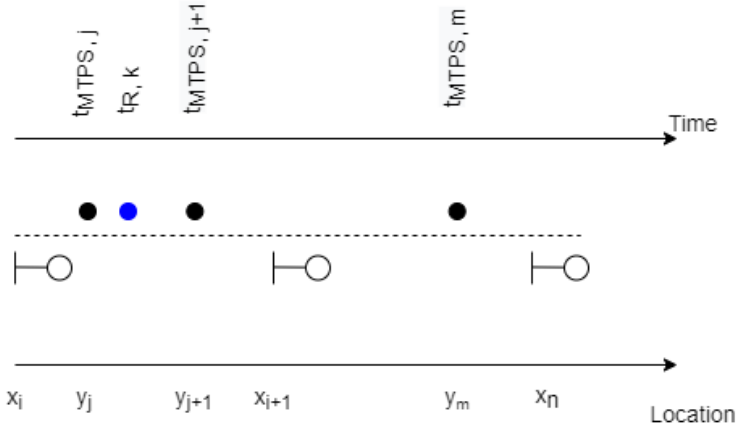


Figure 4.8: Method for determining predecessor position from MTPS data

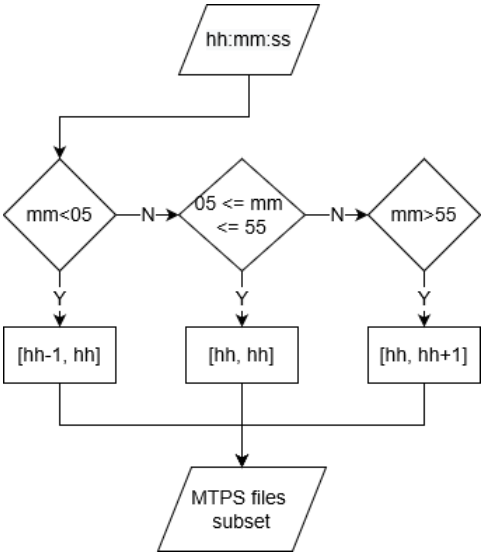


Figure 4.9: Search technique to limit the search space within MTPS log files. The search is based on the MTPS timestamps

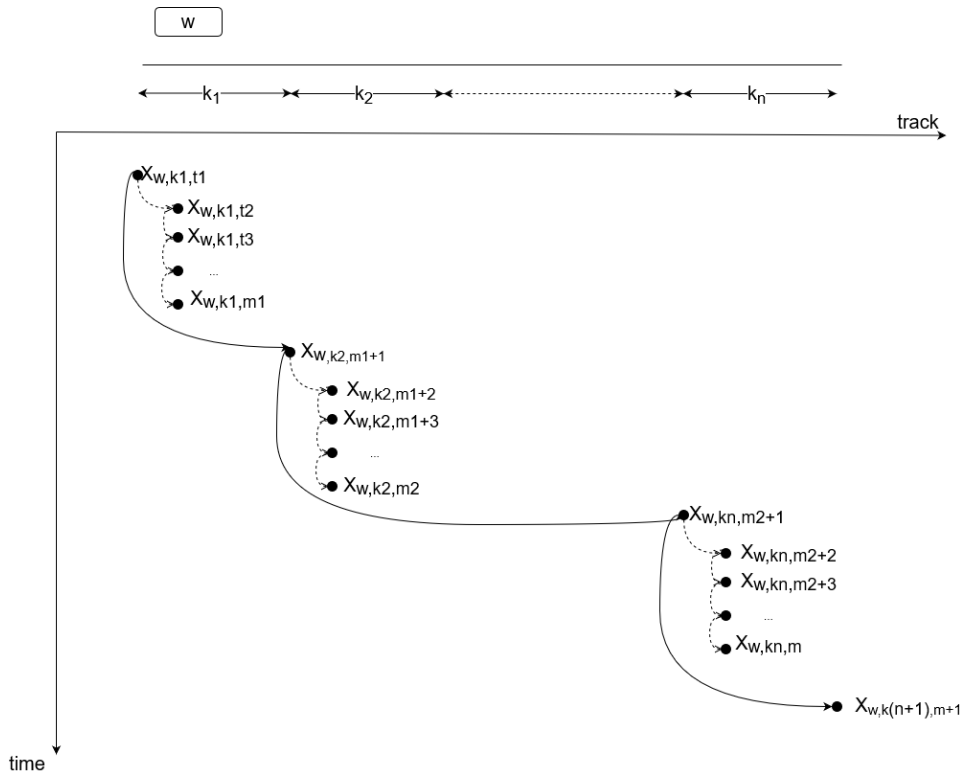


Figure 4.10: Schematic representation of the RouteLint-record reading method by the data mining tool

### 4.3.5. Blocking time diagram routine

The blocking time diagram routine constitutes an offline routine of the data-mining tool. In other words, it is not run for all the train numbers as applies to the data preparation and red signal routine. Instead, the user is able to select specific train runs for which the blocking time diagram will be calculated. The routine receives input from the database regarding train number  $w$ , TPS track-segment  $k$  and time  $t$  of entrance of  $w$  at track  $k$ . After the blocking time diagram is constructed, the timetable pattern is compressed to be latter used for the calculation of the infrastructure occupation. In this study the compression is done manually. Within the blocking time diagram routine, the departure times of all train numbers within a cycle period and the first of the next cycle period are altered until critical blocks come close together but not to overlap. This suggests a trial-and-error procedure which is done visually using the plot created by the *matplotlib* library of Python.

Figure 4.10 explains graphically the time dimension of the procedure with which RouteLint records are read and it proposes a way of how the records can be used to reproduce the blocking time diagram of the train. The blocking time diagram is useful for infrastructure occupation analysis. Consider a train  $w$ . Record  $x_{w,k_1,t_1}$  refers to the train being at track  $k_1$ . The timestamp  $t_1$  is considered as the entry time at track  $k_1$ . Afterwards, this record is directed to the *baseline* routine. Succeeding records referring to the same track  $k_1$  are directed to the *baseline* routine. Timestamp  $t_1$  is the first for track  $k_1$ ,  $m_1$  is the last timestamp for that track, while timestamp  $m_1+1$  is the timestamp of the exit from track  $k_1$  and entrance at  $k_2$ . Likewise,  $x_{w,k_{n+1},m+1}$  is the last record for train  $w$  and  $t=m+1$  the exit time of track  $k_n$ . It is feasible to collect entry and exit time of trains from block track-segments so to reproduce the realised infrastructure occupation diagram of each train. In Figure 4.10, records (the time and track of) which are both stored for the time-distance diagram and used for red signal's determination are connected with continuous lines, while the dots that are used only for the latter purpose are connected with dashed lines.

The algorithm yields the realised blocking time at a micro level (i.e. includes automatic blocks). Train behaviour within an open track cannot be known with the possessed TPS data. For that reason, the speed at which a train traverses through automatic blocks is set equal to the average speed of the

TPS track-segment as revealed from the historical data. The average speed is calculated as follows:

$$\bar{v}_{\text{track-segment}} = \frac{x_{\text{end}} - x_{\text{start}}}{t_{\text{end}} - t_{\text{start}}} \quad (4.3)$$

where  $t_{\text{start}}$  is the observed entrance time of the train to the track-segment,  $t_{\text{end}}$  is the observed exit time of the train from the track-segment (coincides with the entrance time to the downstream track-segment),  $x_{\text{start}}$  and  $x_{\text{end}}$  are the the start and end location (expressed in route-ribbon coordinates), respectively of the-segment.

The assumption of assigning the realised average speed of a TPS track-segment depicting an open track to the blocks of that open track has certain limitations. For example, it would be that the train came to a standstill before a red signal due to a conflict. Consequently, this would extend the blocking time of the corresponding block. Then, it could turn out that the infrastructure occupation would change significantly because at the timetable compression step, other blocks would turn critical.

The blocking time requires time and distance input as well as some constant values. Distance information is collected by combining signal location and topology information from ProRail configuration files. Now, the time input regards the calculation of blocking times. Entrance times at controlled block-sections are already available by the data base of the block-diagram routine (Figure 4.3). Still, the entrance time at automatic blocks must be calculated. The calculation procedure is as follows. The entrance time at the first block-section of the open track  $i$  is known and it coincides with the entrance time at the TPS track-segment which represents the open track  $i$ . Calculating the average speed  $\bar{v}_i$  on open track  $i$  from Equation 4.3, the entrance time of the train to the second automated block  $j$  of the open track  $i$  is given by equation:

$$t_j = t_i + L_j * \bar{v}_i \quad (4.4)$$

where  $t_i$  is entrance time at the open track  $i$  and  $L_j$  is the length of automatic block  $j$ . Then, the entrance time  $t_{j+1}$  at the block  $j+1$  (downstream of block  $j$ ) is given by Equation 4.5. The same equation is used for all subsequent blocks of open track  $i$ .

$$t_{j+1} = t_j + L_{j+1} * \bar{v}_i \quad (4.5)$$

where  $L_{j+1}$  is the length of automated block  $j+1$ .

## 4.4. Assessment framework

This section proposes a framework to assess the performance of both *baseline* (TPS) and *infill* (TPS + MTPS) data in delivering train positioning information. The framework consists of key performance indicators and explains possible interactions between them. Also, this section discloses formulas to quantify the performance indicators. The section is structured as follows. Initially, the required navigation performance (RNP) parameters of the two data sources are discussed. Then, the RNP parameters are transformed into reliability-availability-maintainability-safety integrity (RAMS) parameters. Also, this section introduces two novel KPIs; an indicator for capturing the contribution of GPS in the reliability of determining the red signal as well as an indicator that captures the cases for which *infill* data lead to poorer reliability compared to *baseline* data.

### 4.4.1. Framework architecture

The quality of the data flow proposed in this study ( $v_{\text{max}}$ ) is affected by the quality of the data used by the red signal determination module (Table 4.1). Increasingly, the quality of the red signal module will be assessed via the quality of the train positioning sources used in this study. Hence, the quality measures presented on the remainder refer to the train positioning data sources but imply the red signal model. Recall that the task of red signal determination is used interchangeably with the goal of determining the position of the predecessor. To that end, a framework is proposed to evaluate the performance of *baseline* as well as *infill* (Figure 4.11). Additionally, it is assumed that the  $v_{\text{max}}$  calculation process is totally trustworthy. All performance indicators discussed on the remainder refer to the input of red signal determination module but they are assumed to be equal to those of the output, i.e. advice.

The data-mining tool results all the necessary raw data for the computations of the assessment framework. The raw data are processed to yield the valuable information. The processed data are

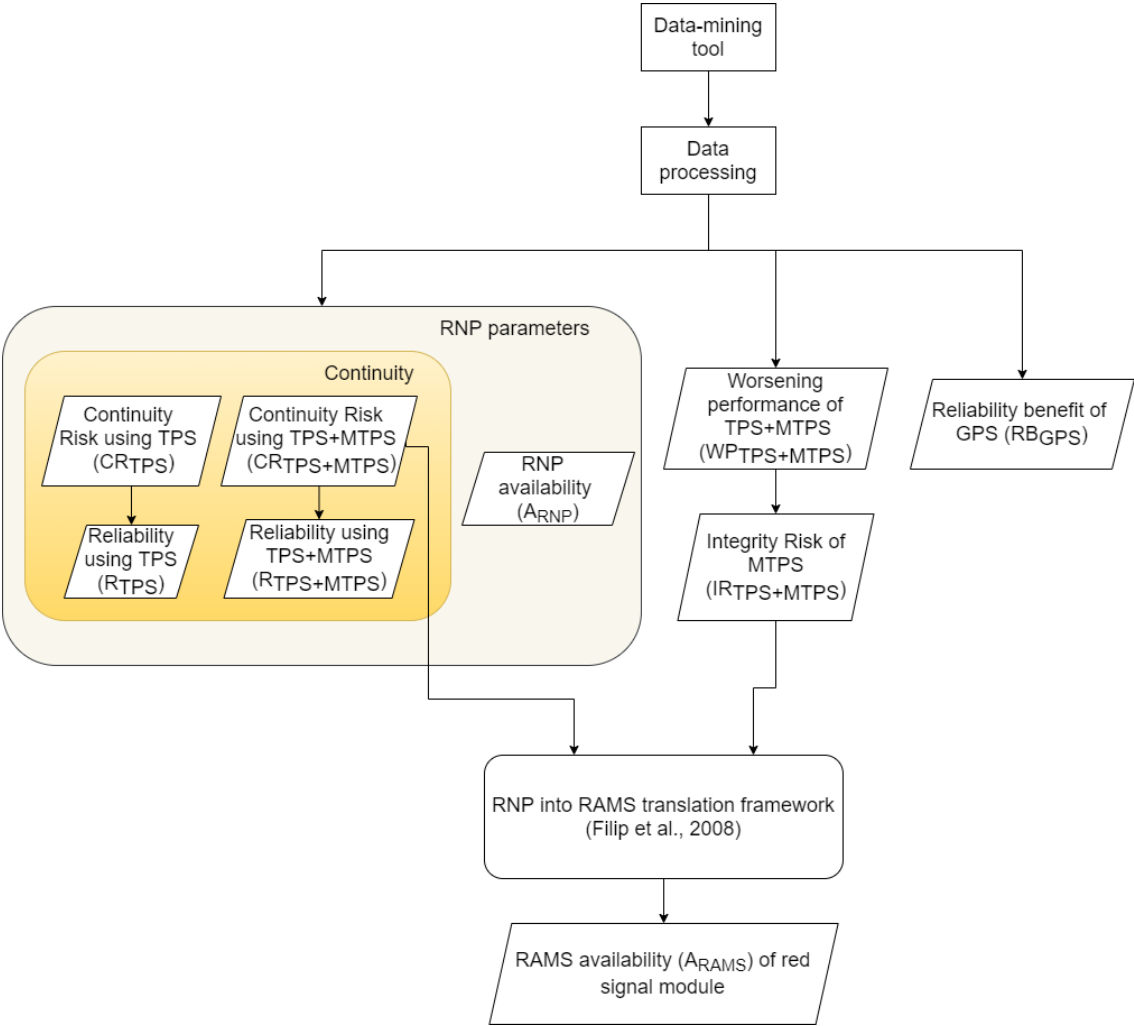


Figure 4.11: Assessment framework

directed to three distinct parts of the framework: the RNP parameter determination, the worsening performance of *infill* and the reliability benefit of GPS. The three parts are explained in detail on the remainder. The worsening *infill* performance indicator is translated into the integrity risk of using *infill* data. The latter is jointly used with the continuity risk of *infill* for the translation of RNP into RAMS parameters.

#### 4.4.2. RNP parameters for the red signal determination

Two parameters of the RNP framework are examined in this study; reliability and availability. First, the reliability parameter is discussed. As explained in Section 3.2.2, it is not always feasible to determine the most relevant red signal. In other words, the data sources used in that sense may show discontinuities. As the number of discontinuities of the input data increases, their reliability decreases. In fact, according to Filip et al. (2008) reliability can be approximated by its continuity. This is in accordance with the definition that Kelly and Davis (1994) give to continuity which is "short-term reliability". The Continuity Risk (CR) of the system (same as that of the data source) equals the probability that it will be unintentionally interrupted and equals:

$$CR = \frac{T}{MTBF} \quad (4.6)$$

Therefore, the formula for reliability ( $R$ ) is:

$$R = 1 - CR = 1 - \frac{T}{MTBF} \quad (4.7)$$

where  $MTBF$  is the mean time between failures and  $T$  is the continuity time interval, or else the observed discontinuity with the minimum duration.  $R$  is expressed as a percentage. Formula 4.7 suggests that reliability is proportional to  $MTBF$  while it is inversely proportional to  $T$ . In other words, large  $MTBF$  is favourable for a data source's reliability, while as  $T$  increases, it has a negative effect on reliability. In fact,  $T$  emphasizes on the importance that the magnitude of the minimum gap in the data stream has on reliability. Also, it is the ideal index to capture the criticality of a gap. In practice,  $T$  is considered as the most critical part of the route where the system should function.

Figure 4.12 illustrates the continuity graph of the data stream as a function of travel time. The information from which this graph is constructed are the output of the data-mining tool. This information is the RouteLint timestamp along with the binary parameter of the tool being able or not to yield the red signal with a certain data source (see also Figure 4.3). The same information is used to calculate  $MTBF$  which is the core parameter for the reliability formula (Formula 4.7). The continuity graph is useful for following analysis in order to correlate the ability to determine the red signal with the realised blocking time. More thoroughly, this graph illustrates the data source's ability to yield the red signal throughout the entire train route. The continuity of the data stream has the form of a binary signal. Hence, it has the value of 1 when it is feasible to determine red signal's location and 0 in the opposite case. As depicted in the Figure, intervals of 1 represent the TBF (Time Between Failure) the number of which is equal to  $n$ , while intervals of zero represent the failure. Note that the term *failure* is used in this study in the sense of the algorithm's inability to locate the red signal. In turn,  $MTBF$  is given by the Formula 4.8. Intuitively, this Formula suggests that as the total duration of a data source's ability to yield the red signal increases, this is favourable for  $MTBF$  and in turn, for reliability (Formula 4.7). In contrast, as the number of gaps increases,  $n$  increases and thus, reliability decreases.

$$MTBF = \frac{\sum_{i=1}^n TBF_i}{n} \quad (4.8)$$

where  $i$  a stretch where the red signal can be determined of duration  $TBF_i$  with  $1 \leq i \leq n$ .

Availability is the other RNP parameter considered as performance indicator in this study. RNP-availability ( $A_{RNP}$ ) quantifies a data source's ability to perform the required function (i.e. determine the red signal) at the start of a train run (TR). It must be stressed that only the *baseline* data source is used for the calculation of  $A_{RNP}$ . In order to quantify  $A_{RNP}$ , a binary parameter  $B_{TR}$  is calculated at the start of each TR.  $B_{TR}$  takes value 1 (available) if the red signal can be determined for the first valid  $x_{w,k,t}$  record, while it takes value 0 (unavailable) in case of the opposite. A  $x_{w,k,t}$  record is valid when it does

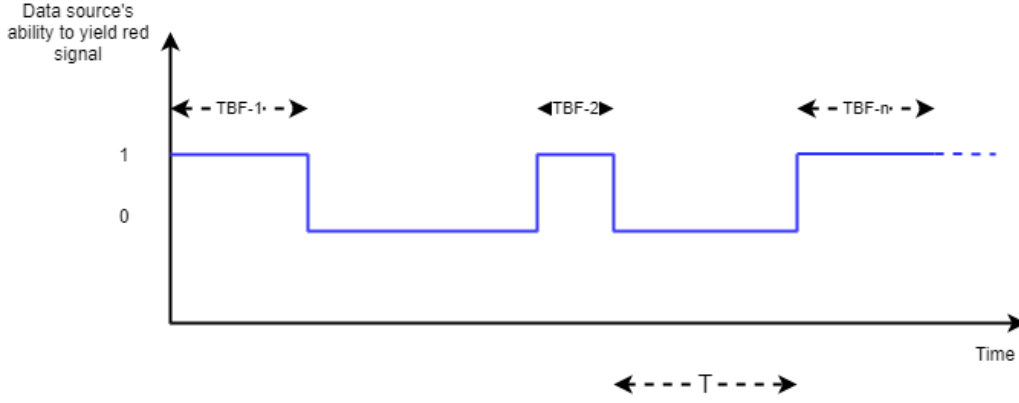


Figure 4.12: Continuity graph of the data stream used for red signal determination

not contain NaN values. Then,  $A_{RNP}$  is calculated as the proportion of all the train runs  $m$  that have scored 1.

$$A_{RNP} = \frac{\sum_{i=1}^m B_{TR=1}}{m} \times 100\% \quad (4.9)$$

#### 4.4.3. Worsening performance of infill data

The use of *infill* data does not guarantee to yield a better (higher) MTBF compared to that of *baseline*. As a consequence, the use of *infill* does not assure improved reliability in determining the red signal compared to *baseline* data. In other words, for the same train run it might be that *infill* yields lower MTBF compared to *baseline*. For these cases, *infill* worsens the performance of the red signal module. This thesis proposes a novel KPI to determine the number of train runs that are worse-off after the introduction of *infill*. The observations of the two samples are matched based on the combination *train number-date*. For each combination  $i$ , the MTBF using *baseline*  $MTBF_{baseline,i}$  and the MTBF using *infill*  $MTBF_{infill,i}$  is calculated. The worsening performance of *infill* data  $WP_{TPS+MTPS}$  is given by the formula:

$$WP_{TPS+MTPS} \equiv IR_{TPS+MTPS} = \frac{\sum_{i=1}^n (MTBF_{infill,i} - MTBF_{baseline,i}) < 0}{n} \times 100\% \quad (4.10)$$

where  $n$  is the number of observations. The nominator of Equation 4.10 expresses the number of observations that are worse-off with the use of *infill* data. Moreover, this study assumes that  $WP_{TPS+MTPS}$  coincides with the integrity risk of using infill data ( $IR_{TPS+MTPS}$ ). The worsening performance of *infill* indicates that the data source does not behave as expected. The exact number of cases for which the data source does not meet the specifications, cannot be predicted. Yet, the system should automatically identify these malfunctions and deliver timely notifications. Within the RNP framework, these cases are captured by the *IR*. For this study, it is believed that such cases can be captured by  $WP_{TPS+MTPS}$ .  $IR_{TPS+MTPS}$  is used in the translation of RNP into RAMS parameters.

#### 4.4.4. Translation of RNP into RAMS parameters

The framework proposed by Filip et al. (2008) is used for translating the two RNP parameters (availability and continuity) into Reliability Availability Maintainability Safety (RAMS) parameters (see also Subsection 2.8.4). Since the proposed red signal framework of this study intends a DAS (non-safety critical system), only the non-safety critical part of the framework is used (Figure 2.1). The non-safety critical part of the framework regards the RAMS-availability ( $A_{RAMS}$ ) of the system which depends on maintainability, correct positioning function and correct diagnostics. This study does not include maintainability in the calculations.  $A_{RAMS}$  is given by the formula:

$$A_{RAMS} = 1 - (IR_{TPS+MTPS} + CR_{TPS+MTPS}) \quad (4.11)$$

where  $IR_{TPS+MTPS}$  is the integrity risk and  $CR_{TPS+MTPS}$  is the continuity risk of using the fusion of TPS and MTPS.

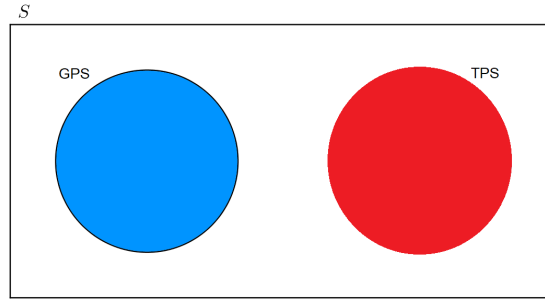


Figure 4.13: Illustration of the positioning solution using event theory

In general,  $CR$  captures the ability of the system to correctly determine the position of the predecessor (and consequently determine the red signal), while  $IR$  models the ability of the system to diagnose a faulty behaviour and provide timely warnings.

#### 4.4.5. Contribution of GPS in determining the red signal

This study introduces a novel KPI to capture the additional benefit MTPS introduces to the function of determining the red signal. The benefit is measured as the change in the aggregate system's reliability after introducing MTPS. This benefit will be captured by the contribution (benefit) of GPS in red signal determination reliability  $RB_{GPS}$ . Since GPS is the new data source when using MTPS, the extra benefit in system's reliability stemming from GPS must be calculated. The following equations hold:

$$R(\text{baseline}) = R(TPS) \text{ and } R(\text{infill}) = R(MTPS) \quad (4.12)$$

where  $R(\text{baseline})$ : reliability of baseline data,  $R(\text{infill})$ : reliability of infill data,  $R(TPS)$ : reliability of TPS and  $R(MTPS)$  reliability of MTPS.

Both  $R(\text{infill})$  and  $R(\text{baseline})$  result from the data-mining tool. Thus,  $R(TPS)$  and  $R(TPS + MTPS)$  are known. The calculation of the reliability of solely GPS data is based on event theory. According to this theory, a data source's reliability is considered as the probability of a positive outcome (i.e. the red signal can be determined) in the data-mining tool originating from certain events with the events being TPS, GPS and MTPS. Then, the reliability of MTPS is given by the formula:

$$R(MTPS) = R(GPS \cup TPS) = R(GPS) + R(TPS) - R(GPS \cap TPS) \quad (4.13)$$

where  $R(GPS)$ : reliability of GPS.

In this study, MTPS is considered to be supplementary to TPS. It is assumed that GPS is supplementary to TPS, too. Therefore, the two information sources are not intersecting in the event space (Figure 4.13). Given this and based on Equation 4.13, the reliability benefit of GPS equals:

$$RB_{GPS} = R(GPS) = R(MTPS) - R(TPS) \quad (4.14)$$

## 4.5. Summary

The main aim of this study is to increase the awareness of a conceptual DAS regarding the actual signal state in order to minimise conflicts in disturbed operations. In order to increase the proposed model's effectiveness, this information must be provided in real time. It was proven that the only missing function to provide this real-time information flow is to determine the red signal in real time. Thus, the initial objective of this study was scoped down to the red signal determination. It was also proven that the goal of determining the red signal is equivalent to the goal of locating the predecessor train. This information is planned to be fed to the on board equipment of a DAS via a novel data stream. Additionally, this section explained how this data stream fits to the train control architecture using a C-DAS-On board.

The determination of the most relevant red signal is based on train positioning data. This thesis opted for a data-driven approach to investigate the potential of two train positioning systems – provided by ProRail – to deliver the red signal to the on board DAS equipment in real-time. The two systems are TPS and MTPS. Using TPS is regarded as the *baseline* approach to deliver the red signal, while it is assisted by *infill*, which constitutes a fusion of TPS with MTPS data. The *infill* approach is the main contribution of this study since MTPS data have never been used for the derivation of the actual signal state. *Baseline* data is easy to handle and yields the red signal when predecessor train is located on an interlocking area or when it is about to move to a downstream track-segment. In contrast, *infill* data require more preprocessing but they are able to yield the red signal when predecessor is located on the open track.

An assessment framework has been proposed to quantify the positioning solution quality of the two data sources. The framework consists of four components: the definition of the required navigation performance (RNP) parameters, the translation of RNP into reliability–availability-maintainability-safety integrity (RAMS) parameters, the worsening performance of TPS + MTPS data and the contribution of GPS data in the reliability of determining the red signal. The attributes of the framework components are quantified by key performance indicators (KPIs). The RNP component regards the reliability and the RNP-availability. Reliability is calculated using the mean time between failures (MTBF) and the minimum observed discontinuity  $T$ . MTBF is an ideal parameter to capture both the total duration and the number of discontinuities of a data stream.  $T$  captures the criticality of a gap. RNP-availability is used to capture the non safety-critical part of the RAMS framework.

This study introduces two novel KPIs. Since MTPS data is used to assist TPS data in determining the red signal, this solution is expected to be more reliable than using solely TPS data. Yet, in practice this is not always the case. To that end, a KPI is proposed to capture the fraction of observations which are worse-off by the introduction of TPS + MTPS data. The other novel KPI addresses the reliability benefit stemming from GPS data. The proposed framework can also be used to assess the positioning quality of other non safety-critical applications of GNSS systems in the railway sector.

# 5

## Numerical results of the data-mining tool

This chapter includes the numerical analysis of the data-mining tool output for the study area. First, the case study area is presented as well as the reason why this area has been selected for applying the tool. Second, the two data sources (TPS and MTPS) are compared with respect to different performance parameters. Third, the KPIs of the red signal determination module using the two data sources are calculated. Fourth, this section tries to investigate the reason behind the worsening performance of infill data. Finally, the interrelationship between data stream continuity and predecessor's position is explained through an example.

### 5.1. Case study

In this section the logic behind the selection of the study area (railway corridor and train series) is presented. Also, the considered data set as well as the availability of the ProRail train positioning systems on the case study area are reported.

#### 5.1.1. Selection of study area

The data mining tool was applied at series 6300, a sprinter series connecting Haarlem to Den Haag Centraal. The initial interest for these series was drawn due to the fact that NS is conducting tests for GoA 2 on it. Figure 5.1 presents series 6300 on the map of the Dutch timetable for the year 2020. Figure 5.2 shows indicative trajectories of the series that share the same track with 6300 (Intercity: 2200, 1800/700, 2100 and Sprinter: 4600) at the direction Haarlem-Den Haag Centraal. The timetable has cycle time equal to 30 min and the departures are shown in full minutes at the Y-axis of Figure 5.2. The timetable pattern as well as the number of trains operating on a 30 min period are the same for both peak and off-peak hour. In fact, this is the general practice in the Dutch timetable. Peak period differs from the off-peak period only with respect to the length of the used rolling stock (longer train sets in peak hour) and not in the number of trains of the period. Finally, series 6300 passes through 10 stations (Haarlem, Heemsteede Aerdenhout, Hillegom, Voorhout, De Vink, Voorschoten, Den Haag Mariahoeve, Laan van NOI, Den Haag Centraal).

Preliminary runs of the data mining tool for both travel directions has shown limited capability of determining the red signal using the *baseline* approach at the direction from Haarlem to Den Haag Centraal. Apart from this and also based on test runs of the tool, for this direction, considerable inability of the tool to determine the red signal is witnessed only at the part of the track between Haarlem and Voorhout (shown in black oval in Figure 5.1). The under consideration area comprises of around 20 km of open track. Figure 5.3 illustrates the layout of the entire track between Haarlem and Leiden Centraal at micro-level, while Appendix D includes detailed drawings of the under consideration track. In principal, the nominal route is considered (included in Appendix D). Still, the tool is able to record train routes other than the nominal in case of disturbed operations. To sum up, this study focuses on train runs at the track between two major stations of the itinerary (i.e. Haarlem and Leiden) which includes the area of interest. The study area contains interlocking areas.

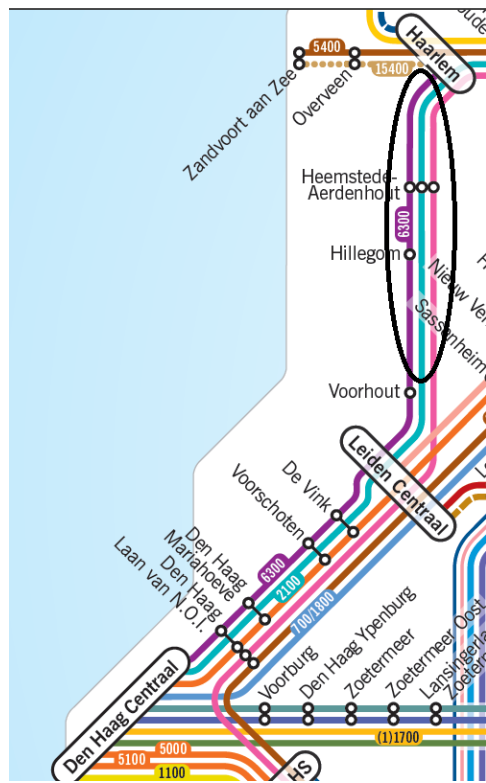


Figure 5.1: 6300 series shown on the map of the Dutch timetable 2020

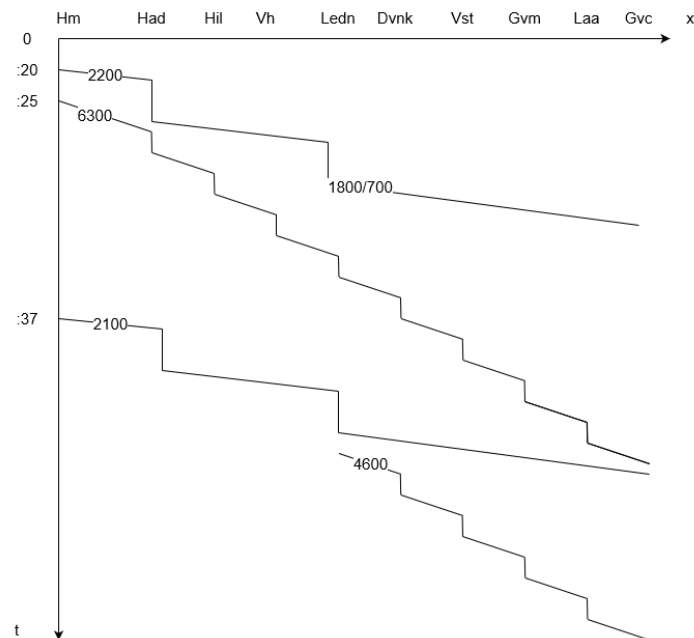


Figure 5.2: Schematic representation of the timetable pattern for the considered railway corridor between Haarlem and Den Haag Centraal

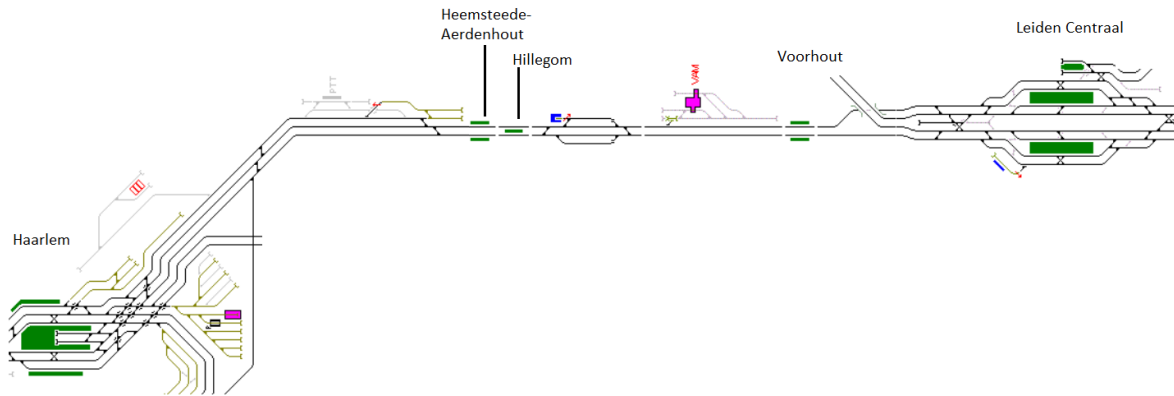


Figure 5.3: Track layout between Haarlem and Leiden Centraal, source: sporenplan.nl

### 5.1.2. Data set selection

It must be revealed whether a train run is conflicting or not. Conflicts are determined by measuring the punctuality of the train at Haarlem (major station of the considered itinerary). ProRail sets a punctuality threshold of 3 min for arrivals at major stations. In this study, arrival punctuality is yielded by comparing the realised running time (RRT) to the scheduled running time (SRT). A train is conflicting when the RRT is longer than the SRT by 3 min. The developed data-mining tool yields the RRT, while the SRT equals 22 min. The conflicting trains equal the 3.1% of the considered train runs. This figure was yielded using historical RouteLint data.

As discussed in Section 4.3, the data-mining tool receives input regarding the date and the train number for which the analysis must be performed. This study possesses RouteLint and MTPS data for sixteen (16) days of data (21-25/10, 9-13, 16-19, 23-25/12/2019). Additionally, the train numbers considered refer almost to an entire day. Note that there is a unique train number per day. Train numbers were retrieved from Timetable 2020 of NS. In total 36 train numbers were examined (from 6321 to 6389 increasing by 2). There are 11 peak hour (6325-6335, 6365-6373) and 25 off-peak hour train numbers. As peak hour train numbers are considered those that depart from Haarlem within the time ranges 06:30-09:00 and 16:00-18:30. Off-peak train numbers refer to all the 6300 series trains that depart from Haarlem between the first departure (around 05:30) and the departure around 22:30 excluding the peak hour trains. Note that the last departure considered in this analysis is not the last departure of 6300 series. This was done for the sake of simplicity due to the mismatch at the naming of the day used in RouteLint and MTPS log files (RouteLint follows the day format of the NS timetable, i.e. operational day starts at 04:00 while MTPS follows the normal day). For example, the whole route of train 6395 that departs from Haarlem on day  $D$  at 23:55 and arrives at Leiden Centraal at 00:18 appears on RouteLint log file of day  $D$ , but the corresponding MTPS records are split in the files of day  $D$  and  $D+1$ . The scheduled travel time for both peak and off-peak trains is 42 min (2520 sec).

### 5.1.3. Availability of the train positioning systems for the examined corridor

Regarding the availability of the raw data sources, RouteLint is assumed available throughout the whole route and it is not discussed further. Still, MTPS's availability must be looked into. The histogram of distances between successive MTPS records along the route between Haarlem and Leiden Centraal as provided by the *TpsMessageHandler*, is used as a way to quantify MTPS availability on the study area (Figure 5.4). Note that these differences indicate distances between successive insulated joints (see also Section 3.2.3). Most records are less than 200 m apart between each other. Yet, there are three significantly big gaps. This is because the *TpsMessageHandler* service is not available for these three distinct areas of the route.

The gaps are between location 21.610-27.945 km ( $L=6335$  m), 38.860-33.014 km ( $L=5846$  m) and 43.250-38.860 km ( $L=4390$  m). In practice, the first gap extends along the whole track connecting Heemstede Aerdenhout to Hillegom, while the other two areas are around 6 km upstream of Voorhout

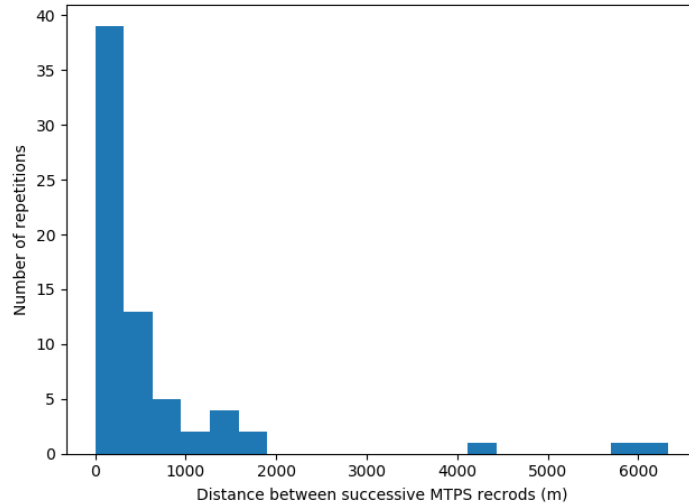


Figure 5.4: Histogram of MTPS records along the considered corridor

and 4.5 km downstream of it. Only an insulated joint that connects the latter two gap areas in Voorhout station is available via *TpsMessageHandler*.

## 5.2. Comparison between baseline and infill data

The information included on the remainder of this chapter is the output of the data-mining tool. The analysis comments on each one of the data sources but also compares them. The tool output for both data sources has been grouped in two samples; peak and off-peak trains. The two samples have been cleared for outliers. Each same *observation* reflects the combination *train number-date* which is unique.

Initially, the performance of the two data sources is quantitatively compared regarding reliability-related parameters, i.e. MTBF and reliability  $R$ . Figure 5.5 includes the box plots of MTBF for the two data sources. According to the Figure, both data sources have outlier values larger than the maximum non-outlier value and only *infill* has outlier values smaller than the minimum non-outlier value. Moreover, *infill* records are quite dispersed compared to the concentrated MTBF observations of *baseline*. Finally, *infill*'s median is higher (791.7 s) than that of *baseline* (543.0 s). Based on this, it can be argued that *infill* leads to a more continuous data stream providing the red signal in real-time by 43.5% compared to *baseline*.

In general, *infill* achieves higher reliability (97.8%) compared to *baseline* (95.9%). Now, both *baseline* and *infill* data are less reliable for peak trains. In detail, *baseline* for peak trains scores 92.4%, while for off-peak 95.9%. The previously presented reliability values were calculated with the median MTBF value of each sample. Additionally, *infill* for peak trains scores 97.0%, while for off-peak 97.8%. This finding points out the effect that the minimum observed discontinuity  $T$  has on reliability. Recall the contribution that  $T$  has on reliability from Equation 4.8 and Equation 4.7. It is not enough to reach a conclusion regarding the reliability of a data source to determine the red signal based solely on MTBF. More specifically, based on historical data it was revealed that peak trains experience more severe discontinuities (the minimum discontinuity  $T$  for peak hour trains is higher than that of off-peak for both data sources).

The level at which *infill* data manage to improve the reliability with which the red signal is determined is also appraised. The results for the general case as well as per train type are illustrated in Figure 5.6. For the general case, GPS increases system reliability by 1.9% (from 95.9% with *baseline* to 97.8% with *infill*). The contribution of GPS for peak hour trains is 1.9% (from 95.9% with *baseline* to 97.8% with *infill*), while for off-peak hour trains the contribution of GPS in red signal determination reliability equals 4.6% (from 92.4% with *baseline* to 97.0% with *infill*). So, GPS contributes more in off-peak hour trains.

Also, the proportion of trains that are worse-off after the introduction of the *infill* data is reported,

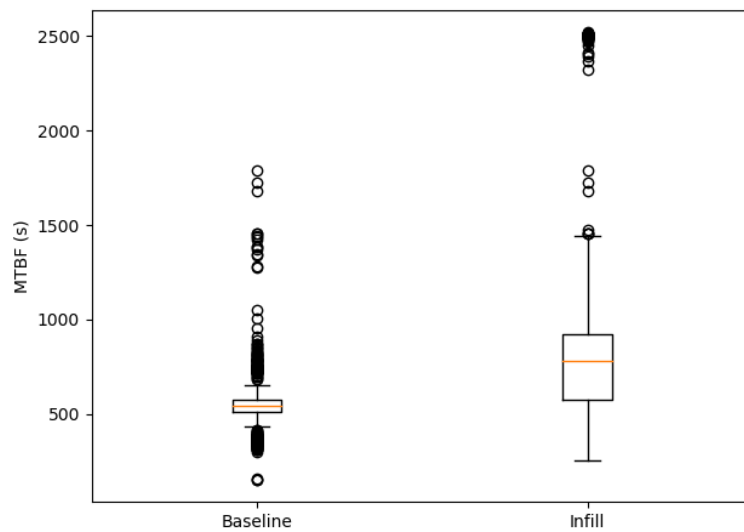


Figure 5.5: Box plot of MTBF for the two data sources. The orange line illustrates the median value of the sample. The box indicates the inner quartile range (IQR), i.e. the range where values between the 25<sup>th</sup> percentile (lower box edge, 1<sup>st</sup> quartile: Q1) and the 75<sup>th</sup> percentile (upper box edge, 3<sup>rd</sup> quartile: Q3) percentile lie within. Box-plot whiskers illustrate the minimum ( $Q1-1.5*IQR$ ) and maximum ( $Q3+1.5*IQR$ ) value of the sample which are not considered outliers.

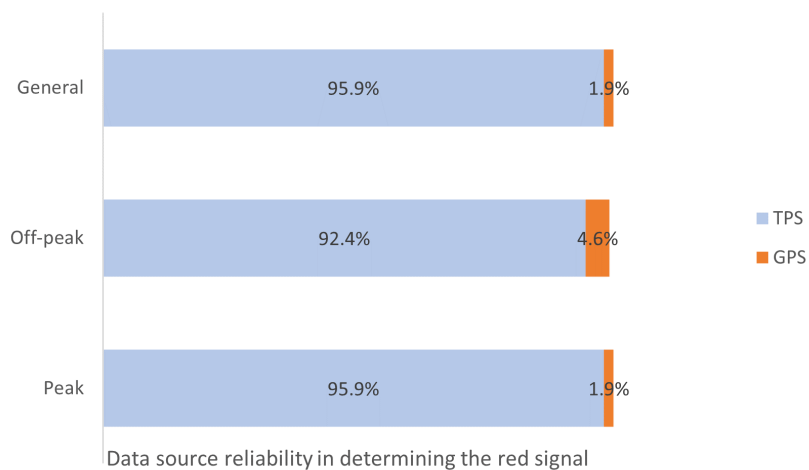


Figure 5.6: Contribution of GPS in determining the red signal when using infill data per type. General: all train types, Peak: peak hour trains, Off-peak: off-peak hour trains,

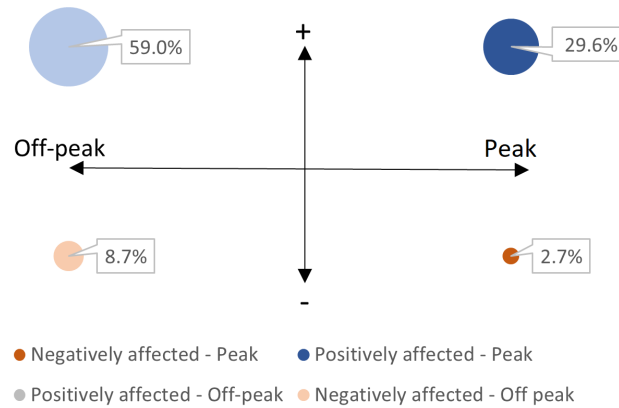


Figure 5.7: Percentages of peak and off-peak trains which are positively or negatively affected after the introduction of the *infill* data source. *Positively*: infill yields higher MTBF compared to baseline, *Negatively*: infill yields lower MTBF compared to baseline. X-axis: train type, Y-axis: positive/negative effect of infill

i.e. the worsening performance of *infill*. In general, 11.4% of all train run observations are negatively affected. Analysing per train type, shows that the majority of the negatively affected train runs refers to off-peak trains (8.7%). (Figure 5.7).

### 5.3. Calculation of key performance indicators

In this section, the key performance indicators (KPIs) are quantified. Each KPI quantifies a different parameter regarding a data source's potential to yield the red signal. It is assumed that the same KPI value expresses the performance of the advice of DAS that uses the aforementioned data sources. Table 5.1 summarizes the numerical values of the KPIs. The values presented on the remainder were calculated for 528 (non-outlier) observations.

First, the RNP parameters are discussed. Regarding reliability,  $R_{TPS}$  equals 95.9%, while  $R_{TPS+MTPS}$  equals 97.8%, (see also Section 5.2). Continuity risk of TPS ( $CR_{TPS}$ ) equals 0.041, while that of TPS + MTPS ( $CR_{TPS+MTPS}$ ) equals 0.022. The RNP-availability ( $A_{RNP}$ ) of the red signal determination reaches 99.24%. using the *baseline* data source. Hence, for the vast majority of the examined train numbers, the *baseline* data source is available to determine the red signal at the start of the trip.

Now the definition of the non safety-critical part of the RAMS framework is quantified through the RAMS-availability  $A_{RAMS}$ . According to this, the performance of a DAS using the developed red signal framework reaches a  $A_{RAMS}$  equal to 86.4%. The value is calculated using  $CR_{TPS+MTPS}$  and  $IR_{TPS+MTPS}$ .

Table 5.1: Key performance indicators

KPI	Value
$CR_{TPS}$	0.041
$R_{TPS}$	95.9%
$CR_{TPS+MTPS}$	0.022
$R_{TPS+MTPS}$	97.8%
$A_{RNP}$	99.2%
$A_{RAMS}$	86.4%
$RB_{GPS}$	1.9%
$WP_{TPS+MTPS} \equiv IR_{TPS+MTPS}$	11.4%

The added benefit in advice reliability of GPS is taken equal to the value of the general case. Thus,  $RB_{TPS+MTPS}$  equals 1.9%.

Now, the worsening performance of infill data is computed.  $WP_{TPS+MTPS}$  is taken equal to the fraction of the total train runs which are negatively affected by the *infill*, i.e. 11.4%. Then,  $IR_{TPS+MTPS}$  is taken equal to  $WP_{TPS+MTPS}$ . Further detail on the previously mentioned values can be found in Appendix C.

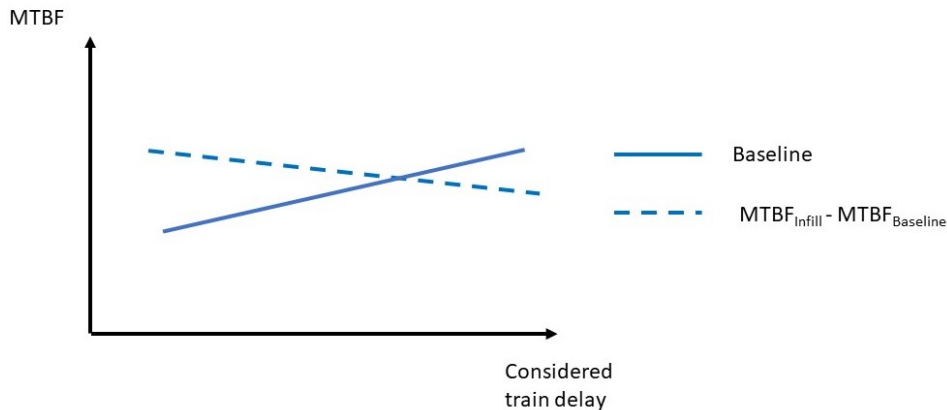


Figure 5.8: Schematic representation of the correlations delay- $MTBF_{baseline}$  and delay- $MTBF_{infill} - MTBF_{baseline}$  for trains that are negatively affected by the introduction of infill data source.

## 5.4. Causality of the worsening performance of infill data

At this point, the study aims to find an explanation behind the worsening effect of *infill* data. To that aim, only the subset of the negatively affected observations is used (i.e. 11.4% of observations). For this subset, a table is constructed that includes the following information for each train: the MTBF yielded by *baseline* data ( $MTBF_{baseline}$ ), the MTBF yielded by *infill* data ( $MTBF_{infill}$ ), the difference of MTBFs ( $MTBF_{infill} - MTBF_{baseline}$ ) as well as the *delay* of the considered train. The Spearman correlation indicator is calculated for all the pairs of the aforementioned attributes. A thorough presentation of the correlations is included in Appendix C.

The correlation analysis showed that  $MTBF_{baseline}$  is positively correlated to delay (solid line in Figure 5.8). Therefore, the more delayed a train is, the more reliably *baseline* data yield the red signal. This can be justified by the fact that *baseline* data disclose signalling information. More thoroughly, the more delayed a train is, the more closely it will attempt to follow its predecessor. In this case, the train will face more restrictive signal aspects. In turn, the train is unlikely to be authorised to a downstream track-segment and thus, it will be easier to yield the red signal. As a consequence, the more the times the red signal can be determined, the less discontinuities appear on the continuity signal of a data stream. In contrast, no strong relation was found between  $MTBF_{infill}$  and *delay*.

Also, the difference of MTBFs is negatively related to delay (dashed line in Figure 5.8). Hence, the more the delay increases, the less *infill* data improves system reliability. The causality of this finding cannot be well supported. The only possible underlying reason to this is the availability of MTPS data with the *TpsMessageHandler* publication service (see also Subsection 5.1.3).

## 5.5. Correspondence of data stream continuity and predecessor position

This section illustrates the correlation between data stream continuity in yielding the red signal and predecessor's position using an example. The analysis included in the following lines supports the claim that *baseline* data can successfully locate predecessor train in cases where it is either on an interlocking area or when it is about to exit an open track, while *infill* extends the solution space of the previous two cases by locating predecessor when it is on the open track. Figure 5.9 presents an example for train 6337 for day 2019-12-13. The Figure matches the locations of the continuity graph of the two data streams with the realised time-distance diagram. Open tracks are depicted at the bottom of the Figure. These are track-segments *LJ*, *LH*, *LG*. Below the labels of the open tracks, the gaps of

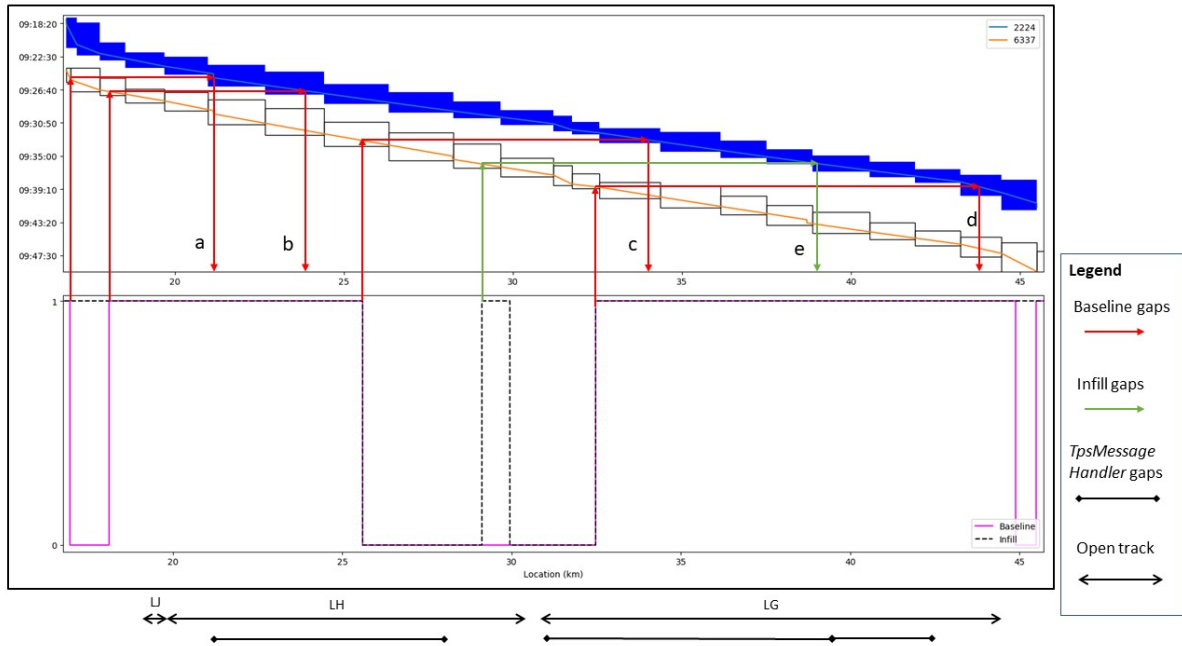


Figure 5.9: Correlation of the continuity of the data stream and the realised time-distance diagram

*TpsMessageHandler* service are demonstrated.

A discontinuity in the graph is correlated with predecessor's position using three arrows. The first arrow (vertical moving upwards, constant location) connects a discontinuity with the trajectory of train 6373. From this intersection point a second arrow (horizontal moving to the right, constant time) connects the trajectory of train 6373 with that of 2224. The third arrow (vertical moving downwards, constant location) illustrates predecessor's position. This position is correlated to open tracks or *TpsMessageHandler* gaps. Arrows related to *baseline* gaps are red while those related to *infill* are green. Each edge of the discontinuities of the data stream of Figure 5.9 are marked with a letter ranging from a to e.

To begin with, *baseline* effectively determines the red signal when predecessor is on interlocking areas. Yet, it fails to yield the desired output when the predecessor is in an open track (cases a to d). *Infill* manages to bridge all these gaps but its global applicability is challenged due to the gaps of the *TpsMessageHandler* service. Only for case e, *infill* manages to yield the red signal since predecessor is located at the connection point of the two *TpsMessageHandler* gaps at location 38 km, approximately. Exact locations of track-segments included in Figure 5.9 can be found in Appendix D.

## 5.6. Summary

It was selected to test the proposed red signal framework on train series 6300 since recently, the same series were chosen by NS to perform ATO tests on top the legacy Dutch signalling system. The analysis is performed for the stretch between Haarlem (Hlm) and Leiden Centraal (Ldn) (direction Hlm-Ldn). This study uses only the *TpsMessageHandler* publication service of MTPS which shows some information gaps for the study area.

In general, *infill* yields more continuous data streams – as expressed by the MTBF – compared to *baseline* (*infill* MTBF equals 791.7 s, while *baseline* MTBF 543.0 s). Also, *infill* was proven to be a more reliable data source compared to *baseline* (*infill* reliability equals 97.8%, while *baseline* reliability equals 95.9%). As regards specific train types, it was revealed that both data sources yield a less reliable solution of the red signal determination for peak trains compared to that of off-peak trains. Reason to this are the more severe discontinuities that peak hour trains observe.

This section contained also the calculation of KPIs. The KPIs include RNP-availability (calculated with *baseline* data only), reliability, continuity risk, RAMS-availability and two novel indicators proposed

by this study; an indicator for quantifying the reliability benefit of GPS in determining the red signal as well as an indicator that captures the cases for which *infill* data lead to poorer reliability compared to *baseline* data. The former KPI was determined equal to 1.9%, while the latter equals 11.4%. In other words, using MTPS improves system reliability by 1.9%, while for the 11.4% of the cases, the introduction of MTPS is not considered beneficial.

The following correlations were found to be statistically significant for the train runs that are negatively affected by the introduction of *infill* data. As the delay of the considered train increases: a)  $MTBF_{baseline}$  increases and b) *infill* data worsen the reliability. This worsening effect possibly stems from the limited availability of MTPS data at the considered area.

# 6

## Model assessment on a simulator

This chapter contains information relevant to the performed simulations. First, the simulator is introduced. Then, its components along with its capabilities and weaknesses are discussed. Also, the DAS model incorporated in the simulator is elaborated. A correlation of the simulator functions to the train control architecture using a C-DAS-On board is presented. Then, the setup of the experiment is explained in which the simulation input, the capacity analysis of the simulations as well as the assumptions on which the experiment is based are defined. Finally, there is an elaboration on the simulation results.

### 6.1. Motivation of simulation

The purpose of the simulation is to examine the plausibility of the following hypothesis:

increased advice reliability → increased driver acceptance → better capacity usage.

where *advice reliability* is input to the simulation, *capacity usage* is the measurable variable and *driver acceptance* is the connecting factor between the input and the measurable.

The fundamental hypothesis of the simulation requires three assumptions. First, it is assumed that the driver trusts the advice. This is a fundamental but hard assumption. Second, it is assumed that the driver follows the advice carefully by adjusting the train controls as soon as this has been announced. Third, it is assumed the better capacity usage is one of the objectives of the DAS. These three assumptions are sufficient to support the logical connection of the hypothesis. Then, the behaviour of the output can be directly connected to the input quality. This will be done using sensitivity analysis.

As explained in Subsection 4.2.2, the speed advice calculation requires two major input sources. One component is a route plan which is sent onboard by the TMS, while the other regards a model of displaying the advice only when an input source can deliver the actual signal state. The simulation intends only the latter component of the advice calculation of a DAS.

This study opts for using a simulator. The alternative of a simulator was selected among other alternatives due to the fact that the simulator is owned by ProRail. Also, the simulator constitutes an ideal means for capturing the response of the driver to advice with certain reliability and how this is translated into railway capacity usage. The simulator used in this study is *NEO-DMI Suite with 3D Viewer*, for simplicity called NEO-DMI on the remainder.

The DAS model included in NEO-DMI does not provide a model of sending the route plan to the on board DAS equipment in real-time. This limitation of the simulator does not hinder the potential of the simulation to test the fundamental hypothesis.

### 6.2. NEO-DMI Suite with 3D Viewer

This section presents information regarding the simulator used in this study. The different modules from which the simulator comprises of are discussed. Also, the simulator functions related to the train

control are presented. Solely functions of the onboard train equipment are discussed. Special acknowledgements are given regarding the simulator input.

### 6.2.1. Simulator general characteristics - Architecture

NEO-DMI is owned and maintained by the Dutch IM ProRail. NEO-DMI is an event-based simulator which performs simulations at a microscopic level. In the remainder of this chapter, the discussion is limited to the simulator functions used only in this study. The simulator is constantly updated and currently, has several other capabilities which lie outside the scope of this study.

Under its current version, NEO-DMI facilitates only script-based simulation. More thoroughly, the different simulator modules do not interact between each other. An interactive simulation requires time-based input. For example, using an interactive simulator, if the train ran faster than planned and provided that the simulator facilitated a track-clear detection model, the operator would see a signal turn into a restrictive aspect. Instead, in this scripted simulator, all modules receive the same pre-defined input which gives the user the impression of a dynamic character of the simulated environment. This is achieved by having all the modules perform tasks according to the location of the simulated train along the track. To do so, the simulator receives distance-based input in a scripted format. All input files include an attribute followed by its location starting from location 0 (in metres) which indicates the starting point of the simulation.

The operating principle of this script-based simulator is presented using an example. The example describes the approach followed to model a signal-aspect change. In a script, the experimenter includes the command *X, S, yellow* which can be interpreted as: "when train is at location *X*, turn the aspect of signal *S* (which is placed at a location downstream of *X*) from green (was set to green on the infrastructure file) to yellow". Thus, when the train is at location *X*, the operator will see the upcoming signal turn from green to yellow. This suggests that irrespective of the train running earlier or later at location *X*, the aspect change will occur.

NEO-DMI comprises of three core modules: *DMI*, *train* and *3DV* (3D View) module. Figure 6.1 demonstrates the architecture of the simulator. The three modules use scripted (static) input and interchange dynamic information through dedicated interfaces between them. A human operator is required to perform the simulation. In the remainder of this chapter, the term *driver* refers to the human operator that runs a scenario on the simulator. The driver receives visual input from the *DMI* and *3DV* modules and delivers manual output to the train module.

The infrastructure included in the simulator is at a micro level and is set as input for the *3DV* module in a scripted format. The *3DV* can reproduce every piece of infrastructure.

The *train* module incorporates the train control levers. The driver gives manual input to the train module by adjusting the levers. The output of the *train controls* sub-module is directed to the train dynamics module. In case emergency braking is needed, the braking sub-module receives input from the ATP-onboard sub-module of the *DMI* module.

The *train dynamics* module contains a train dynamics model. The train movement is replicated via the train dynamics sub-module. The sub-module receives dynamic input from the train controls. Also, essential input to this sub-module is a file that includes the technical characteristics of the rolling stock such as maximum speed, service and maximum braking as well as maximum acceleration. For scenarios that run under ATB-EG, the minimum braking criterion to cope with the braking rules of ATB-EG is included in the afore mentioned file. The train dynamics sub-module calculates the acceleration, speed and distance from the start of the train every 2 sec and sends it to the *DMI* module. This output is also directed to the *3DV* module to simulate the train movement.

The *DMI* module integrates the *DMI* as well as the ATP-onboard functionality. Input for this module is a dedicated script for each of the following attributes of the scenario: ATP system, possible ATB-code changes, the SSP, delay and advice. SSP is the same irrespective of the ATP used. The ATB-code change file is applicable only for ATB-EG operation and it allows to model the signal aspect speed profile (SASP) in the form of ATB-code changes originating from the changes in signal aspects (see also Subsection 6.3.2). The delay script is also distance-based. This allows for emulating a delay information published by the TMS when the train reaches a certain location. The speed advice is rather static and it is included in a dedicated script. Since advice is loaded before train's departure this can be considered as a S-DAS function.

The *DMI* displays the actual speed, the train's delay, the simulated time and distance from the start

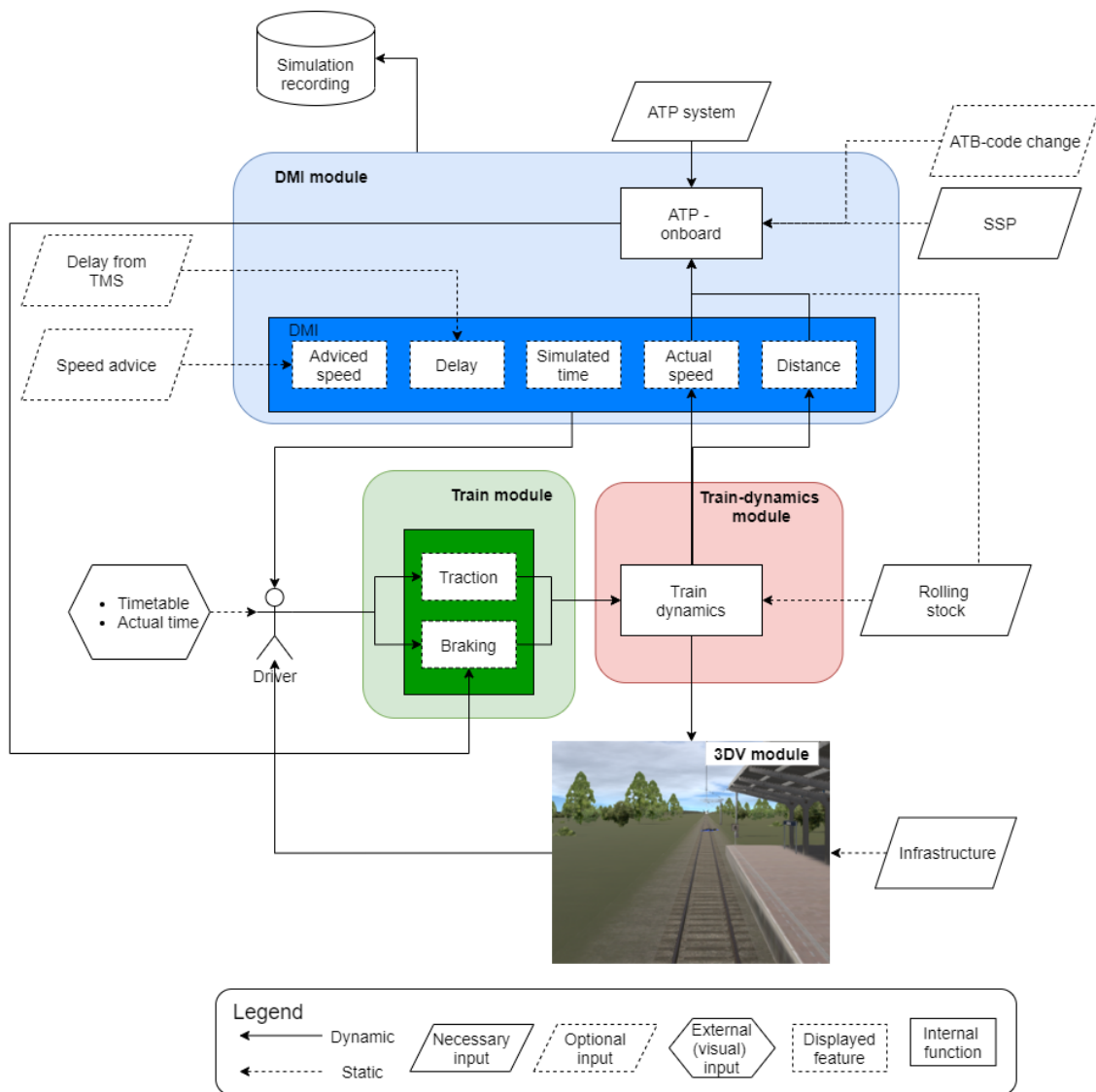


Figure 6.1: Architecture of the NEO-DMI Suite with 3D Viewer simulator

and in case a DAS is used, the advised speed. The delay is modelled in the following format: *location, seconds*. A sign is added to the *seconds* to indicate the amount of time the simulated train is behind (+) or ahead (-) of the schedule. The actual speed and distance originate from the train dynamics function. The ATP onboard constantly compares the actual speed with the allowed speed at that location of the track, delivers audible notifications when the speed limit is exceeded and triggers emergency braking when safety threshold has been violated. The latter action is realized through an interface between the DMI and the train module. In case of ATB-EG operation, ATP-onboard is also responsible to check whether the braking criterion is met. What is more, the DMI module can reproduce the audible sounds of every ATP system. Finally, the DMI records the simulation and stores it on a .csv file.

Note that some of the previously presented scripts are necessary while others are optional for the simulation (Figure 6.1). More specifically, the simulator is able to run without the advice, delay and ATB-code change scripts. In contrast the following scripts are vital to the simulation procedure: ATP system, SSP, rolling Stock and infrastructure. It must also be pointed out that there are dynamic data flows such as that between the train control levers and train dynamics module or the intervention of ATP-onboard in case of an overspend. In opposition to that, all information flows coming from the scripted input is static.

### 6.2.2. Correlation between train control and simulator functions

Figure 6.2 correlates functions of the train control architecture using a C-DAS-On board (see also Subsection 4.2.2) with the simulator modules (see also Subsection 6.2.1). The Figure correlates the two architectures using labels *a* to *g*. Note that only the onboard functions of the train control are contemplated, while the trackside functions are illustrated in an opaque font in Figure 6.2 since the simulator does not facilitate a model of them (see also 6.2.1).

In Figure 6.2, label *a* corresponds to the route plan feed from the DAS trackside to DAS on board. Note that NEO-DMI only allows for *a* being static. The calculation of the static advice is explained in Subsection 6.3.3. The calculation of the static advice is contained in label *f*, which combines the speed profile calculation and advice generation modules of the on board DAS. Note that there is no recalculation of the optimal speed profile based on actual operations (loop ICL2). Data stream *e* provides the maximum allowed speed to the speed profile calculation module and it is embedded in the speed advice script. Data stream *e* constitutes a novelty of this study to the train control scheme that uses an DAS-On board. Data flow *e* differs from data flow *c* only due to the fact that the former incorporates the reliability of the data source. In the simulator, data flow *c* is realised by the driver. He/she continuously observes the 3DV window and constantly monitors the actual speed. The ATP-onboard module is the same in both the train control architecture and the simulator (data flow *d*). The role of the ATP-onboard module in both architectures is to supervise the speed (data flow *g*). Lastly, in the train control architecture, the supervised speed is given by the track side equipment (data flow *b*). In the simulator, this is modelled by feeding the DMI module with a dedicated scripts for the SSP and ATB-code change. Table 6.1 summarizes the previous analysis.

Table 6.1: Matching of simulator functions to the functions of the train control architecture using a conceptual N-DAS-On board. The labels stem from Figure6.2

Label	Train Control function	Corresponding function in simulator
a	TMS to DAS-On board communication	Not included
b	Supervised speed	ATB-code change & SSP
c	Max allowed speed considered by the driver	3DV window
d	ATP on board	ATP on board
e	Max allowed speed provided to the speed profile generation	Embedded in speed advice script
f	Speed profile & advice generation module	Performed manually
g	Speed supervision	Speed supervision

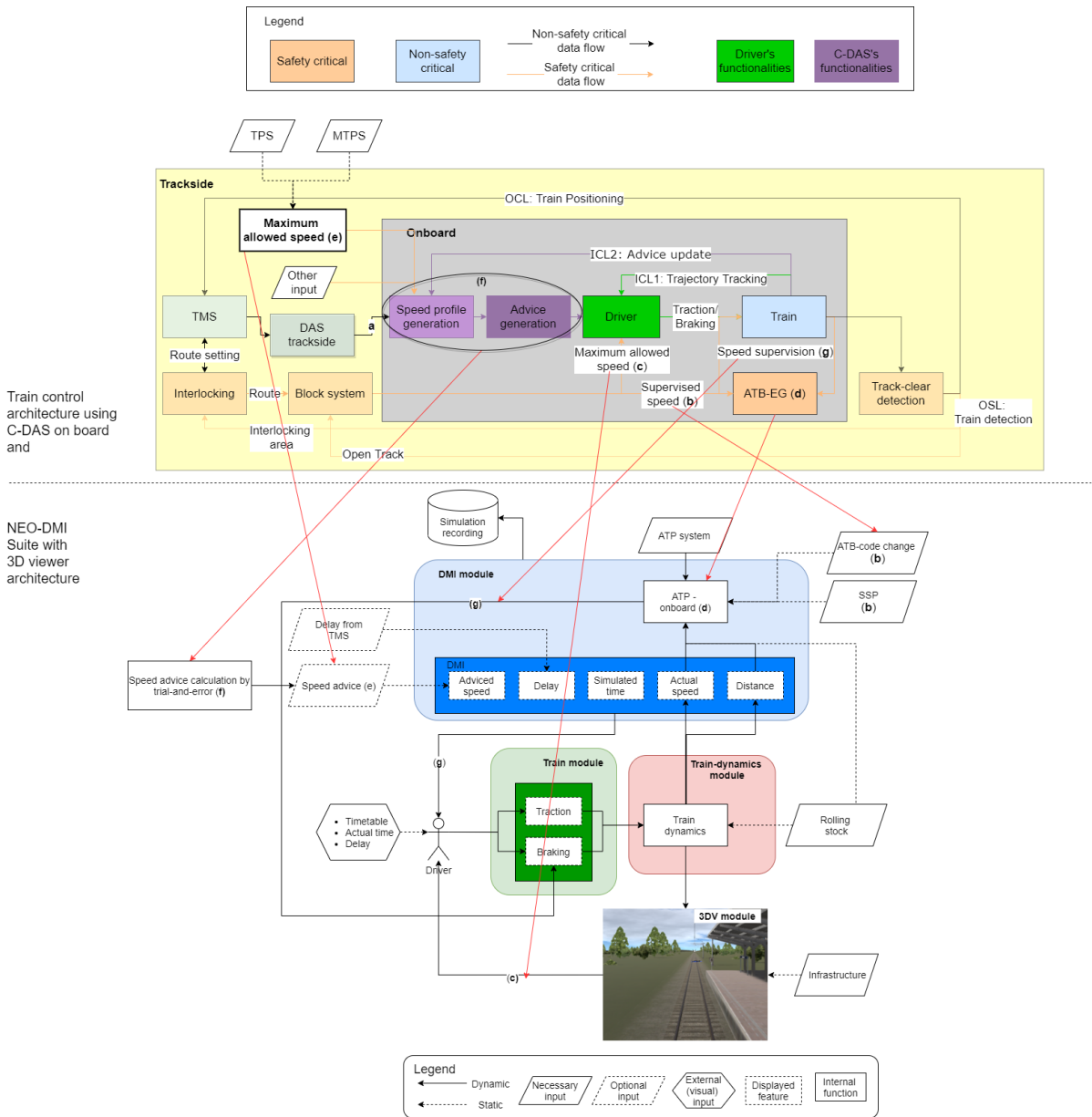


Figure 6.2: Correlation of modules between train control architecture using a C-DAS-On board and a maximum allowed speed module and NEO-DMI architecture

## 6.3. Experiment setup

This section discusses minor additions to the simulator so as to fit for the purpose of this study. Additionally, the development of the scripted input is explained. This regards the approach of modelling the advice reliability, train delay and other necessary input. Then the capacity analysis of the corridor is discussed. Also, this section gives approaches to model the train driving rules in the simulation environment. The section concludes by declaring the assumptions and limitations of the simulation setup.

### 6.3.1. Adjustments to the original simulator architecture

Apart from the scripted input, it was decided to include other information sources to perform the simulation. This information aims to make the train driving more realistic. First, a clock is used to display the actual time. An online Global Mean Time (GMT) service is selected for this purpose. Second, the driver must take into consideration the actual timetable. To that end, the simulated timetable is constructed as follows. Based on the Dutch Timetable 2020 and assuming departure from Haarlem at 0:00 the event times of the route until Leiden Centraal are included in Table 6.2. Assuming that the current GMT time (i.e. the time when the simulation begins) is 07:23, the simulated timetable is created by adding the simulation start time to the times of the original timetable (Table 6.2). Note that for intermediate stations, it is assumed that the train arrives and departs from the station within the same full minute. Both events are described by a single event time. Still, that is not the case for Leiden Centraal, the major station of the study area.

Comparing the actual operations with the timetable and the world clock, driver's situational awareness is enhanced. These two information sources are displayed on a dedicated monitor, distinct from the one that includes the simulator modules (Figures E.1). Each one has a dedicated window within the screen. It is assumed that the monitor setup does not challenge the driver's situation awareness.

Table 6.2: Simulated timetable of the series 6300 departing from Haarlem at 0:00 and heading to Leiden Centraal. The case study area stations are selected as explained in Subsection 5.1.1

Station (-Event)	Theoretic Timetable	Simulated timetable
Haarlem	0:00	7:23
Heemstede-Aerdenhout	0:04	7:27
Hillegom	0:10	7:33
Voorhout	0:17	7:40
Leiden Centraal-Arrival	0:22	7:45
Leiden Centraal-Departure	0:24	7:47

### 6.3.2. Development of general scripted input

The study area of the simulation is the area discussed in Chapter 5, i.e. the stretch between Haarlem and Leiden Centraal. Initially, the basic scripts (both necessary and optional, see also Subsection 6.2.1) to run the simulation are constructed. The scripts discussed in the following are ATP system, rolling stock characteristics, infrastructure, static speed profile (SSP) and ATB-code change.

As regards the ATP system the script file just contains the name of the ATP used by the scenario, i.e. ATB-EG or ETCS-L2. The rolling stock type used in the simulations is the SNG with six carriages, which is often used by NS for 6300 series. This train type has maximum accelerating capacity equal to  $0.6 \text{ m/s}^2$ , emergency braking equal to  $1.2 \text{ m/s}^2$ , braking rate to satisfy the ATB-EG braking criterium  $0.1 \text{ m/s}^2$  and maximum speed 140 km/h. The same maximum speed is considered for both ATB-EG and ETCS L2 operation.

The infrastructure script includes signals (both controlled and automatic), speed signs, coasting signs "S" (indicating next station), level-crossings, bridges and platforms. The infrastructure was retrieved from technical drawings (OBE-sheets, see also 3.2.3) and stored in a .csv file. Each piece of infrastructure was labelled with its name followed by its location expressed in km-linten. Then, the locations are transformed from kilometres into metres from the starting point of the simulation. For

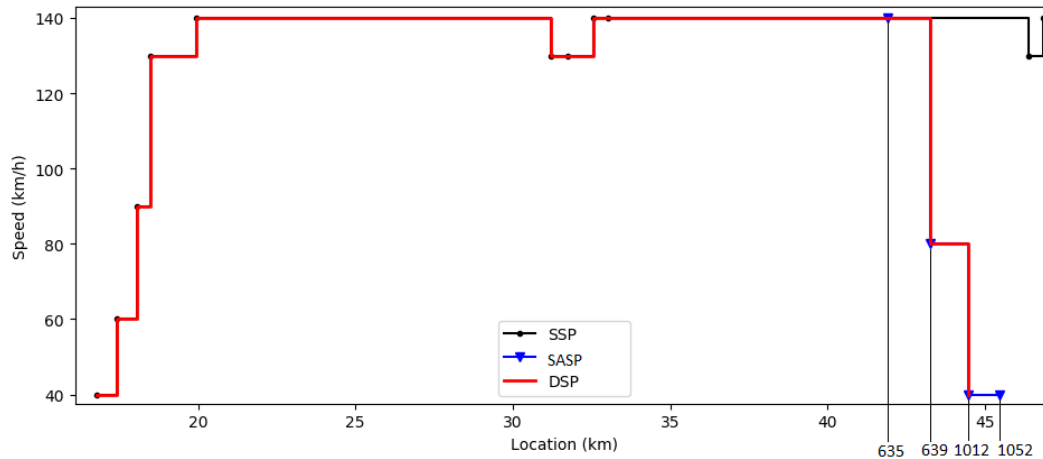


Figure 6.3: Construction of the dynamic speed profile (DSP) by merging the static speed profile (SSP) with the signal aspect speed profile (SASP)

ETCS-L2 scenarios, ETCS marker boards are placed on the same locations as these of the NS'54 signals.

Now, the construction of the SSP is explained. The SSP is applicable to both ATB-EG and ETCS L2 operation. In the SSP script, speed values are stored in km/h accompanied by a location. In order to construct this script, the locations of speed signs as well as the speed value which they display must be retrieved. This information is collected from OBE sheets.

Under ETCS L2 operation, this study does not consider any movement authority that demands for a speed change different from that imposed by the SSP. Therefore, no other scripts regarding ETCS L2 are developed. Yet, for ATB-EG operation an extra script is needed. The ATB-code change script is a trick to make the DMI show on the DMI window information coming from the ATP system, information which is not included in other scripts. By default, the DMI will display the ATB-code change and make the bell sound associated with a speed code change included in the SSP script. Yet, the same should be done for ATB-code changes coming from the signalling. This is achieved with the ATB-code script. On this script, the code change (and thus, speed change) imposed by a signal can be defined.

The ATB-code change script requires the signal locations as well as the ATB-codes stemming from their aspects. The signal locations can easily be derived from OBE sheets. So, the missing information to reconstruct the speed profile imposed by the signalling system under ATB-EG operation is the actual signal state and consequently, the speed limit stemming from it. The determination of the actual state depends on the actual operations. Yet, the simulator supports only static input and thus the signalling state will be static, too. For simplicity, this study assumes the signalling state of the examined track under nominal operations. According to a video on YouTube which displays footage from an onboard camera recording the route from Haarlem to Leiden Centraal, it was found that all signals showed a green aspect except from the last three signals before Leiden Centraal station (signals 639, 1012 and 1052 in Figure 6.3). Once the signal aspects were deduced, the speed profile stemming from the signalling system was constructed (Figure 6.3).

For a signal showing a green aspect, the speed limit stemming from it equals the speed value of the SSP at that part of the track, while in case the signal aspect is accompanied by a numeral and/or a flash, the speed limit must be interpreted as explained in Section 3.1. So, in the example of Figure 6.3 signal 635 shows a green aspect and given the value of 140 km/h of SSP at that location, the signal enforces a speed limit equal to 140 km/h. The matching of signal aspects to speed limits (shown in parenthesis) for the signals included in Figure 6.3 are: signal 1052–Yellow (40 km/h), signal 1012–Yellow-4 (40 km/h) and signal 639–Yellow-8 (80 km/h). Figure 6.3 includes the SSP of the track of the study area as well as the DSP for ATB-EG operation. The speed limit for ETCS L2 coincides with the SSP shown in Figure 6.3. The DSP value at every location of the track is calculated using Equation 4.1. Note that a DSP for ETCS includes the braking curves (European Railway Agency, 2016). Yet, the ETCS braking curves are not discussed in this study.

### 6.3.3. Scripted input regarding speed advice and aggregate delay

Figure 6.4 illustrates the interface between the developed data-mining tool and NEO-DMI. The interface is achieved by using the tool's output as input for the simulator. The data-mining tool yields the aggregate published delay per track-segment as well as the continuity of the data stream per train. Both files are time-based, while the simulator works on the basis of distances. Thus, a linear interpolation on the observed time-distance profile (mentioned as x-t diagram in Figure 6.4) is performed so as to define the location along the track where a delay was published (to the Routelint DMI) and the location where the position of the red signal could not be determined. The observed blocking time diagram for this train run has been calculated with the blocking time routine of the tool (see also Section 4.3.5). The produced distance-based delay as well as speed advice files are fed to the DMI module (see also Figure 6.1) of NEO-DMI.

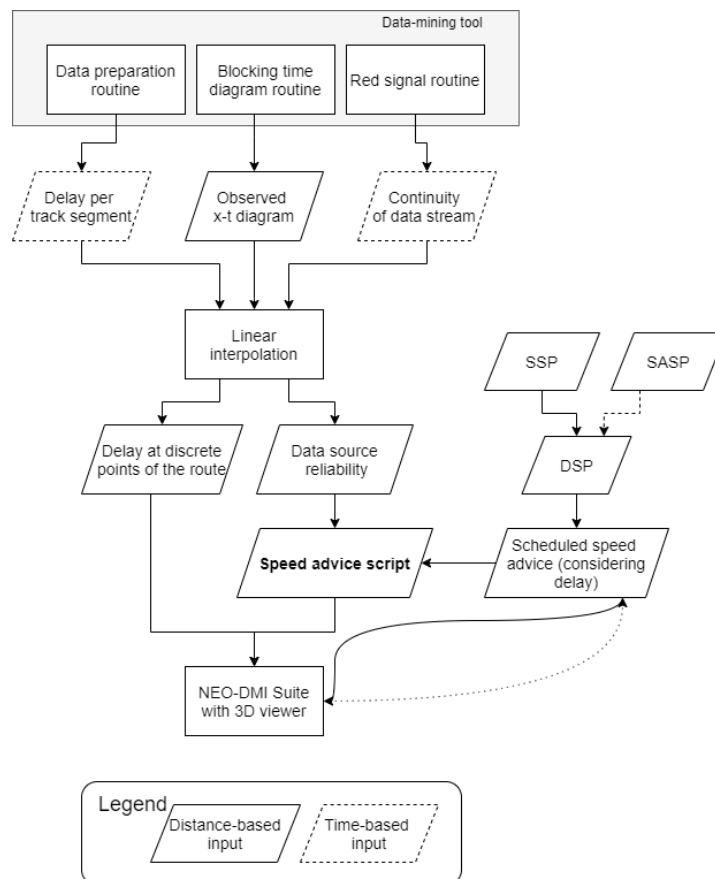


Figure 6.4: Interface between the data-mining tool and NEO-DMI simulator

Main goal is to construct the script that includes the speed advice (marked in bold in Figure 6.4). In this study, the speed advice file is augmented with the reliability of the data source and constrained by the DSP.

For ATB-EG operation, the DSP considers both the SSP and the signal aspect speed profile (SASP). For ATB-EG, SASP is modelled by the ATB-code change script (see also Subsection 6.2.1). By incorporating the ATB-code change script, this study models the speed advice's compliance with the NS'54 signalling system. For ETCS L2 operation, DSP coincides with the SSP. Still, the DMI module automatically displays and supervises the ETCS braking curves with respect to the speed restrictions imposed by the DSP.

At this point, the process for developing the scheduled speed advice script is explained. This comes as the result of a trial-and-error process. More thoroughly, an initial scheduled speed advice script is developed which includes some indicative speed values. These values are carefully selected so as to be in accordance with the DSP. Also, this initial script caters for the aggregated delay of the train (as

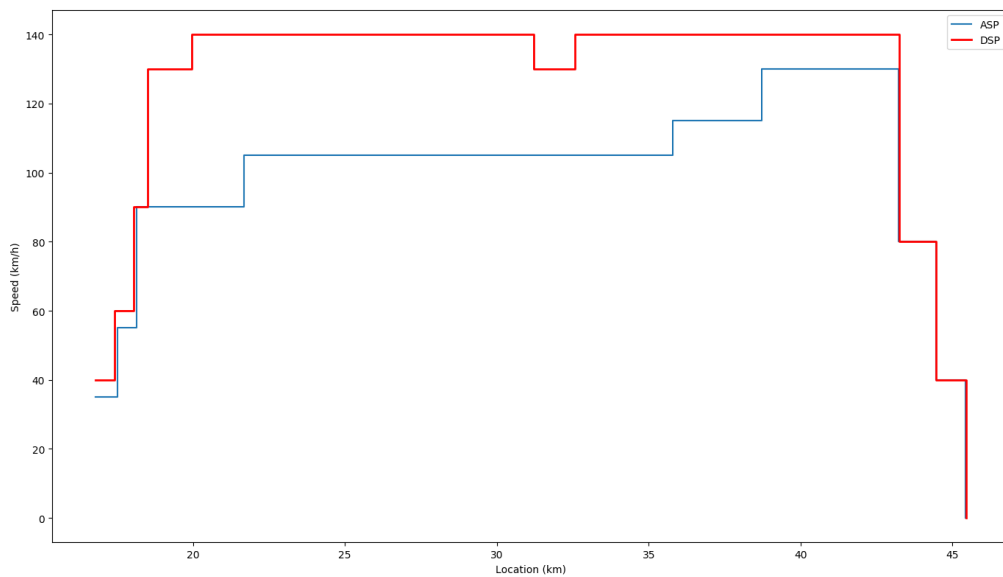


Figure 6.5: Advised speed profile (ASP) and dynamic speed profile (DSP) stemming from NS'54 along the route for a scenario

published in RouteLint). Then, the simulation is initiated. Principal attention is drawn to punctuality in case the amount of delay allows for it. Punctuality is checked consulting on the simulated timetable (see also Subsection 6.3.1). Punctuality at the major station (i.e. Leiden Centraal) is a priority but it is attempted to achieve punctuality also on the intermediate stations. In case the simulated train falls behind schedule, the values of the initial speed advice script are increased. In case of the opposite, the speed values are decreased or coasting is initiated earlier. The coasting point for the simulation is determined by looking at the average coasting point as it occurs from the observed speed-distance profiles retrieved from historical data. The process is repeated until speed advice that yields a punctual train run given the delay is derived. The feedback loop is marked as a dashed line connecting the NEO-DMI block with the scheduled speed advice block in Figure 6.4.

An example of the advised speed profile (ASP), i.e. the definitive version of the scheduled speed advice script, is illustrated in Figure 6.5. The timetable has the majority of the recovery time allocated between Haarlem and Voorhout. After Voorhout (location 38.6 km) there is only little recovery time. This is the reason why in Figure 6.5, the advised speed (130 km/h) approached the speed limit (140 km/h) after location 38.6 km. It can be seen that ASP respects DSP during the whole route.

The construction of the scheduled speed advice profile follows some criteria. These are:

- In nominal operations, speed advice is set 5 km/h less than the speed limit so as not to cause interventions from the ATP (e.g. from speed profile upgrading from 40 km/h to 60 km/h to 90 km/h results in advice of 35, 55, 85 km/h, respectively). In contrast, in case of disturbed operations the speed advice is set equal to the speed limit.
- In case of advice related to a speed limit improvement, the advice adjustment follows the operational rules. According to these rules, the speed improvement refers to the full train length and thus, the entire train must pass the location until the driver is allowed to accelerate. Assuming an average train length of 100 m, the speed advice is displayed 100 m after the location of a speed limit improvement.
- In case a speed advice needs to be displayed that is not related to a location of a speed limit change, the location as well as the value of this speed advice are determined by the trial-and-error earlier in this subsection.
- Points of applying coasting are not included in the speed advice because there is no way to model the "cut traction command" in the speed advice script. The driver must always be focused on the

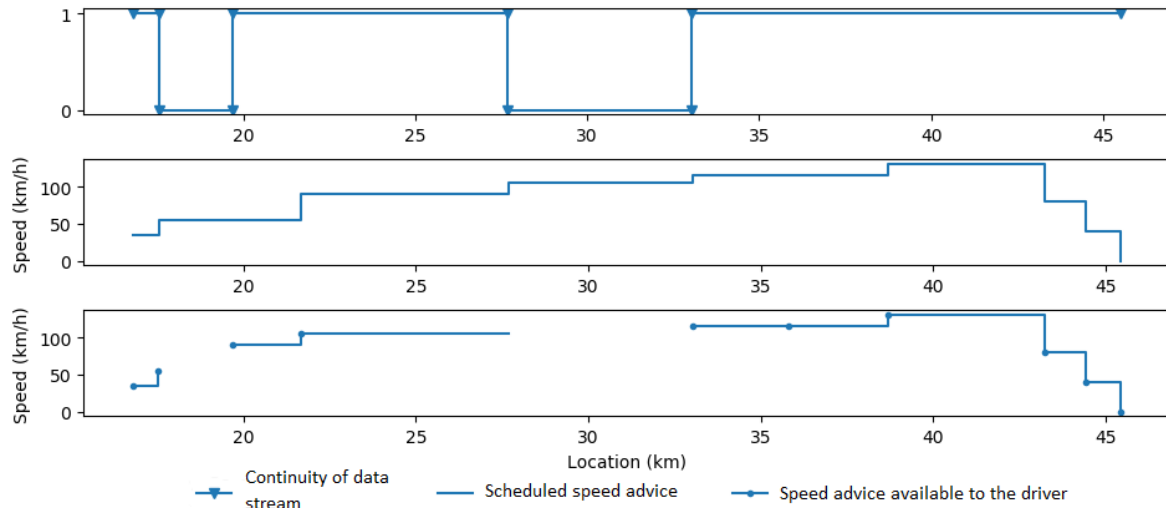


Figure 6.6: Procedure of developing the speed advice profile available to the driver for a scenario using baseline data. Upper: Continuity of data stream, Mid: Scheduled speed advice, Bottom: Speed advice available to the driver

3DV window, prepared to cut traction and disregard the speed advice once the train passes the "S" sign indicating a coasting point.

Once the definitive version of the scheduled speed advice script has been established, the speed advice is combined with the reliability information coming from the continuity of the data stream (Figure 6.4). The process to combine the continuity of the data stream (top sub graph in Figure 6.6) with the scheduled speed advice profile (mid sub graph in Figure 6.6) is shown in Figure 6.6. The data stream contemplated in the example is *baseline*. Sub-graphs of Figure 6.6 are correlated based on location. The speed advice profile available to the driver (bottom sub graph in Figure 6.6) is the product of the top and mid sub graph of Figure 6.6. For example, at a location before 20 km it was impossible to yield the red signal, while right after that location this turned possible. Additionally, around that location the scheduled speed advice was 60 km/h. As a consequence, before that location no speed advice is available to the driver while after that a speed advice of 60 km/h will be shown on the DMI window. This study models the former case (unavailable speed advice) by assigning a speed advice equal to zero (0 km/h) for these locations. Thus the driver must be aware that an advice of 0 does not suggest the train coming to a stand-still but that no speed advice is available for that part of the route.

#### 6.3.4. Capacity analysis of the examined corridor

In order to calculate the effect that the proposed framework has on corridor capacity, a blocking time diagram including the simulated 6300 series must be reproduced. Based on the simulated blocking time diagram, the effect that advice reliability has on capacity will be discovered by calculating the infrastructure occupation. Infrastructure occupation is the fraction of time required to operate a number of trains on a railway corridor for a given timetable pattern (Goverde et al., 2013). Infrastructure occupation is calculated using the timetable compression method which is based on blocking time theory (see also Section 4.3.5). The compressed timetable is free of buffer time between train trajectories. Yet, the scheduled running times include the recovery time for each train. Note that the recovery time is added to the technical minimum running time in order for the train to make up for small disturbances. The buffer time is set between successive train runs to prevent a delay being transmitted to other trains. The recovery time extends the running time, while the buffer time reduces the number of trains that can be scheduled (Pachl, 2014). Infrastructure occupation  $C$  is given by the formula:

$$C = \frac{\text{minimum cycle time}}{\text{planned cycle time}} \times 100\% \quad (6.1)$$

where *minimum cycle time* is the time duration between the departure times of the first train of two successive cycles and it is calculated using the compressed timetable.  $C$  is expressed as a percentage.

At this point, the objective is to determine the simulated blocking time diagram. The DMI records several parameters of the simulation every 2 s. For the construction of the simulated blocking time diagram only the location and time data are required. These two parameters allow for reproducing the time-distance profile of the simulated train. Recall that the tool has been run only for 6300 series. Thus, the data-mining tool is run for train numbers of series 2200, 1800/700, 2100 and 4600 that are in the same cycle time (i.e.  $T=30$  min) with the simulated train and for the train of 2200 series of the next cycle (i.e. first train of the next cycle).

The blocking time diagram for both the simulated and the observed trains is constructed according to the methodology explained in Section 4.3.5. Then the blocking time diagram of the simulated train must be integrated with the blocking time diagram derived from historical data. To achieve that, the time and distance values of the simulated trajectory are adjusted adequately. Note that in order to perform an appropriate capacity analysis, the whole corridor between Haarlem and Den Haag Centraal is considered and not only until Leiden Centraal. Yet, the simulation ends in Haarlem. For that reason, the simulated 6300 series are matched with the observed segment of 6300 series between Leiden Centraal and Den Haag Centraal. This is achieved by adjusting the departure time from Leiden Centraal of the simulated train with the same time of the observed train.

Section 3.3 discussed the blocking time components. This study contemplates two signalling systems. Both NS'54 (i.e. a three-aspect two-block signalling system) and ETCS L2 is used which also requires track-clear detection and it is based on fixed blocks. Therefore, the same components for both signalling systems are considered in the calculation of blocking times even though the calculation may differ. This study uses the blocking time components shown on Table 6.3 which are used in practice by ProRail except mentioned differently. The major difference between the two signalling systems regards the approach time of a block. On the one hand, the approach time for NS'54 equals the travel time  $TT_{previous\ block}$  of the train on the previous block. On the other hand, the duration from the time to brake from the train's speed on previous block  $\bar{v}_{previous\ block}$  until standstill is used for ETCS L2. In this formula, an average braking rate for the SNG rolling stock is used which equals  $0.6\text{ m/s}^2$ . As regards the running time, this equals the actual running time plus possible scheduled dwell time. Finally, the time to release the signal depends on the train's speed at the exit of the block  $v_{block\ exit}$  and on the train length  $L_{train}$  for both signalling systems.

Table 6.3: Blocking time components used in this thesis

Blocking time component (s)	NS'54	ETCS L2
Setup	3 (open track), 12 (interlocked area)	
Sight and reaction	9	7 <sup>1</sup>
Approach	$TT_{previous\ block}$	$\bar{v}_{previous\ block} / 0.6^1$
Running	Block running time (+ Dwell)	
Clearing	$L_{train} / v_{block\ exit}$	
Release	3	

<sup>1</sup> Suggested by daily university supervisor

After having yielded the compressed timetable, the nominator of Equation 6.1 equals the subtraction of the departure time of series 2200 for the considered period from the departure time of series 2200 for the next period.

### 6.3.5. Modelling operational rules in the simulation environment

The driver must adhere to a number of operational rules which are performed in daily practice. The first operational rule regards the dwell time at small stations. The published timetable of the Dutch railway network does not include departure and arrival times for intermediate stations. In nominal operations, both events must be performed within the published full minute. In practice, for intermediate stops and for Sprinter trains (as series 6300) a minimum dwell time of 24 s is applied. Having said that, during a simulation, once the train has arrived at an intermediate stop, the driver must wait for 24 s until departure. The driver can consult on the simulated clock included in the DMI to fulfil this necessity. The dwell time includes door opening and closure as well as passenger alighting and boarding.

Additionally, the driver must react to a speed limit improvement after the full train has passed the corresponding location. Reason for this is that a speed limit upgrade applies to the full train length and not just the train head (Brünger & Dahlhaus, 2014). In the simulator, the driver performs this operational rule by consulting the distance indication on the DMI. Consulting on the NS Trip Planner regarding the rolling stock of 6300 series used in peak/off-peak train, it was concluded that they have a length equal to 160 m and 60 m, respectively. Consequently, when the simulated train regards a peak period train, the driver reacts to a speed limit increase after 160 m or after 60 m in case of the opposite. Finally, the "S" signs placed upstream of a station are used in practice to point out the location to start applying coasting. The driver can see these signs via the 3DV window and uses them for the same reason. Yet, the location of the "S" sign serves only as an indication. The actual location of the track where the driver cuts off traction is a function of the actual speed, the driver's expert knowledge as well as the current operations (disturbed or not).

In case there is sufficient running time supplement, the driver is encouraged to follow the optimal driving strategy aiming for energy efficiency (Albrecht, 2014). According to this strategy, the driver must apply the following sequence of driving regimes: maximum acceleration – cruising at the optimal cruising speed, which may be below the maximum speed, depending on the running time supplement – coasting – maximum service braking until standstill. In case of disturbed operations, the coasting phase is omitted.

In the case of a down speed, the braking behaviour depends on the ATP system used. Under ATB-EG operation, the driver starts braking when the ATB-onboard model starts to intervene (continuous bell) given the change in ATB code (single bell sound). Then, sufficient braking is applied only to meet the braking criterium until reaching the threshold of the target speed (three bell sounds). No more than that is applied so as not to lose on capacity. In case of ETCS-L2 operation, the curve of the permitted supervision limit is followed.

### 6.3.6. Assumptions-Limitations

To start with, the advice is calculated offline. The speed constraints stemming from the signalling are modelled in the calculations of the advised speed profile. Still, the simulator does not facilitate a model of proving whether a conflict has occurred during the simulation. Consequently, although the advice is designed to be compatible with information coming from the signalling, it cannot be guaranteed that the advice has led to a conflict in the simulation environment. In fact, a conflict can only be observed after reproducing the blocking time diagram of the simulated train and of the observed trains from historical data (see also Subsection 6.3.4).

A fundamental assumption of this study is that the driver trusts the advice and follows it carefully. Moreover, it is assumed that the driver adjusts the train controls to follow a new speed advice as soon as this has been announced. The time error between the two events is deemed unimportant.

It is selected to present speed advice. This form of advice is considered as adequate to fulfil the objective of this study as discussed in Subsection 2.7.4. Traditionally, it is assumed that the selection of presenting speed advice (form of the advice) as well as the simulator interface (included in Appendix E) do not have a negative effect on the human factors of the problem.

At this point, it is important to discuss the level of driving experience required to perform a simulation. According to a study (D. Large et al., 2014), the human operator of a scientific-oriented train simulator can be inexperienced without this challenging the railway safety rules (over-speeds and SPADs) (see also 2.7.4). This finding justifies the recruitment of inexperienced drivers due to the inability to engage professional drivers for this study. Therefore, the inexperienced driver is not expected to affect the main objective of the simulation. Based on this, the simulations are performed mainly by the author.

It is important to look into the time character of the two major sources of DAS input; the route plan and the signalling constraints. Initially, the developed red signal framework intended a C-DAS. Yet, the simulator does not facilitate a model of it. Instead, the static speed advice is manually produced. Then the advice is enhanced with the signalling constraints. The latter data source gives a dynamic character to the DAS. It is assumed that the limitation of not having a DAS that performs a real-time calculation of new route plans does not affect the purpose of the simulation to test the fundamental hypothesis

## 6.4. Scenario development

A scenario-based assessment is set to test the hypothesis presented in Section 6.1. Each simulation scenario comprises of three decision variables: aggregate predecessor delay, train type (peak/off-peak) and advice reliability. Initially, a scenario is built based on the delay of the predecessor train as well as the type of the considered train. Predecessor's aggregate delay is modelled as explained in Subsection 6.3.3. Moreover, train type is modelled in the simulation environment by the location where a traction increase is applied due to a speed limit improvement. Recall that a speed limit refers to the whole train length. This necessity is modelled by having the driver react at different distances after the location of the speed increase (see also Subsection 6.3.5).

The scenarios consider a range of predecessor train's delay. Note that delays are recorded in RouteLint per track-segment and that only track-segments between Haarlem and Leiden Centraal are considered. Both delay and train type are recorded by the data-mining tool. The location of announcing a delay was explained in Subsection 6.3.3. For each one out of the six scenarios, a train run that fulfilled the criteria (combination predecessor delay and train type) was randomly selected from the historical data.

Following, each scenario is run with one of the four different advice variants. Thus, each *advice variant* corresponds to different advice reliability. Having said that, for each variant of a scenario the same delay script is used while the speed advice script differs since it is the data source that embeds advice reliability. Here, it is assumed that the advice has the same quality as the reliability of the data source that provides input to the DAS used. So, on the remainder, when *advice reliability* is mentioned, the reliability of the input data source is implied. The advice variants are:

- No DAS. No advice is provided to the driver. This variant will capture the driver's ability to cope with certain operational cases having no support from external systems. In practice, although no advice is displayed, this variant is assumed to have zero reliability so as to make it comparable with the other variants. In the following, this variant is called *No DAS*.
- N-DAS over ATB-EG with baseline data feed. The advice quality equals the reliability achieved with the *baseline* data source. In the following, this variant is called *Baseline*.
- N-DAS over ATB-EG with infill data feed. The advice quality equals the reliability achieved with the *infill* data source. In the following, this variant is called *Infill*.
- N-DAS over ETCS L2 with flawless data feed. The advice of this variant is considered to have perfect (100 %) reliability. On the remainder it is called *ETCS L2*.

## 6.5. Scenario analysis

The analysis of scenarios presents the calculation of input regarding advice reliability and delay. Also, this section includes numerical results of the simulation.

### 6.5.1. Input determination for the scenarios

Three scenarios have been constructed to assess the hypothesis. It was revealed from historical data that the train-date combinations included in Table 6.4, satisfied the necessity for the decision variables train type and predecessor's delay. The delays for both the train and its predecessor regard the maximum aggregate delay observed on the stretch between Haarlem and Leiden Centraal. Table 6.4 also includes the components  $T$  and  $MTBF$  for calculating reliability. According to Table 6.4, the historical data reveal that scenarios 1 and 2 arrived on time at Leiden Centraal, while scenario 3 arrived with 8 min delay.

Table 6.4: Scenario setup

No.	Train type	PD <sup>1</sup> (min)	TD <sup>2</sup> (min)	MTBF <sub>baseline</sub> (s)	MTBF <sub>infill</sub> (s)	Train	Date
1	Peak	+0	+2 <sup>3</sup>	504.8	750.6	6373	13/12/2019
2	Off-peak	+3	+2 <sup>3</sup>	545.2	1173.3	6359	18/12/19
3	Peak	+7	+8 <sup>4</sup>	595.2	843	6325	24/10/19

<sup>1</sup> Predecessor delay,

<sup>2</sup> Train delay,

<sup>3</sup> Observed at track LG. On-time arrival at Leiden Centraal,

<sup>4</sup> Observed at track within Leiden Centraal station.

The following lines explain the entire analysis for Scenario 1; from the construction of the input to the calculation of the infrastructure occupation. The same procedure is followed for the other two scenarios. The scenario presented in the following considers a case where a 0 min delay has been observed for the predecessor and the considered train is a peak hour train. Scenario 1 regards train 6373 as observed on December the 13<sup>th</sup>, 2019. The train experiences a delay of +2 min at maximum. According to the timetable 2020, the train numbers included in the same cycle period are: 2260, 1860, 2173 and 4658 and 2262 is the train number of the successive cycle period. The data-mining tool is run for these train numbers and for day 2019-12-13 in order to derive their observed time-distance diagram. The predecessor train that experiences a delay of 0 min is train 2260.

The continuity of the data stream for the two data sources for Scenario 1 is shown in Figure 6.7. Initially, the discontinuities (0 or 1 on Y-axis) are given according to time (primary X-axis). The time values are interpolated to the realised time-distance profile so as to yield the locations of the corresponding discontinuities (secondary X-axis). Following, these locations are used to construct the speed advice script. According to Figure 6.7, *infill* manages to entirely bridge the gap of *baseline* data between locations 17.549-19.700 km and 45.500-46.076 km, while it partially bridges the *baseline* gap between 27.677-33.014 km.

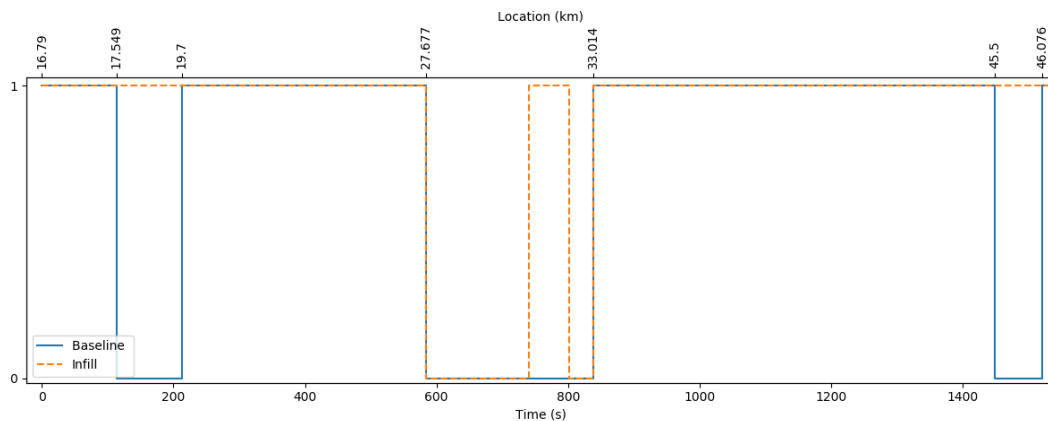


Figure 6.7: Continuity of *baseline* and *infill* data stream for Scenario 1. The graph expresses the continuity of each data stream with respect to time. The landmark locations of the discontinuities are determined via interpolation using the realised time-distance profile

Figure 6.8 demonstrates the compressed simulated blocking time diagram for Scenario 1. In this figure, critical blocks are marked with a red circle. The overlapping blocks in Leiden Centraal station do not constitute conflicts since all trains share different tracks in this occasion.

Table 6.5 includes the advice available to the driver for the advice variants that include reliability, i.e. Baseline, Infill and ETCS L2. The locations of Table 6.5 are adjusted so as to indicate distance from the start of the simulation. So, value 16.79 km (departure point at Haarlem station) is subtracted from all locations. Note that the speed advice for variants *baseline* and *infill* caters for the down speed before Leiden station (location 45.5 km in Figure 6.3 or adjusted location 28713 m in Table 6.5). In order to achieve a feasible train run, the advised speed between Voorhout station (adjusted location

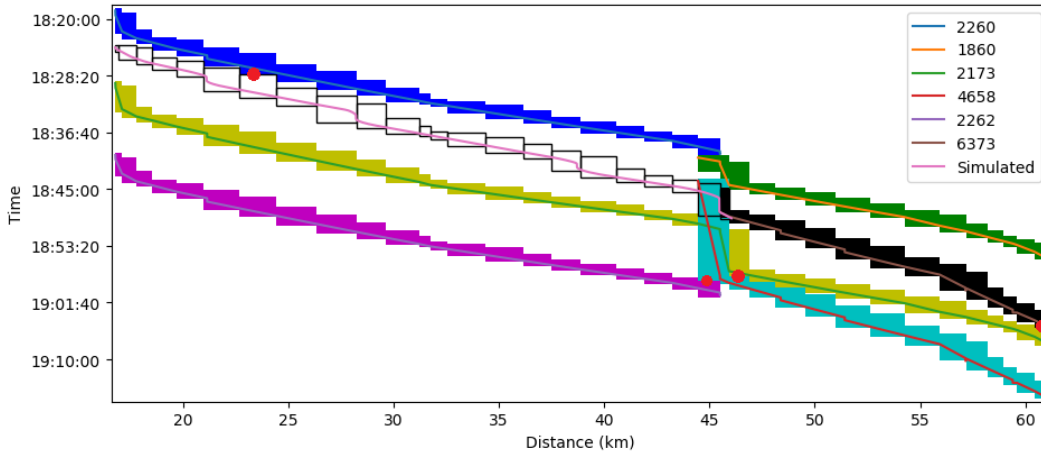


Figure 6.8: Compressed blocking time diagram of Scenario 1 using *Baseline* data. Red dots indicate the critical blocks.

21910 m) until the location of the down speed to 80 km/h is set equal to 130 km/h. Yet, advising a lower speed (120 km/h) for ETCS L2 is enough to reach Leiden Centraal station on time. Note that advice is calculated until Leiden Centraal stations (i.e. until 45.5 km or 28710 m). Also note that speed advice equal to zero in Table 6.5 does not imply the train coming to a stand still. Instead, it indicates the start of a discontinuity (see also Subsection 6.3.3).

The calculation method of the advised speed profile available to the driver with *baseline* reliability of Scenario 1 is included in Figure 6.6. Likewise, the advised speed profile available to the driver with *infill* is calculated. It is important to mention the calculated advice takes into consideration the +2 min delay of Scenario 1 which, from interpolation, it was announced in RouteLint at location 2898 m. Hence, speed advice at locations after 2898 m has slightly higher values so as to take advantage of the slack time included in the timetable. Finally, the advised speed profile available to the driver with *ETCS L2* reliability is the ASP line shown in the example of Figure 6.5.

Table 6.5: The advised speed profile available to the driver according to different advice variants of Scenario 1

		Advice variant			
Baseline		Infill		ETCS L2	
Location (m)	Speed advice (km/h)	Location (m)	Speed advice (km/h)	Location (m)	Speed advice (km/h)
0	35	0	35	0	35
722	55	722	55	722	55
759	0	1359	90	1359	90
2910	90	4890	105	4890	105
4890	105	10887	0	19000	115
10887	0	14304	115	21920	120
16224	105	15018	0	28713	40
19000	115	16224	115		
21920	130	21920	130		
26550	80	26550	80		
27765	40	27765	40		
28713	40	28713	40		

### 6.5.2. Simulation results

Figure 6.9 summarizes the simulation results for the three scenarios. Detailed values of the results can be found in Table 6.6. In Figure 6.9, advice variants of the same scenario are connected with a line. for all scenarios. As a general observation, infrastructure occupation (*C*) increases as predecessor's

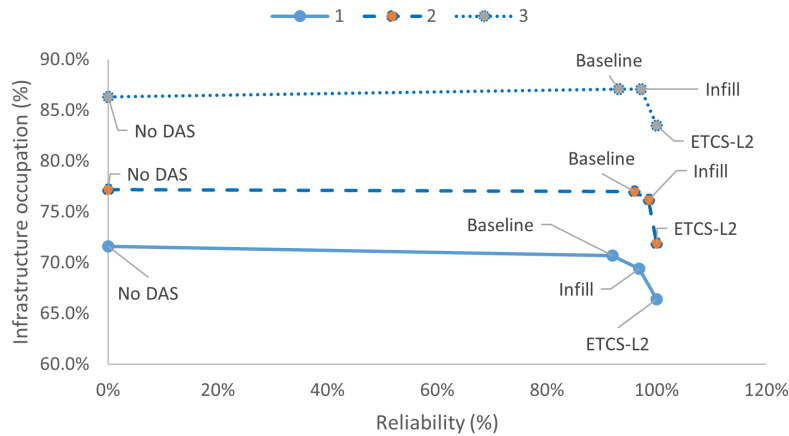


Figure 6.9: Simulation output regarding infrastructure occupation for the different scenarios and their reliability variants

Table 6.6: Scenario results

No. Scenario	Advice variant	Conflict	R(%)	C (%)
1	No DAS		0%	71.6%
	Baseline		91.9%	70.7%
	Infill		96.8%	69.4%
	ETCS-L2		100%	66.4%
2	No DAS	×	0%	77.2%
	Baseline	×	95.9%	77.0%
	Infill	×	98.5%	76.2%
	ETCS-L2		100%	71.9%
3	No DAS		0%	86.3%
	Baseline		93.1%	87.1%
	Infill		97.2%	87.1%
	ETCS-L2		100%	83.5%

delay increases. Also, ETCS L2 variant leads to better infrastructure occupation than the ATB-based variants. Note that the simulated speed profile of the No-DAS, Baseline and Infill variants of Scenario 2 leads to a conflict (Table 6.6). Those conflicts occur at the critical block between 2200 and 6300 series which is located on the open track after Heemstede Aerdenhout station (Appendix F).

For Scenarios 1 and 2, a decreasing trend of infrastructure occupation can be observed as advice reliability increases. This finding reinforces the initial hypothesis of this study. Also, for these two scenarios, advice with *infill* reliability leads to better *C* than *baseline*. Thus, the contribution of this study, i.e. fusing TPS with MTPS for real-time train positioning addressing a C-DAS, indeed leads to better capacity usage compared to a C-DAS that would use the current data stream (*baseline*) of ProRail systems on board NS trains.

For Scenario 3, No-DAS variant leads to smaller *C* than the *baseline* and *infill*. Additionally, *baseline* and *infill* variant of Scenario 3 yield equal *C*. Based on these findings, two conclusions can be made. On the one hand, in disturbed operations –such this of Scenario 3– the hypothesis of increased reliability leading to better capacity usage, does not hold. On the other hand, not using a DAS can lead to better capacity usage in that case. The latter conclusion may arise because the produced advice in this study is static and manually produced, thus does not consider the real-time operations.

## 6.6. Discussion

The NEO-DMI simulator is used to assess the behaviour of the proposed red signal framework on a DAS. The hypothesis being tested states that the reliability of the advice produced by a DAS is negatively related to the capacity usage. This hypothesis is tested based on scenarios using sensitivity

analysis.

NEO-DMI is an event-based simulator which performs micro-simulation using distance-based scripts. NEO-DMI has three modules: train, DMI and 3 DV. NEO-DMI includes a model for all the on-board functions of the train control architecture. This study uses the S-DAS model included in NEO-DMI.

All input relevant to a simulation is scripted. Each feature is modelled by setting the attribute feature along with its location from the start of the simulation where it should occur. The basic calculation regards the speed advice which is available to the driver. Advice reliability is embedded in the available speed advice to the driver. This advice is calculated offline using an iterative process. The goal of this iterative process is to construct a speed advice which satisfies all the following attributes: reliability of the data stream with which the red signal is determined, speed limit stemming from the DSP and punctuality (if possible).

The simulations are performed per scenarios. Each scenario has three decision variables: aggregate delay of the predecessor, train type and advice reliability. The former two decision variables were retrieved from historical RouteLint observations. Then, the third decision variable was calculated by the data-mining tool using the former two decision variables as input.

Advice reliability is segmented into four variants: No DAS as well as DAS using baseline, infill and ETCS L2 data feed. The variants are set in increasing order with respect to advice reliability. The hypothesis was tested against three scenarios; a peak train having zero delay (scenario 1), an off-peak having +3 min delay (scenario 2) and a peak train having +7 min delay (scenario 3). Thus, only scenario 3 is conflicting. The hypothesis is well supported by scenarios 1 and 2. In other words, as the advice reliability increases, infrastructure occupation decreases. Nevertheless, this statement does not hold for the conflicting scenario 3. In fact, baseline variant yields infrastructure occupation equal to that of infill, while driving without a DAS leads to better capacity usage than the afore mentioned variants.

# Conclusions and Recommendations

The final part of this thesis consists of the conclusions and recommendations which are the result of this thesis. After a brief discussion, the research questions of Chapter 1 are answered. Then, the contributions of this study to both academia and industry are presented. Finally, recommendations for future research and improvement of the proposed model are discussed.

## 7.1. Conclusions

This section includes a short discussion as well as the answers to the research questions.

### 7.1.1. Discussion

This thesis intended to address the problem of advice produced by a DAS leading to conflicts. It was selected to tackle this problem by providing a real-time data feed to the DAS equipment regarding the actual signalling information. The goal of acquiring signalling information can be scoped down to retrieving only the red signal since the other necessary functions can be offered by ProRail systems. Two train positioning systems provided by ProRail, were tested for their ability to yield the red signal; TPS and MTPS. The data sources show certain latency in delivering the desired function. This latency was quantified by the reliability (as defined in RAMS) of the data stream which is closely related to the continuity of a data stream as defined in the the RNP framework. A DAS will use this input to calculate the advice. Inevitably, the advice will suffer with at least the reliability of the input data. This study assumed the advice reliability being equal to that of the input data.

The contribution of this study pertains in the way MTPS is combined with TPS to yield the red signal in real-time. The case study findings revealed that the contribution indeed leads to more reliable advice for the majority of the cases. The reliability of *baseline* (TPS) and *infill* (TPS + MTPS) information in yielding the red signal was examined through historical data.

The numerical results showed that indeed *infill* data manage to yield a more continuous data stream of providing the DAS on board with the red signal in real-time and thus, increase the DAS's awareness regarding the actual signal state. Especially on open tracks, the novel data source (*infill*) manages to bridge the gaps that *baseline* data experience. In detail, *infill* data manage to decrease the frequency with which the red signal knowledge is lost by 43.5%. This frequency is captured by the mean time between failures (MTBF). The median value of MTBF increased from 543.0 s with *baseline* data to 779.3 s with *infill* data. MTBF is the core component of the formula calculating reliability (the ability of a system to work without interruptions) as defined in the RAMS framework. The introduction of *infill* data increases the total system reliability by 1.9% (from 95.9% with *baseline* to 97.8% with *infill*). Still, the introduction of MTPS does not always lead to increased system reliability. In fact, for a 11.4% of the cases, the introduction of MTPS makes the solution worse-off with respect to reliability. Possible reason to this is the limited availability of MTPS data on the examined corridor.

In the end, simulator experiments were deployed to validate the proposed red signal framework. The results showed that for some cases, this framework can lead to better capacity usage when it is

fed to a DAS.

### 7.1.2. Answers to research questions

First, the sub-questions are answered:

1. *Which data sources are available to improve the awareness level of a DAS regarding actual signalling status on open tracks equipped with ATB-EG?*

This study meets this goal by wisely combining existing ProRail systems and proposing a framework of the missing function. The approach to increase the actual signal state awareness is by providing the maximum allowed speed on board in real-time which embeds the signal aspect speed profile (SASP). The only missing function for constructing the SASP is a module that delivers the red signal. The remaining necessary information from ProRail systems is shown in Table 7.1.

The contribution of this study is that it determines the red signal by locating the predecessor mostly when it is on an open track. Train positioning data are relevant to achieve this. ProRail systems that provide train positioning information and which can be used for the aforementioned goal are TPS and MTPS. TPS performs train positioning using real-time information from the Dutch train describer system TROTS. TROTS performs train positioning by combining track occupation information with train numbers. MTPS is a train positioning system that uses both TPS and GPS data. In case a train is running in an area with more than one parallel tracks, MTPS manages to yield train positions that are referenced to the correct track. A map-matching technique is used to perform that task.

Also, certain configuration files are required. These files regard the topology of signals and blocks, the location of signals as well as the correlations of aspects of adjacent signals. Dynamic input regarding the actual train position and the adjusted route plan is required, too. All necessary input for the SASP construction are included in Table 7.1.

Table 7.1: Necessary information to reproduce the signal aspect speed profile

Attribute	Source	Content	Time-dimension
Signal/block topology	Configuration file	Signal/block-IDs adjacent to each signal/block-ID	Static
Signal Location	"	Signal coordinates [in route-ribbon]	Static
Aspect correlation	"	Aspect correlation of adjacent signal-IDs	Static
Train position	TIMTIM	Train coordinates [in route-ribbon]	Dynamic
Planned route	RouteLint	Planned downstream track-segments	Dynamic
Red signal	This study	signal-ID	Dynamic

2. *Which architecture allows for an effective interface of DAS to additional data sources to increase reliability on signal aspect information?*

This study selected a C-DAS-On board architecture because it offers a real-time connection to the TMS which can help for upgrading the proposed framework in the future to address disturbed operations in real-time. Another reason to this, is that TPS, one of data sources used for red signal determination, is already available on board NS train via RouteLint. Consequently, the signal aspect speed profile is easy to be directed on board and thus a DAS architecture that calculates optimal speed profiles on board should be opted for. DAS-On board is such an architecture. Thus, the migration to this solution is deemed as easier compared to other DAS architectures.

3. *Which mathematical algorithm can efficiently support the combination of multiple data sources to improve awareness of DAS over ATB-EG?*

A data-driven approach was selected to analyse the potential of TPS and TPS assisted by MTPS data to yield the red signal. It is a data-driven approach since the algorithm is based on the format of RouteLint data. The developed data-mining tool yields whether the red signal can be determined with a given data source. Thus, the tool only determines the potential of a data source to yield the red signal and it does not conclude on an actual *signal-ID* that indicates the signal showing a red aspect.

4. *How does the advice reliability of a DAS — whose awareness of the actual signal state on open tracks has been improved with a data-driven method — affect a corridor's capacity when compared to DAS/ETCS L2 operation?*

In order to answer this question, the following hypothesis is constructed:

increased advice reliability → increased driver acceptance → better capacity usage.

where *advice reliability* is input to the simulation, *capacity usage* is the measurable variable and *driver acceptance* is the connecting factor between the input and the measurable.

The hypothesis requires some assumptions to support the logical connection of the hypothesis. The assumptions are the following:

- The driver trusts the advice,
- The driver follows the advice precisely,
- Better capacity usage is among the DAS objectives.

Then, the behaviour of the output can be directly connected to the input quality. The hypothesis was tested on a simulator using scenarios. For each scenario, predecessor trains have different amount of delay and the advice is affected by the reliability of four variants. The variants are: No DAS used, DAS that produces advice with reliability equal to that of TPS data, DAS that produces advice with reliability equal to that of TPS + MTPS data, and a DAS using the perfect data of ETCS L2. The former three advice variants operate over ATB-EG, while the latter variant operates over ETCS L2. Based on a sensitivity analysis, it was found that indeed the hypothesis holds for undisturbed cases or cases with minor disturbances. Yet, the hypothesis does not hold for considerably delayed cases. A possible reason to this is that the advice with which the signalling information is combined is static and manually constructed. It does not come from an optimization procedure as done in practice by the speed profile calculation module of a DAS.

Having questioned the research sub-questions, the main research question can be answered.

*What are the actions that must be taken towards improving a conceptual DAS's awareness of the actual signal state on open tracks equipped with ATB-EG aiming for better capacity usage on Dutch railway corridors?*

First and foremost, the way in which the actual signal state is provided to the DAS equipment must be determined. This thesis opted for the solution of acquiring real-time information of the signalling through locating the most relevant red signal to a train. In turn, the most relevant red signal was yielded by locating the predecessor train in real-time.

Next, the correct data sources that can provide this real-time train positioning must be determined. This study concluded that TPS and MTPS can satisfy this need. Moreover, configuration data are necessary. Then, a framework which assesses the quality of train positioning using these data sources must be established. Reason to this is that railways need a similar framework to the aviation industry (Required Navigation Performance) for assessing GPS utilization on railway applications. Another reason is to quantify the quality of input data to a DAS system which highly affects the quality of the product (advice).

Then the DAS architecture must be selected. This study selected a C-DAS-On board architecture because it offers a real-time connection to the TMS and it already delivers the signalling constraints on board. Therefore, it is advised to opt for this DAS architecture (DAS-On board) which calculates the speed profiles on board.

This study also defined the interface between the actual signal state framework and the onboard DAS equipment. It was selected to feed the signal aspect speed profile through a data stream that provides the maximum allowed speed of the track.

In the end, it is essential to test whether the proposed model can in fact lead to better capacity usage. Preliminary results of the case study showed that the proposed framework can lead to decreased infrastructure occupation in certain cases.

## 7.2. Contributions

The contributions to the industry regard the railway industry in general as well as ProRail. The contributions are:

- The delivery of a framework that can serve as the foundation for developing a C-DAS-On board with increased awareness of the actual signal state. Such a DAS is expected to pose less conflicts making it more accepted by the driver and therefore increase the DAS's effectiveness. Since one of the DAS goals is to improve capacity usage, reliable advice (as the outcome of reliable input) will lead to increasing the number of trains operating on a railway corridor. The proposed conceptual DAS can constitute a low-cost alternative for addressing capacity issues on certain bottlenecks of the Dutch railway network until the complete roll out of ETCS L2.
- ProRail benefits from this study since further potential of its systems has been revealed.
  - This study delivered the missing module which combined with other ProRail systems can be used for developing a C-DAS with increased awareness of the actual signal state.
  - MTPS was proven to be a liable solution in assisting TPS for real-time train positioning. Also, the weaknesses of MTPS were revealed which can be taken into consideration for further improvement of the system.

On the other hand, this study contributes to academia in three distinct ways:

- An interface between the module that provides the real-time knowledge of the signal state and the on board DAS equipment has been introduced. Research studies or existing DAS systems reported that they achieved to cope with conflicts by following this approach but none of them gave details into how this was done.
- An assessment framework was delivered which can be used for appraising the performance of the C-DAS who is fed with the actual signal state and in general for non-safety critical railway functions that use GNSS systems. Sub-contribution of this contribution is that two new KPIs were proposed which are considered in relative literature.
- It was proven, on a simulation environment, that there is a relation between advice reliability and capacity usage.

## 7.3. Recommendations

Based on the conclusions and contributions discussed on this chapter as well as the limitations described in the previous chapters, certain recommendations are proposed. The recommendations regard the improvement of the current model and points for future research on the topic are proposed.

### 7.3.1. Recommendations for improvement of the current model

The following points for the improvement of current the model are recommended:

- Determine the *signal-ID*. The data-mining tool reveals the ability of a data source to locate the predecessor train. Increasingly, it informs whether the red signal can be inferred. Still, a routine that realizes the actual *signal-ID* has not been developed in this study. It is highly recommended to develop this routine since it is an indispensable component of the framework for constituting a C-DAS aware of the actual signal state.
- Reproduce the signal aspect speed profile (SASP). Such a module is necessary for deriving the approaching signal aspect in real-time. Still, no such routine has been developed in the context of this thesis.
- Validate the red signal determination. This study considered TPS and MTPS as totally trustworthy. Given this, when the predecessor train could be located on a single block-section, it would known

for sure that the signal protecting that section showed a red aspect. Increasingly, after having reproduced the SASP up to the location of the train, the aspect of the signal the train approached would be determined with 100% accuracy. Yet, the integrity of the red signal framework must be validated. This will further reveal the quality of the framework and it is expected to further increase the acceptance of the system from the market's perspective. The validation can be performed by comparing the actual signal aspects a train is facing from a video captured with a camera mounted on the train, and running the tool for the same historical train run. In short, by validating the signal aspect knowledge, the red signal determination framework will be validated, too. Needless to say that the proposed validation requires the implementation of the previous two points of recommendation.

- Improve the efficiency of the data-mining tool. In Subsection 4.3.1 it was discussed that the tool reads records which correspond to TPS events that are irrelevant to the red signal determination. This suggests that the time efficiency of the tool can be increased if these events are omitted from the process. This can be considered as a point of improvement of the data-mining tool.
- Include the *GpsGenericMessageHandler* publication service of MTPS in the analysis. Recall that *TpsmessageHandler* publishes train positions, referenced on the correct track which are expressed in the railway track positioning system, while *GpsGenericMessageHandler* expresses track-referenced train positions in GPS coordinates. Also, each publication service has a unique set of positioning solutions for the same train. This study used only the *TpsmessageHandler* service which was found to suffer from information gaps on the study area. If the *GpsGenericMessageHandler* service is used combined with the *TpsmessageHandler*, it is believed that the availability of MTPS along the examined railway corridor will drastically be improved.
- Use *infill* data for the RNP-availability calculation. This study calculates RNP-availability using solely *baseline* data. Instead, using *infill* is likely to further increase the RNP-availability of the proposed red signal framework.
- Blocking time diagram compression using optimization. The blocking time diagrams were manually compressed. This method is believed to have certain inaccuracies and thus, lead to a somehow inaccurate evaluation of the infrastructure occupation. Given this, it is recommended to opt for an optimization method for compressing the simulated blocking time diagrams.
- Assessment of the red signal framework on a dense corridor. The proposed framework has been tested on a peripheral corridor of the Dutch railway network. Still, testing the framework on dense traffic corridors within the Randstad area (e.g. Hoofddorp-Schiphol-Amsterdam Zuid) can shed light into the actual potential of the framework with respect to capacity. Also, the model has been tested only for a single direction and for a certain part of the corridor between Haarlem and Den Haag Centraal. It is recommended to test the tool for both directions and for the entire corridor.
- Perform more experiments on the corridor of the study area. More experiments are required to test the fundamental hypothesis of this study, especially for conflicting trains.
- Run simulations with a professional driver. The simulations were performed by the author who has no experience in real train driving. It is recommended to perform the simulations with a professional train driver. By doing so, a more trustworthy value regarding the proposed framework's potential to improve capacity will be revealed.

### 7.3.2. Recommendations for future research

The proposed framework for constituting a DAS aware of the actual signal state on open tracks was tested on a S-DAS, since that was the only DAS model available on NEO-DMI. Thus, the tests were based on static advice. Yet, it is recommended to test the framework on a C-DAS. In this case, the route plan will be adjusted in real-time. The proposed model will constrain the calculated speed profile by delivering real-time signalling information to the speed profile calculation module. Then, the effect of having both dynamic route plan adjustments and a data feed of the actual signal state on corridor capacity can be estimated.

The advice was manually constructed catering for the speed limits imposed by the dynamic speed profile. Although, the constraints originating from the signalling system were taken into consideration, these constraints remain static on the simulation environment. The framework must be tested on a tool that allows for time-based simulation. Time-based simulation will allow for a dynamic behaviour of the signalling system according to the actual train status. Then, it can be appraised how well the red signal determination framework respects the actual signalling state. Conflicts can be observed if this recommendation is implemented.

This thesis established a hypothesis in order to perform the simulations. The hypothesis dictates that as advice reliability increases, the driver trusts the advice more and follows it. Given that the better capacity utilization is within the objective function of the DAS, improved advice reliability leads to better capacity usage. It is evident that this hypothesis is based upon two hard assumptions; first, driver's acceptance towards the advice and second, precise following of the advice. In short, the human factors related-parameters of the hypothesis were considered as constant while in practice they are not. For that reason, it is recommended to take both *driver acceptance* and *precision* with which the advice is followed as observable parameters. Then the true effect of advice reliability on actual rail operations using a C-DAS-On Board can be captured.

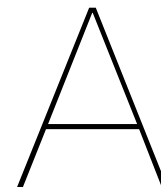
# References

- Abril, M., Barber, F., Ingolotti, L., Salido, M. A., Tormos, P., & Lova, A. (2008). An assessment of railway capacity. *Transportation Research Part E: Logistics and Transportation Review*, 44(5), 774–806.
- Albrecht, T. (2013). Human factor challenges in the development of a driver advisory system for regional passenger trains. *Rail Human Factors: Supporting reliability, safety and cost reduction*, 129–138.
- Albrecht, T. (2014). Energy-efficient railway operation. In I. A. Hansen & J. Pacht (Eds.), *Railway timetabling & operations* (pp. 91–114). Hamburg: Eurailpress.
- Albrecht, T., Binder, A., & Gassel, C. (2013). Applications of real-time speed control in rail-bound public transportation systems. *IET Intelligent Transport Systems*, 7(3), 305–314.
- Albrecht, T., Gassel, C., Binder, A., & Luipen, J. v. (2010). Dealing with operational constraints in energy efficient driving. , 22–22.
- Albrecht, T., Goverde, R. M. P., Weeda, V. A., & van Luipen, J. (2006). Reconstruction of train trajectories from track occupation data to determine the effects of a Driver Information System. In *Computers in Railways X* (Vol. 1, pp. 207–216). Prague, Czech Republic: WIT Press.
- Albrecht, T., Lüddecke, K., & Zimmermann, J. (2013). A precise and reliable train positioning system and its use for automation of train operation. In *2013 IEEE International Conference on Intelligent Rail Transportation Proceedings* (pp. 134–139).
- Albrecht, T., & van Luipen, J. (2006). What role can a driver information system play in railway conflicts? *IFAC Proceedings Volumes*, 39(12), 251–256.
- Albrecht, T., van Luipen, J., Hansen, I. A., & Weeda, A. (2007). Bessere echtzeitinformationen für triebfahrzeugführer und fahrdienstleiter. *Der Eisenbahningenieur (Hamburg)*, 58(6), 73–79.
- Barbu, G. (2000). Requirements of rail applications. In *GNSS rail user forum* (p. 5).
- Becker, U., Hänsel, F., May, J., Poliak, J., & Schnieder, E. (2006). Vehicle autonomous positioning as a basis for a low cost train protection system. , 12.
- Beugin, J., Filip, A., Marais, J., & Berbineau, M. (2010). Galileo for railway operations: question about the positioning performances analogy with the RAMS requirements allocated to safety applications. *European Transport Research Review*, 2(2), 93–102.
- Bombardier-Transportation. (2008). *EBI Drive 50 Driver assistance system*. Retrieved 2020-05-24, from [http://bombardier.at/content/dam/Websites/bombardiercom/supporting-documents/BT/Bombardier-Transportation-ECO4-EBI\\_Drive-EN.pdf](http://bombardier.at/content/dam/Websites/bombardiercom/supporting-documents/BT/Bombardier-Transportation-ECO4-EBI_Drive-EN.pdf)
- Brünger, O., & Dahlhaus, E. (2014). Energy-efficient railway operation. In I. A. Hansen & J. Pacht (Eds.), *Railway timetabling & operations* (pp. 65–89). Hamburg: Eurailpress.
- Buurmans, C. P. G. (2019). *Automatic train operation over legacy automatic train protection systems* (Unpublished master's thesis). Delft University of Technology.
- CENELEC, E. (2001). 50126: Railway applications-the specification and demonstration of reliability. *Availability, Maintainability and Safety (RAMS)*.
- Daamen, W. (2018). *Lecture notes in empirical analysis for transport and planning*. Delft University of Technology.
- D'Ariano, A., Corman, F., & Pacciarelli, D. (2014). Rescheduling. In I. A. Hansen & J. Pacht (Eds.), *Railway timetabling & operations* (pp. 254–257). Hamburg: Eurailpress.
- Darlington, P. (2019). KeTech – Connected Driver Advisory System. *RailEngineer*(180), 36–39.
- de Fabris, S., Longo, G., & Medeossi, G. (2008). Automated analysis of train event recorder data to improve micro-simulation models. In (pp. 575–583). Toledo, Spain.
- de Fabris, S., Longo, G., & Medeossi, G. (2011). An algorithm for the calibration of running time calculation on the basis of GPS data. In (pp. 577–585). New Forest, UK.
- Dong, H., Zhu, H., & Gao, S. (2018). An Approach for Energy-Efficient and Punctual Train Operation via Driver Advisory System. *IEEE Intelligent Transportation Systems Magazine*, 10(3), 57–67.
- EGNSSA. (2019). *Report on Rail User Needs and Requirements- Outcome of the European GNSS' user consultation platform* (Tech. Rep.). European Global Navigation Satellite Systems Agency.

- Endsley, M. R. (1995). Toward a theory of situation awareness in dynamic systems. *Human factors*, 37(1), 32–64.
- European Railway Agency. (2016). *System Requirements Specification*. ERA.
- European Space Agency. (2015). *GPS Performances*.
- Filip, A., Beugin, J., Marais, J., & Mocek, H. (2008). Safety concept of railway signalling based on Galileo Safety-of-Life Service. In (pp. 103–112). Toledo, Spain.
- Ghofrani, F., He, Q., Goverde, R. M. P., & Liu, X. (2018). Recent applications of big data analytics in railway transportation systems: A survey. *Transportation Research Part C: Emerging Technologies*, 90, 226–246.
- Goverde, R., Corman, F., & D'Ariano, A. (2013). Railway line capacity consumption of different railway signalling systems under scheduled and disturbed conditions. *Journal of Rail Transport Planning & Management*, 3(3), 78–94.
- Goverde, R., & Theunissen, E. (2018). *Onderzoeksmethodologie ATO-over-ATB* (Tech. Rep.). Delft: Delft University of Technology.
- Hänsel, F., Ganzelmeier, L., Becker, U., & Schnieder, E. (2004). Mobile testbed for the accuracy and availability measurement of satellite navigation systems. *Proceedings of Networks for Mobility (Fovus)*, Stuttgart.
- Hoffmann, M., & Böttcher, J. (2018). Entwicklung und Einführung der Zuglaufregelung. *Deine Bahn*(10).
- Jin, J., & Kadhim, R. (2011). Driver Advisory Information for Energy Management and Regulation. , 12.
- Kecman, P. (2014). *Models for predictive railway traffic management* (PhD Thesis). Delft University of Technology.
- Kecman, P., & Goverde, R. M. P. (2012). Process mining of train describer event data and automatic conflict identification. In (pp. 227–238). New Forest, UK.
- Kelly, R. J., & Davis, M. (1994). Required Navigation Performance (RNP) for Precision Approach and Landing with GNSS Application. , 30.
- Kent, S. (2009). *RSSB Advisory Information for Drivers for Energy Management and Regulation Stage 1 Report-Appendices* (Tech. Rep. No. Stage 1 Report-Appendices). DeltaRail.
- Langley, R. B. (1999). The Integrity of GPS. *GPS World*, 60–63.
- Large, D., Golightly, D., & Taylor, E. (2014). The effect of driver advisory systems on train driver workload and performance. In (pp. 335–342).
- Large, D. R., Golightly, D., & Taylor, E. (2017). Train-driving simulator studies: Can novice drivers deliver the goods? *Proceedings of the Institution of Mechanical Engineers, Part F: Journal of Rail and Rapid Transit*, 231(10), 1186–1194.
- Li, Z., Chen, L., Roberts, C., & Zhao, N. (2018). Dynamic Trajectory Optimization Design for Railway Driver Advisory System. *IEEE Intelligent Transportation Systems Magazine*, 10(1), 121–132.
- Lochman, L. (2009). Background for ertms. *Compendium on ERTMS*, 32.
- Luijt, R. S., van den Berge, M. P. F., Willeboordse, H. Y., & Hoogenraad, J. H. (2017). 5 years of Dutch eco-driving: Managing behavioural change. *Transportation Research Part A: Policy and Practice*, 98, 46–63.
- Lüthi, M. (2009). *Improving the efficiency of heavily used railway networks through integrated real-time rescheduling* (PhD Thesis). Swiss Federal Institute of Technology (ETH), Zurich.
- Marais, J., Beugin, J., & Berbineau, M. (2017). A Survey of GNSS-Based Research and Developments for the European Railway Signaling. *IEEE Transactions on Intelligent Transportation Systems*, 18(10), 2602–2618.
- Medeossi, G., Longo, G., & de Fabris, S. (2011). A method for using stochastic blocking times to improve timetable planning. *Journal of Rail Transport Planning & Management*, 1(1), 1–13.
- Mehta, F., Rößiger, C., & Montigel, M. (2010). Latent energy savings due to the innovative use of advisory speeds to avoid occupation conflicts. *WIT Transactions on the Built Environment*, 114, 99–108.
- Mitchell, I. (2009). The sustainable railway—use of advisory systems for energy savings. *IRSE News*, 151, 2–7.
- Neri, A., Capua, R., & Salvatori, P. (2018). Track Constrained RTK-like Positioning for Railway Applications. *NAVIGATION*, 65(3), 335–352.

- Nicholson, T. J. (2010). Total automation: Impacts & systems. In *1st professional development course on railway signalling and control systems (RSCS 2010)* (pp. 271–280).
- Pachl, J. (2014). Timetable design principles. In I. A. Hansen & J. Pachl (Eds.), *Railway timetabling & operations* (pp. 21–23). Hamburg: Eurailpress.
- Panou, K., Tzieropoulos, P., & Emery, D. (2013). Railway driver advice systems: Evaluation of methods, tools and systems. *Journal of Rail Transport Planning & Management*, 3(4), 150–162.
- Poulus, R., Kempen, E. van, & Meijeren, J. van. (2018). *Automatic train operation. Driving the future of rail transport* (Tech. Rep.). TNO.
- Powell, J. P., Fraszczyk, A., Cheong, C. N., & Yeung, H. K. (2016). Potential benefits and obstacles of implementing driverless train operation on the tyne and wear metro: A simulation exercise. *Urban Rail Transit*, 2(3-4), 114–127.
- Quaglietta, E., Pellegrini, P., Goverde, R. M. P., Albrecht, T., Jaekel, B., Marlière, G., ... Nicholson, G. (2016, February). The ON-TIME real-time railway traffic management framework: A proof-of-concept using a scalable standardised data communication architecture. *Transportation Research Part C: Emerging Technologies*, 63, 23–50.
- Rahn, K., Bode, C., & Albrecht, T. (2013). Energy-efficient driving in the context of a communications-based train control system (CBTC). In *2013 IEEE International Conference on Intelligent Rail Transportation Proceedings* (pp. 19–24).
- Railway-News. (2015, April). *New High-Tech Systems to be Installed on Main Line Trains*. Retrieved 2020-09-08, from <https://railway-news.com/new-high-tech-systems-to-be-installed-on-main-line-trains/>
- Rao, X., Montigel, M., & Weidmann, U. (2016). A new rail optimisation model by integration of traffic management and train automation. *Transportation Research Part C: Emerging Technologies*, 71, 382–405.
- SBB. (2017). *Mit neuen Assistenzsystemen zu mehr Kapazität und Sicherheit | SBB*. Retrieved 2020-06-08, from <https://company.sbb.ch/de/medien/medienstelle/medienmitteilungen/detail.html/2017/12/0512-1>
- Schumann, T. (2014). *Fahrerassistenz und Betriebsoptimierung im Bahnverkehr (Schwerpunkt: Güterverkehr)*. Retrieved 2020-06-08, from [https://elib.dlr.de/89410/1/Fahrerassistenzsysteme-im-SGV\\_TU-Berlin\\_140520.pdf](https://elib.dlr.de/89410/1/Fahrerassistenzsysteme-im-SGV_TU-Berlin_140520.pdf)
- Seinenboek* (Tech. Rep.). (2005). Nederlandse Spoorwegen Reizigers.
- Smith, K. (2019). *Rise of the machines: Rio Tinto breaks new ground with AutoHaul*. Retrieved 2020-11-09, from [https://www.railjournal.com/in\\_depth/rise-machines-rio-tinto-autohaul/](https://www.railjournal.com/in_depth/rise-machines-rio-tinto-autohaul/)
- Steinfeld, A., Jenkins, O. C., & Scassellati, B. (2009). The oz of wizard: simulating the human for interaction research. In *Proceedings of the 4th acm/ieee international conference on human robot interaction* (pp. 101–108).
- Thales. (2019). *Why digital is riding with the mainline train driver | Thales Group*. Retrieved 2020-09-08, from <https://www.thalesgroup.com/en/worldwide-transport/main-line-rail/magazine/why-digital-riding-mainline-train-driver>
- Theeg, G., & Vlasenko, S. (2009). Railway signalling & interlocking. *International Compendium. Hamburg, Eurail-press Publ*, 448.
- Tschirner, S., Andersson, A., & Sandblad, B. (Eds.). (2013). *Designing train driver advisory systems for situation awareness*. Taylor & Francis. doi: 10.1201/b13827
- UITP. (2011). *Press kit: Metro automation facts, figures and trends – a global bid for automation: Uitp observatory of automated metros confirms sustained growth rates for the coming years* (Tech. Rep.). International Association of Public Transport (UITP).
- Venkateswaran, K. G., Nicholson, G. L., Roberts, C., & Stone, R. (2015). Impact of Automation on the Capacity of a Mainline Railway: A Preliminary Hypothesis and Methodology. In *2015 IEEE 18th International Conference on Intelligent Transportation Systems* (pp. 2097–2102). Gran Canaria, Spain: IEEE.
- Vincze, B., & Tarnai, G. (2006). Evolution of Train Control Systems..
- Wang, P., & Goverde, R. M. P. (2017). Development of a train driver advisory system: ETO. In *2017 5th IEEE International Conference on Models and Technologies for Intelligent Transportation Systems (MT-ITS)* (pp. 140–145).

- Wang, P., Goverde, R. M. P., & van Luipen, J. (2019). A connected driver advisory system framework for merging freight trains. *Transportation Research Part C: Emerging Technologies*, 105, 203–221.
- Weidmann, U., Bruckmann, D., Fumasoli, T., Herrigel, S., & Schranil, S. (2015). *Innovationen im Bahnsystem: SBB-Fonds für die Forschung zum Management im Verkehrsbereich* (Tech. Rep.). ETH Zurich.
- Yang, L., Liden, T., & Leander, P. (2013). Achieving energy-efficiency and on-time performance with Driver Advisory Systems. In (pp. 13–18).
- Yin, J., Tang, T., Yang, L., Xun, J., Huang, Y., & Gao, Z. (2017). Research and development of automatic train operation for railway transportation systems: A survey. *Transportation Research Part C: Emerging Technologies*, 85, 548–572.
- Yuan, J., & Medeossi, G. (2014). Statistical analysis of train delays and movements. In I. A. Hansen & J. Pahl (Eds.), *Railway timetabling & operations* (pp. 218–222). Hamburg: Eurailpress.
- Zheng, Y., & Cross, P. (2012). Integrated GNSS with different accuracy of track database for safety-critical railway control systems. *GPS Solutions*, 16(2), 169–179.
- Zhu, H., Gao, S., & Dong, H. (2018). Improving Train Driving Performance under Disturbances by Intelligent Driver Advisory System. In *2018 International Conference on Intelligent Rail Transportation (ICIRT)* (pp. 1–5).
- Zhu, H., Sun, X., Chen, L., Gao, S., & Dong, H. (2016). Analysis and design of Driver Advisory System (DAS) for energy-efficient train operation with real-time information. In *2016 IEEE International Conference on Intelligent Rail Transportation (ICIRT)* (pp. 99–104).



## Detailed tool results

Table A.1 includes the results of the data-mining tool using baseline and infill data for train 6335 on 13/12/2019. The Table demonstrates the information being stored by the data-mining tool. First, every single track of the route between Haarlem platform 4 (HLM-4) to Den Haag Centraal platform 7 (GVC-7) is included. Second, the entrance time at each track is recorded. It is assumed that the exit time of a track coincides with the entrance time of the downstream track. The number of the predecessor train  $P$  and the delay of the train that is being examined as well as that of the predecessor are recorded. Finally, the tool calculates per data source and per track, the time that it was unfeasible (TTU) as well as the fraction of the travel time of the track it was feasible (FTF) for the data source to determine the red signal.

Table A.1: Tool results for simple and MTPS-infill algorithm, Train: 6335, Date: 13/12/2019

Track	Entrance time	$P^1$	Delay (min)		Baseline		Infill	
			$P$	6335	TTU <sup>2</sup> (sec)	FTF <sup>3</sup> (%)	TTU (sec)	FTF (%)
HLM-4	08:56:20				0	100	0	100
ZSPL-122	08:56:05				0	100	0	100
LJ	08:58:09	2222	5	2	47.0	46.3	0	100
LH	08:59:36	2222	4	4	296.7	52.0	178.5	71.1
LIS-302	09:09:54	2222	4	4	23.3	0.0	23.3	0.0
LG	09:10:01	2222	4	3	72.1	83.8	72.1	83.8
LEDN-9A	09:17:42	722	3	1	91.7	43.7	57.2	64.9
LEDN-510B	09:20:02	722	3	1	42.6	0.0	17.5	58.8
LF	09:21:10	722	3	1	11.2	98.0	11.2	98.0
GVM-1	09:30:18				0.0	100.0	0.0	100.0
LE	09:32:03				0.0	100.0	0.0	100.0
LAA-909	09:36:07				0.0	100.0	0.0	100.0
GVC-7	09:37:39				0.0	100.0	0.0	100.0

<sup>1</sup> Predecessor train number;

<sup>2</sup> Total time that it is unfeasible (TTU) to determine red signal's location for that track;

<sup>3</sup> Fraction of the travel time (TT) on a track-segment for which it is feasible to determine the red signal;  
 $FTF = (TT - TTU) / TT$ .

Figure A.1 includes all the TPS records for train 6335 for its trajectory through track *LJ* as displayed on the RouteLint HMI. Figure A.1a shows the event of the train entering track *LJ*, while Figure A.1f shows the event of the train entering track *LH*, which coincides with the exit time from track *LJ*. For both Figure A.1a and A.1b, train 6335 is not authorised to the downstream open track *LH*, therefore *LH*'s entry signal shows a red aspect. In contrast, for the cases depicted in Figure A.1c-A.1e, 6335 is authorised on the same open track (*LH*) as predecessor, so red signal's location cannot be determined by *baseline* data.

Treinnr	08:58:09	Vertraging
2133	LEDN-510B	+1
99971	LEDN-9A	+4
	LG	
	LIS-302	
99971	LH	+4
2222	LH	+5
	LH	
6335	LJ	+2
2135	SJ	+1
2224		

(a)

Treinnr	08:58:37	Vertraging
2133	LEDN-510B	+1
99971	LEDN-9A	+4
	LG	
	LIS-302	
99971	LH	+4
2222	LH	+5
	LH	
6335	LJ	+2
2135	SJ	+1
2224		

(b)

Treinnr	08:58:49	Vertraging
2133	LEDN-510B	+1
99971	LEDN-9A	+4
	LG	
	LIS-302	
99971	LH	+4
2222	LH	+5
	LH	
6335	LJ	+2
2135	SJ	+1
2224		

(c)

Treinnr	08:59:18	Vertraging
2133	LEDN-510B	+1
99971	LEDN-9A	+4
	LG	
	LIS-302	
99971	LH	+4
2222	LH	+5
	LH	
6335	LJ	+2
2135	HW-602	+0
2224		

(d)

Treinnr	08:59:36	Vertraging
2133	LEDN-510B	+1
99971	LEDN-9A	+4
	LG	
	LIS-302	
99971	LH	+4
2222	LH	+5
	LH	
6335	LJ	+2
2135	SL	+1
2224		

(e)

Treinnr	08:59:36	Vertraging
2133	LF	+1
2133	LEDN-510B	+1
99971	LEDN-9A	+4
	LG	
	LIS-302	
99971	LH	+4
2222	LH	+5
6335	LH	+2
2135	SL	+1
2224		

(f)

Figure A.1: RouteLint display of all the TPS records that capture the passage of train 6335 through open track LJ

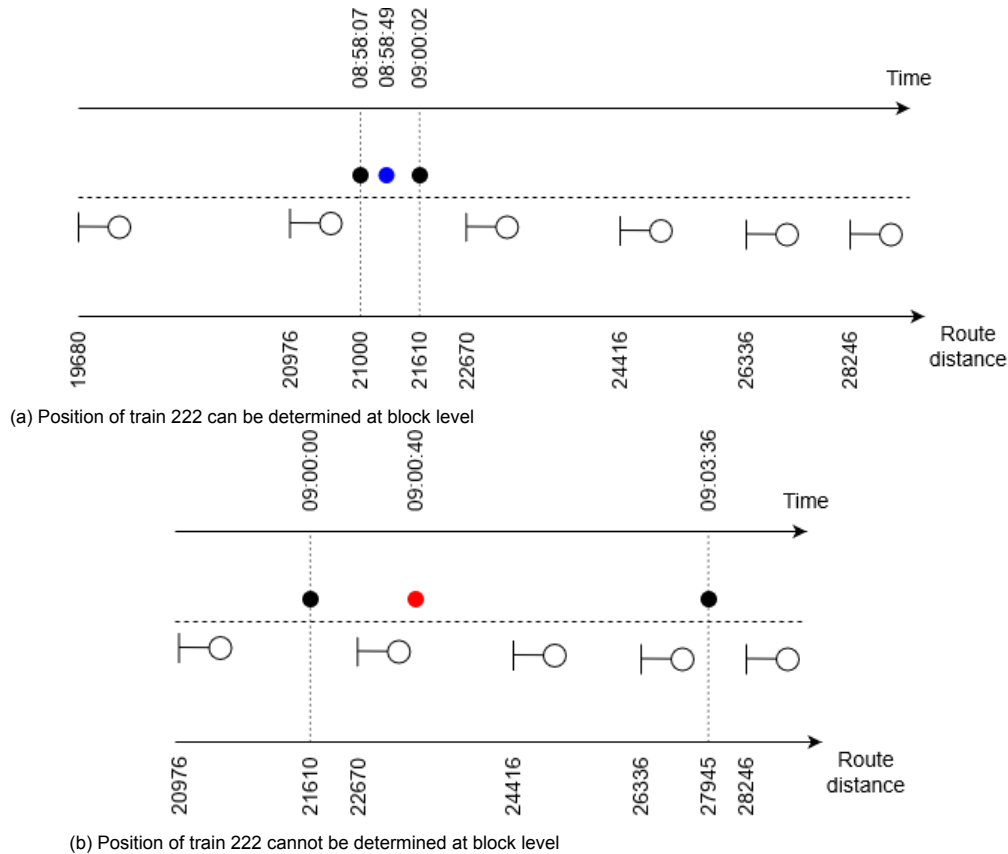


Figure A.2: Example where it is (a) feasible and (b) unfeasible to determine the position of train 2222 (predecessor of train 6335) and thus, red signal using infill data. Figures are not in scale.

Now, assume that the *infill* routine is launched for the case of Figure A.1c. The tool is searching in MTPS files for train 2222 for timestamp 08:58:49. The algorithm yields that 2222 was at 08:58:07 at location 21000 m and at 09:00:02 it was at location 21610 m. All the afore mentioned locations are within the same block, therefore 2222 is at this block and signal at location 20976 m shows a red aspect. The example is depicted in Figure A.2a.

An example where it is unfeasible to determine red signal's location with MTPS is shown in Figure A.2b. The timestamp that is being searched is for train 2222 for 13/12/2019 at 09:00:40. The MTPS timestamp earlier than that and closer (time-wise) to it, is at 09:00:00 at location 21610 m, while the next consecutive timestamp is at 09:03:36 at location 27945 m. As the Figure illustrates, the available consecutive MTPS measurements are for several blocks apart. Therefore, predecessor could be wherever in the intermediate blocks and as a consequence, the red signal cannot be determined.

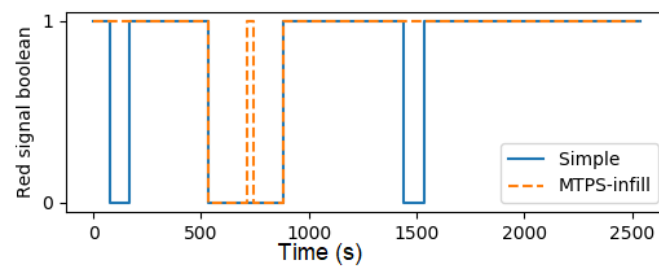
Figure A.3 includes an example where *infill* yields a higher MTBF than that of the *baseline* (Figure A.3a) as well as an example where the opposite occurs (Figure A.3b). Figure A.3a presents a comparison between the continuity of the data stream using *baseline* and *infill* for train 6337 on 13/12/2019, while Figure A.3b demonstrates the same signals for train 6335 for the same day. In Figure A.3 x-axis represents the time from the start of the trip, while y-axis includes the binary variable which defines the data source's ability to define the red signal.

In Figure A.3a, MTPS-infill algorithm alleviates the simple algorithm's discontinuity starting around 100 s, cannot improve that around 600 s, while it totally eliminates discontinuity around 1500 s. Also, *infill* somehow bridges the gap from 500 to 800 s by a little. For this scenario, MTBF improved by 47.7% (from 501.4 s (baseline) to 741.0 s (infill)). In Figure A.3b *infill* fills to a large extent the gap between 200 and 300 s, while it partially bridges the baseline's discontinuity between 600 s and 900 s. Contrary to the previous example, in this case *infill* worsens MTBF by 25.4% (from 475.7 s (simple) to 336.1 s (infill)). This occurs because MTBF is affected not only by the amount of time the data stream is able to yield the red signal but also it is affected by the number of gaps it experiences. In Figure A.3a, the

Table A.2: Tool results for simple and MTPS-infill algorithm, Train: 6337, Date: 13/12/2019

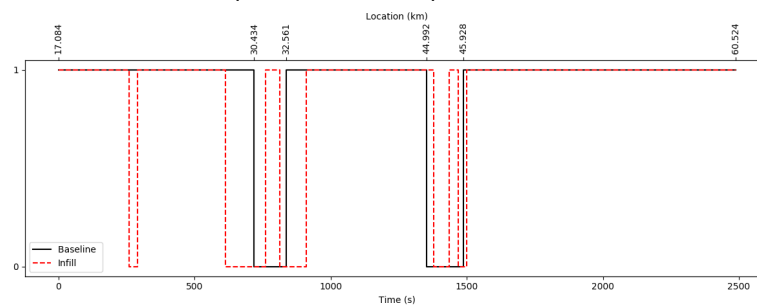
Track	Entrance time	P	Delay (min)		Simple		MTPS	
			P	6337	TTU (sec)	FTF (%)	TTU (sec)	FTF (%)
HLM-1	09:24:01				0.0	100.0	0	100
ZSPL-122	09:25:26	2224	1	0	72.6	4.4	0.0	100.0
LJ	09:26:04	2224	1	1	13.6	83.4	0.0	100.0
LH	09:28:04	2224	0	2	327.0	47.9	294.4	53.1
LIS-302	09:38:31	2224	0	2	20.5	10.9	20.5	10.9
LG	09:38:54	2224			0	100.0	0	100.0
LEDN-9A	09:47:13	1824	1	1	98.8	38.9	0.0	100.0
LEDN-510B	09:49:55				0.0	100.0	0.0	100.0
LF	09:50:35				0.0	100.0	0.0	100.0
GVM-1	09:59:34				0.0	100.0	0.0	100.0
LE	10:01:57				0.0	100.0	0.0	100.0
LAA-909	10:05:23				0.0	100.0	0.	100.0
GVC-7	10:06:28				0.0	100.0	0.0	100.0

number of continuous instances decreased by 1 (from 4 to 3) with the introduction of MTPS, while in the example of Figure A.3b the number of continuous instances increased by 2 (from 4 to 6) despite the aggregate time of discontinuity being reduced in both cases with the introduction of MTPS.



(a)

Infill improves MTBF compared to baseline



(b)

Infill worsens MTBF compared to baseline

Figure A.3: Example of MTPS-infill algorithm having (a) the desirable and (b) the undesirable effect

# B

## Detailed related files

The format of a RouteLint log file is presented in Table B.1. Information is divided in several columns (fields) of the log file. Table B.1 corresponds to the RouteLint interface example shown in Figure B.1.

Treinnr	09:34:46	Vertraging
2224	LG	+0
	LG	
	LIS-302	
6337	LH	+1
	LH	
	ZSPL-LJ	
2231	ZSPL-122	+3
6339	HLM-1	
2231	MH	+3
73329	LIS-304	+5

Figure B.1: Example of RouteLint interface

Table B.1 includes a detailed overview of a RouteLint record.

Table B.2 correlates each TNS-status with its corresponding colour on the RouteLint interface as well as the description of TNS-status. TNS-status depends on the movement of trains on the vicinity with respect to a train's position. The *Description* field of Table B.2 contains this information. A schematic representation of the movements mentioned in the *Description* field of Table B.2 is shown in Figure ???. Also, the meaning of the TNS-status is given. The Table reveals four distinct colours; red, white, orange, grey. The TNS-status can be classified based on their colour. The data-mining tool considers these four colour groups. Note that each TNS-status is accompanied by a TNS-track field indicating the track-segment which the TNS-status refers to. The meaning that each colour group has for the (proper) train as well as for trains on the vicinity is the following:

- Red: (Proper) Train is unauthorised to the track-segment,
- White: (Proper) Train is unauthorised to the track-segment,
- Orange: A train has triggered the ARI,
- Grey: (Proper) Train is authorised to the downstream track-segment, while this track-segment refers to an open track.

Table B.1: Detailed example of Routelint record. The record corresponds to a line of the Routelint log file

Field	Value	Field-continue	Value-continue
Timestamp	2019-10-01T09:34:46.293+02:00	TNS-4-status	AV
Train number	6339	TNS-4-track	LIS-302
Time	93446293	TNS-4-route-ribbon	Asd-Rtd
Delay		TNS-4- route-ribbon-location	32561
Track segment	HLM-1	TNS-4-train-number	6337
Start route-ribbon	Asd-Rtd	TNS-4-delay	100
Start route-ribbon's locations	17500	TNS-5-status	AV
End route-ribbon	Asd-Rtd	TNS-5-track	LG
End route-ribbon's locations	16705	TNS-5-route-ribbon	Asd-Rtd
Total number of downstream TNS	7	TNS-5- route-ribbon-location	44455
Total number of upstream TNS	2	TNS-5-train-number	6337
TNS-0-status	PK	TNS-5-delay	100
TNS-0-track	ZSPL-122	TNS-6-status	VV
TNS-0-route-ribbon	Asd-Rtd	TNS-6-track	LG
TNS-0- route-ribbon-location	17787	TNS-6-route-ribbon	Asd-Rtd
TNS-0-train-number	2231	TNS-6- route-ribbon-location	44455
TNS-0-delay	300	TNS-6-train-number	2224
TNS-1-status	PV	TNS-6-delay	0
TNS-1-track	ZSPL-LJ	Upstream-train-0- track	MH
TNS-1-route-ribbon	Asd-Rtd	Upstream-train-0- train-number	2231
TNS-1- route-ribbon-location	18536	Upstream-train-0-delay	300
TNS-1-train-number	2137	Upstream-train-1-track	LIS-304
TNS-1-delay	-100	Upstream-train-1- train-number	73329
TNS-2-status	PV	Upstream-train-1- delay	500
TNS-2-track	LH		
TNS-2-route-ribbon	Asd-Rtd		
TNS-2- route-ribbon-location	31754		
TNS-2-train-number	2137		
TNS-2-delay	-100		
TNS-3-status	VV		
TNS-3-track	LH		
TNS-3-route-ribbon	Asd-Rtd		
TNS-3- route-ribbon-location	31754		
TNS-3-train-number	6337		
TNS-3-delay	100		

Table B.2 contains the meaning of a *TNS-status* and its colour as displayed on the Routelint HMI. Each label of the 'TNS-status' field of Table B.2 has a certain meaning in the Dutch language. Yet, only its translation in the English language is given in the 'Description' field.

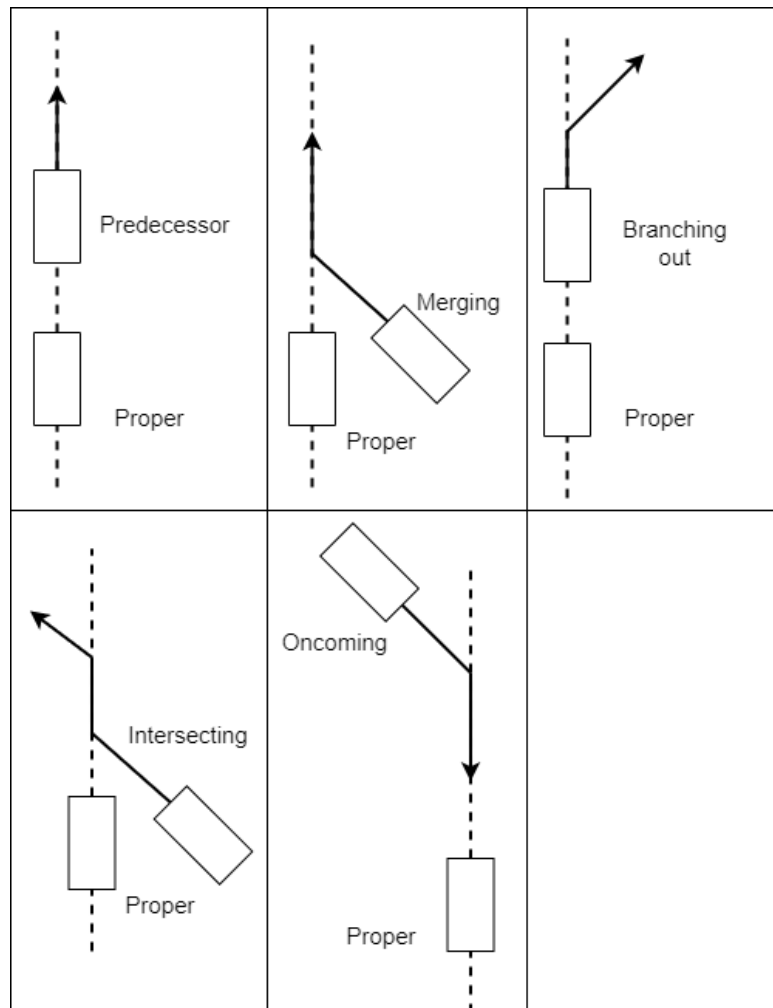
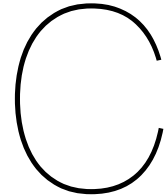


Figure B.2: Examples of movements of trains on the vicinity with respect to (proper) train's position as they appear on the description of TNS-status

Table B.2: Correlation of TNS-status with colour and description

TNS-Status	Description	TNS-Colour
PE	Planned for proper train	Red
NE	Normally authorized for proper Train	White
RE	On sight movement authorised for proper train	Red
PI	Planned for merging train	Red
AI	Authorised for merging train	Orange
BI	Occupied by merging train	Red
PU	Planned for branching out train	Red
AU	Authorised for branching out train	Orange
BU	Occupied by branching out train	Red
PK	Planned for intersecting train	Red
AK	Authorised for intersecting train	Orange
BK	Occupied by intersecting train	Red
PV	Planned for predecessor train	Red
AV	Authorised for predecessor train	Orange
BV	Occupied by predecessor train	Red
VV	Predecessor train on open track	Grey
PT	Planned for oncoming train	Red
AT	Authorised for oncoming train	Orange
BT	Occupied by oncoming train	Red
VT	Oncoming train on open track	Grey



# Statistical analysis

This Appendix includes statistical analysis of the tool output performed for 6300 series. In the following, knowledge and formulas regarding statistics were retrieved from Daamen (2018). The section contains a qualitative analysis of baseline and infill data, calculation of the required navigation performance (RNP) parameters, descriptive statistics of parameters related to reliability, the calculation of the contribution of infill data in system reliability and correlation assessment between calculated parameters.

## Qualitative analysis of baseline and infill data

The analysis focuses on the continuity of each data source in determining the red signal. A qualitative comparison of the two samples is performed using their histograms. Figure C.1 includes a comparison of the histograms for the two data sources. Three distinct areas can be distinguished at the histogram of the *infill*. One area is around 700 s. This area is where most observations are concentrated. Another area, around 2500 s can be distinguished for *infill* distribution. This value approximates the scheduled travel time (SRT). Since, for that area MTBF equals the SRT, no or minor discontinuities have been witnessed for these records. Therefore, it can be argued that this area of the graph represents the cases where the *infill* data source achieves to deliver a continuous data stream providing the red signal throughout the whole train journey. Yet, this area constitutes a small minority of the total *infill* records. The third area lays around 1300 s. This value approximately equals the half of the scheduled journey time. Based on this observation and consulting on the formula of MTBF (see Formula 4.8),  $n$  must equal 2. Therefore the data stream is likely to have experienced a single gap for this cases. Still, only a small proportion of the *infill* observations falls under this category.

Moreover, two areas can be distinguished for the distribution of *baseline*. The first one is located around its median value (approximately 500 s) where the majority of observations is concentrated. The other area lays around 1400 s which is believed to also represent observations with a single gap throughout a train run.

Now, the analysis focuses on the effect that the two data sources have on peak and off-peak trains. For that reason, the original samples per data source are divided into subsets for these two train categories. Figure C.2a illustrates that the histogram of peak-hour trains has higher peak than that of the off-peak trains. For *infill* the median value is the same for the two train types but the probability to draw that value is higher for peak hour trains (Figure C.2b). The findings from the two figures lead to the conclusion that a peak hour train using a DAS is more likely to have more reliable input when using both the *baseline* and the *infill* data compared to an off-peak train.

## Required navigation performance parameters

Two parameters of the required navigation performance are discussed: availability and continuity. Regarding availability, the tool reaches 99.24 %. In detail, out of the 528 non-outlier observations of the *baseline* (Table C.1), the tool was able to deliver the desirable function for 524 instances.

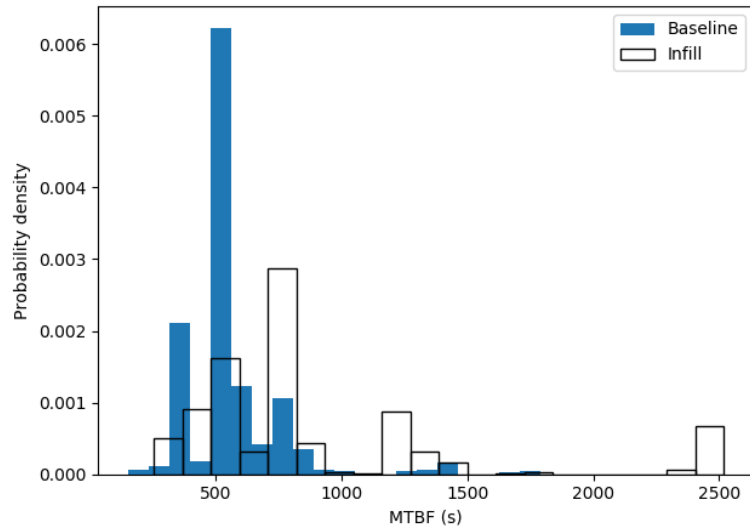
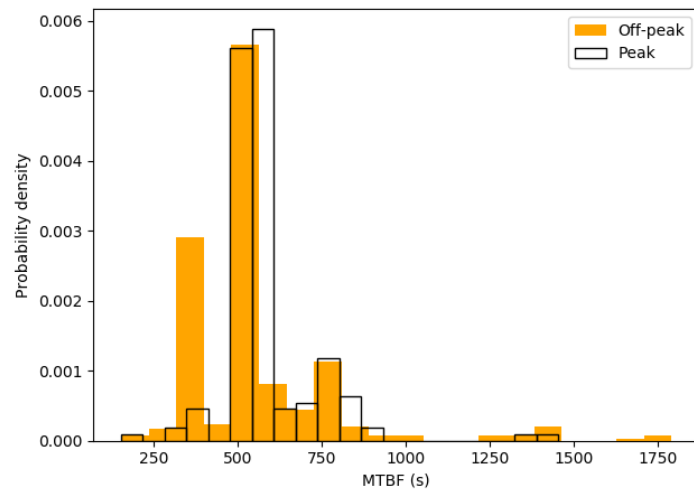


Figure C.1: MTBF histogram for both baseline and infill data source

Table C.1 includes the descriptive statistics of the two data sources regarding reliability. The columns refer to the samples considered. Thus, for each of the data sources three samples are examined: the general set of observation, a subset including only peak hour trains and another one for off-peak trains. The majority of the rows refer to MTBF, a row refers to the minimum observed discontinuity  $T$  and the rest of the rows refers to reliability as shown in Equation 4.7. Value  $T$  is the minimum (critical) gap that has been observed in the continuity graph of the data stream (Figure 4.12) out of all the observations of the sample. For example, 40.8 is the minimum gap that has been observed out of the 170 observations of peak-baseline sample. The number of initial observations for the *infill* is smaller than that of the *baseline* since there were no available MTPS records for some days for specific train numbers. After excluding the outliers from the observations of the two samples, two subsets were created depicting peak and off-peak hour trains for both the data sources.

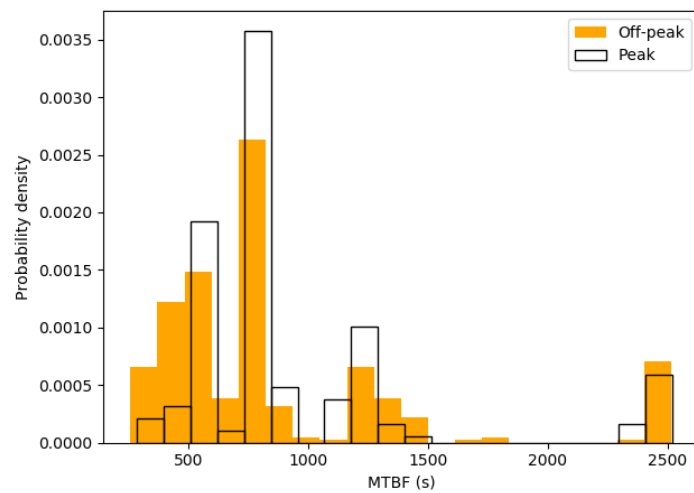
The normality check (Shapiro-Wilk) for the MTBF of each one of the samples proves that they do not follow the normal distribution. In fact it is revealed that Weibull distribution best fits the samples.

For both data sources peak hour trains show higher MTBF. Hence, peak hour trains experience larger intervals where the red signal can be determined. This can be explained due to the close following of trains during peak hours. The closer a train follows its predecessor, the more likely it is for it to face more restrictive aspects. In contrast, in case of a green wave, the red signal may lay way downstream, further than the coverage range of TPS.



(a)

Baseline data



(b)

Infill data

Figure C.2: Histograms of the MTBF for both peak and off-peak hour trains for the two data sources

Table C.1: Descriptive statistics regarding the reliability of the two algorithms

		Data source					
Variable	Attribute	Baseline			Infill		
		General	Peak	Off-peak	General	Peak	Off-peak
	$n_0$ <sup>1</sup>	555	-	-	543	-	-
	Outliers <sup>3</sup>	27	-	-	0	-	-
	$n^4$	528	170	358	531	168	363
	p-value <sup>5</sup>	e-28	e-17	e-23	e-27	e-17	e-23
	Best fit distribution	<sup>11</sup> 4e-5	3e-5	4e-5	6e-6	1e-5	5e-6
MTBF	Average	568.0	584.9	559.9	896.5	939.1	876.9
	Std <sup>6</sup>	202.1	141.0	225.1	554.2	517.1	570.2
	CV <sup>7</sup>	0.36	0.24	0.40	0.62	0.55	0.65
	Min	152.5	152.5	153.7	256.9	285.4	256.9
	Max	1791.9	1454.1	1791.9	2519.3	2519.3	2517.3
	25%(Q1)	513.7	532.0	392.7	573.3	594.7	552.6
	50%	543.0	550.2	538.2	779.3	791.7	774.2
	75%(Q3)	572.6	578.8	568.9	923.0	1168.0	880.9
T <sup>12</sup>	Min	22.2	40.8	22.2	17.1	23.9	17.1
CR1 <sup>8</sup>	-	0.041	0.074	0.041	0.022	0.030	0.022
CR2 <sup>9</sup>	-	1.8e-3/1s (11.0%/1min)			1.9e-3/1s (11.4%/1min)		
R1 <sup>10</sup>	-	95.9 %	92.4 %	95.9 %	97.8 %	97.0 %	97.8 %

<sup>1</sup> Initial number of observations;

<sup>2</sup> Number of values excluded because irrational;

<sup>3</sup> Excluded values greater than 3\*sigma;

<sup>4</sup> Considered number of observations;

<sup>5</sup> p-value used for testing for normality (Shapiro-Wilk) ;

<sup>6</sup> Standard deviation;

<sup>7</sup> Coefficient of Variation = Standard deviation/ Average;

<sup>8</sup> T/MTBF<sub>median</sub> · Non-dimensional value;

<sup>9</sup> 1/MTBF<sub>median</sub> · Value expressed for a time interval of 1 min;

<sup>10</sup> (1-CR1)\*100%;

<sup>11</sup> Weibull distribution best fits all samples. Goodness of fit is tested using the square error between observed and calculated values;

<sup>12</sup> Critical gap in the continuity of the data stream

## Contribution of infill data in reliability

Hereby is discussed the extent to which *infill* improves the solution compared to *baseline*. To do so, the MTBF of each pair of *train number* and *date* for *baseline* was correlated to the relevant pair of *infill*. The variable *Difference* refers to the subtraction of a MTBF<sub>Baseline</sub> from a MTBF<sub>Infill</sub>. Hence, when *infill* yields a smaller MTBF than *baseline* for a specific *train number–date*, *Difference* takes a negative value. The column *Set of records* refers to the set that it was taken into consideration to perform the test. Field *General* refers to same set of the records as that used in Table C.1.

The number of records for the *General* set equals 543. The negative observations sum up to 59 out of 517 or else, a 11.4% of the observed records is negatively affected by the introduction of the *infill* approach. Increasingly, the 76.3% of the negatively affected observations refers to off-peak trains. Hence the majority of the negative affected are off-peak trains.

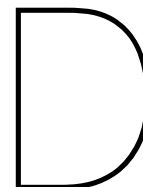
## Correlation between parameters

Since the samples are not normally distributed, a Spearman correlation is performed to yield possible dependencies between different parameters of each sample. Values in bold in the column *p-value* of Table C.2 illustrate the correlations between *Variable 1* and *Variable 2* that were found to be statistically significant ( $p < 0.05$ ). *Variable 2* refers to the MTBF of different data sources or their difference. Then the order (more to less correlated) was found based on the magnitude of the Spearman correlation value  $r_s$ . In Table C.2, the parameter 'Difference' corresponds to the value  $MTBF_{infill} - MTBF_{baseline}$ . Consulting on Table C.2, the following conclusions can be drawn:

- For the negatively affected observations, the difference is negatively correlated to the train's delay and,
- In general,  $MTBF_{Baseline}$  is positively correlated to train's delay.

Table C.2: Comparison of baseline, infill data as well as their difference with respect to delay

Set of records	Variable 1	Variable 2 (MTBF)	$r_s$	p-value	Order
General	Delay	Baseline	0.24	<b>1e-8</b>	3
		Infill	0.14	<b>1e-3</b>	5
		Difference	0.00	1.00	
	Predecessor's delay	Baseline	-0.01	0.7	
		Infill	0.07	0.1	
		Difference	0.15	<b>5e-4</b>	4
Negatively affected	Delay	Baseline	0.28	<b>0.02</b>	2
		Infill	0.17	0.17	
		Difference	-0.35	<b>4e-3</b>	1
	Predecessor's delay	Baseline	-0.07	0.6	
		Infill	-0.03	0.81	
		Difference	0.12	0.33	



## Technical drawings

Figure D.1 includes a simplistic representation of the track between Haarlem and Leiden Centraal. In this Figure, locations are given in route-ribbon coordinates. Given that the considered track belongs entirely to the Ass-Rtd (Amsterdam Sloterdijk-Rotterdam) route-ribbon, only locations are given in km. Figure D.1 includes station names followed by their location. It also includes the names as well as the start and end of track-segments as included in TPS. Track-segments "HLM-1", "LEDN-9A" and "LEDN-105B" are just indicative. In the analysis in their place are also included other track-segments of the interlocked areas of the two stations. Note that the Figure is not in scale.

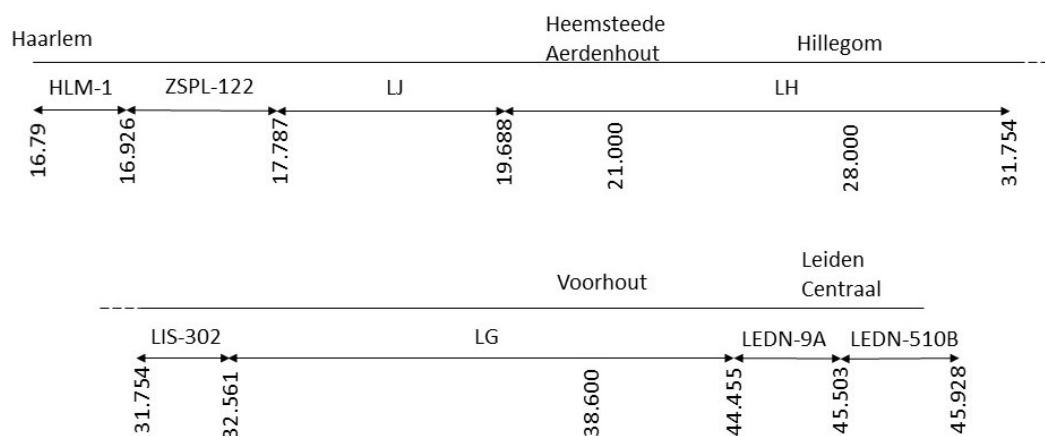
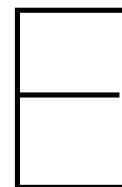


Figure D.1: Simplified track layout



## Simulator-user interface

Figure E.1 illustrates an example of the simulator-user interface. The three core modules of the simulator are distributed into three dedicated windows. *3DV* window replicates driver's view outside the cab and it is located on the top right part of the screen. It is essential for two reasons. First, it allows the driver to consult on line side signals and speed signs so as to be aware of the maximum allowed speed of the track at every instant. Apart from that, it allows the driver to locate the stop target sign on a platform. Precise stopping location is deemed important in order to have a good match between the observed and simulated speed profile at stations. Matching the speed profiles at stations will reveal difference in driving style between the simulated and the observed operations.

The *DMI* window contains a speedometer and other indications regarding the train operation and it is located on the left side of the screen. The actual speed is indicated in two ways: at the radial scale by the rotating needle, and with a numeral at the centre of the speedometer. Also, in the speedometer there are two locations where advised speed is indicated. Advised speed is marked by a white dot at the radial scale as well as by a white underlined numeral. If the actual speed is lower than the advised (as in the example of Figure E.1), a white triangle pointing up appears at the right edge of the underline. In case the actual speed matches the advice the triangle disappears and in case the actual speed exceeds the advised, the triangle points down.

Other fields of the DMI include an indication regarding the ATP that is currently operating (ATB-EG in Figure E.1), messages about the current scenario (bottom left corner), a coloured box with or without a numeral illustrating the current ATB code (40 km/h in Figure E.1). A box labelled as "DAS" and outlined by a train head is jointly a button and an indication of the DAS function. The DAS function can be (dis-)activated by clicking on the button. An activated DAS function is marked by a white indication with an arrow on top. The opposite state is highlighted by a yellow figure without the arrow. Finally, the bottom right part of the DMI window contains the time from the start of the simulation with a second precision as well as the distance in meters from the start of the simulation.

Ultimately, the *train* window contains the traction and brake lever and it is located at the bottom right corner of the screen. The driver adjusts traction and brake by clicking and sliding the white knob.

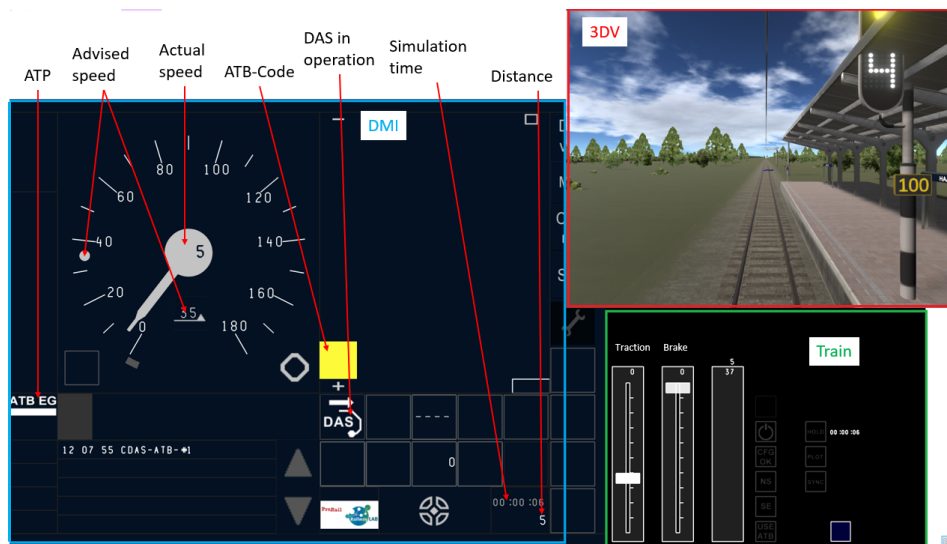


Figure E.1: Display of the NEO-DMI Suite with 3D Viewer simulator



# Blocking time diagrams of the simulator experiments

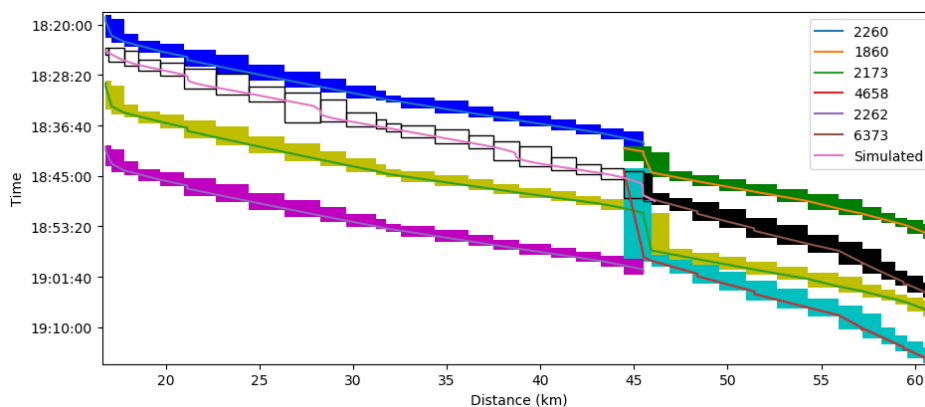


Figure F.1: Scenario 1 - No DAS - Compressed

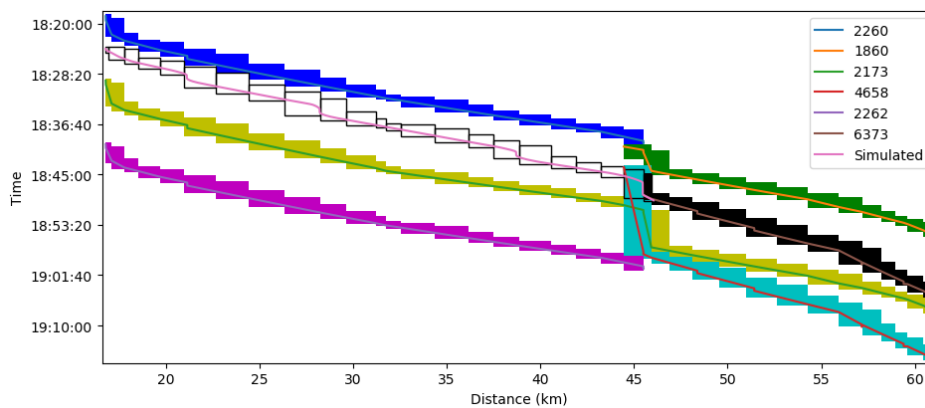


Figure F.2: Scenario 1 - Baseline - Compressed

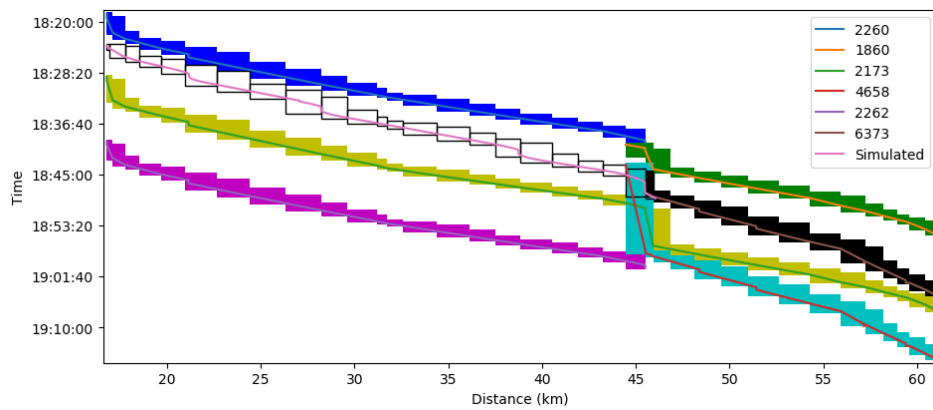


Figure F.3: Scenario 1 - Infill - Compressed

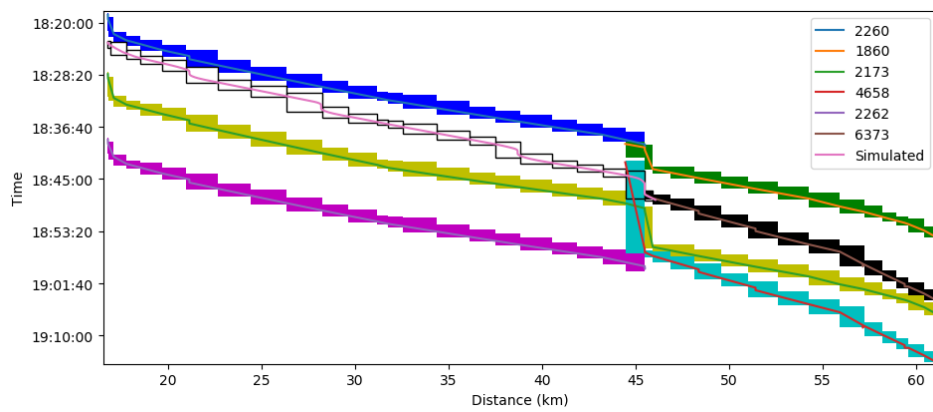


Figure F.4: Scenario 1 - ETCS L2 - Compressed

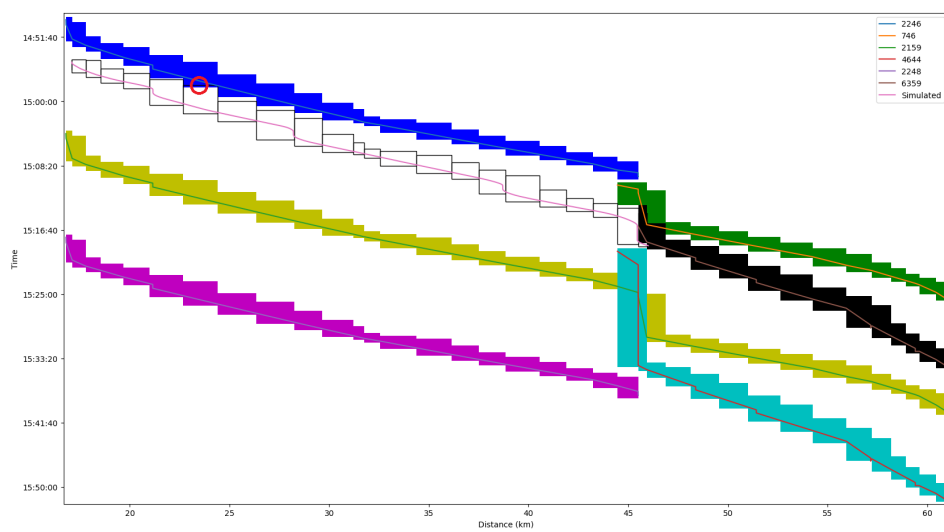


Figure F.5: Scenario 2 - No DAS - Uncompressed

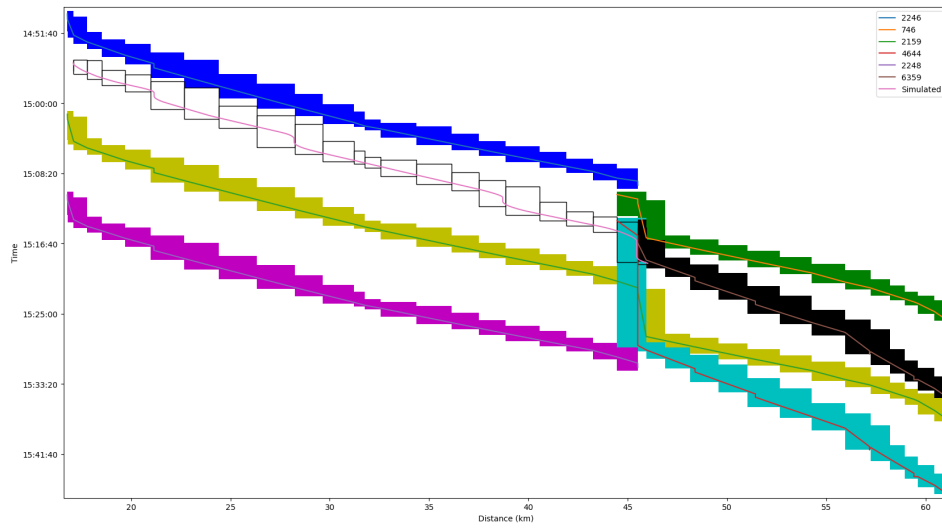


Figure F.6: Scenario 2 - No DAS - Compressed

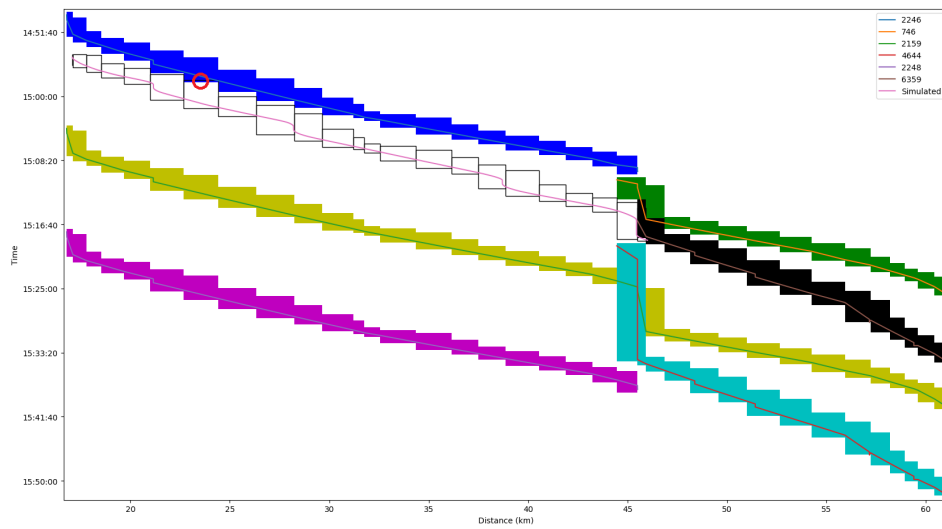


Figure F.7: Scenario 2 - Baseline - Uncompressed

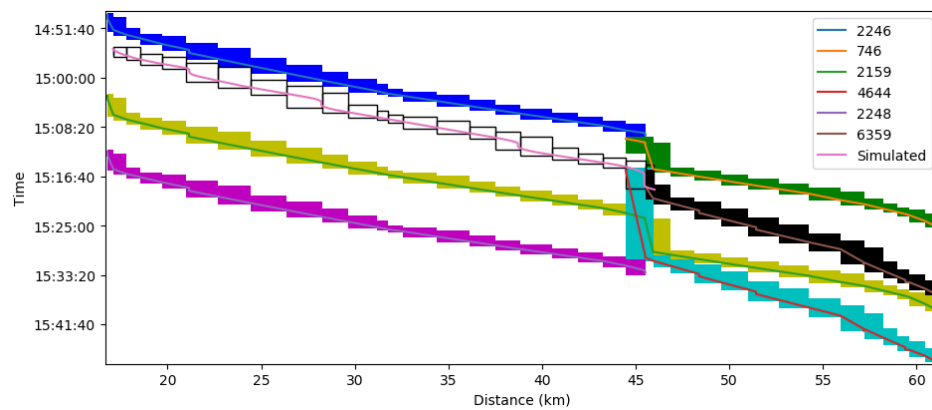


Figure F.8: Scenario 2 - Baseline - Compressed

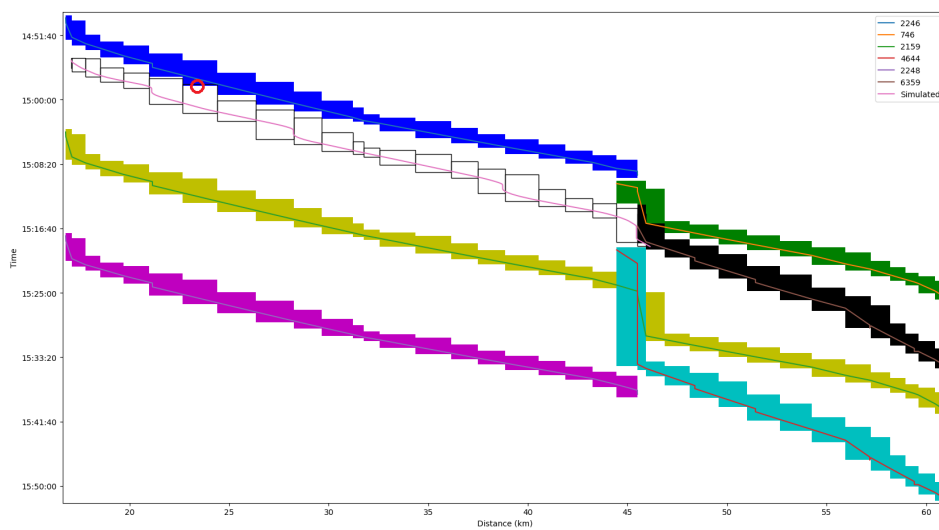


Figure F.9: Scenario 2 - Infill - Uncompressed

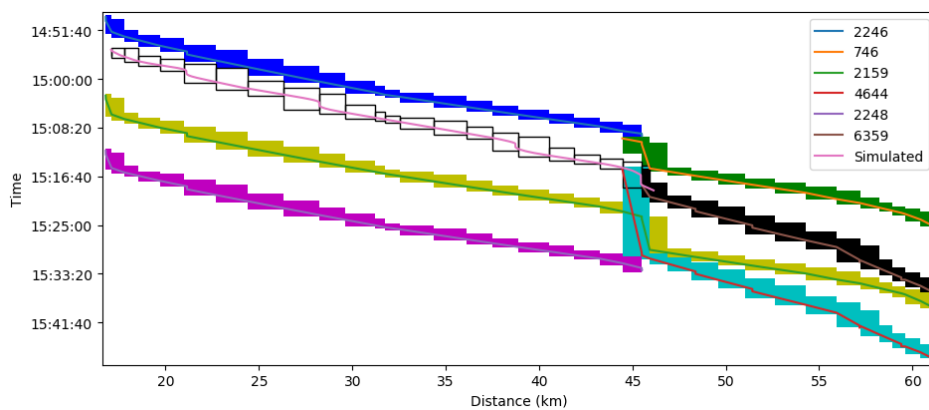


Figure F.10: Scenario 2 - Infill - Compressed

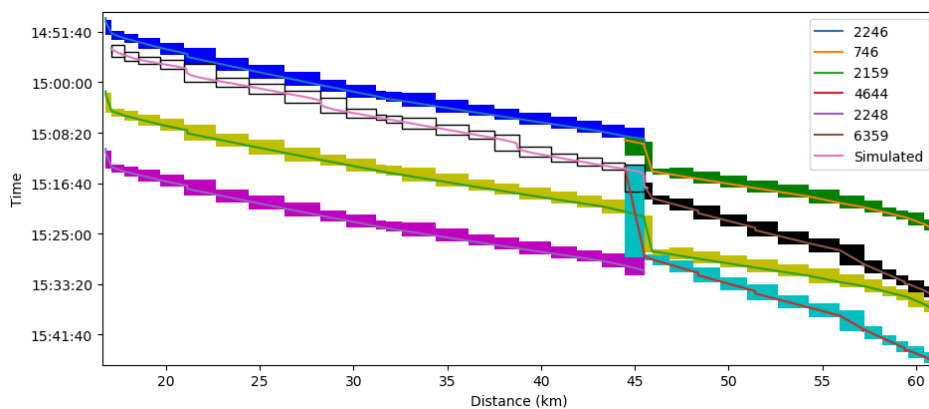


Figure F.11: Scenario 2 - ETCS L2 - Compressed

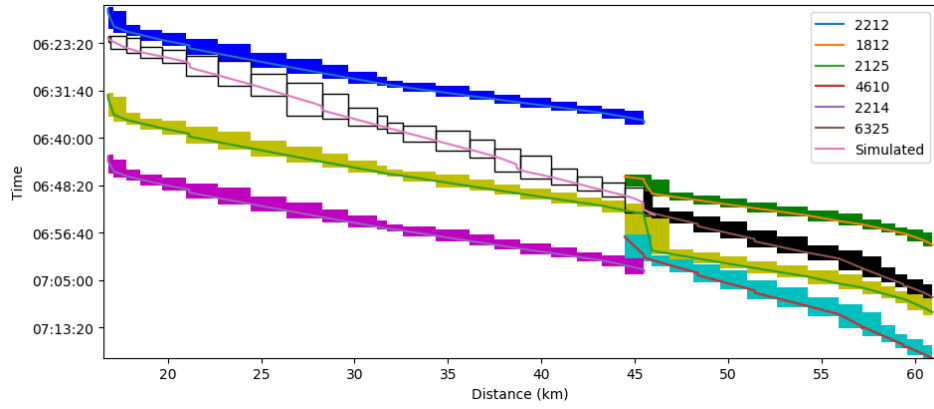


Figure F.12: Scenario 3 - No DAS - Compressed

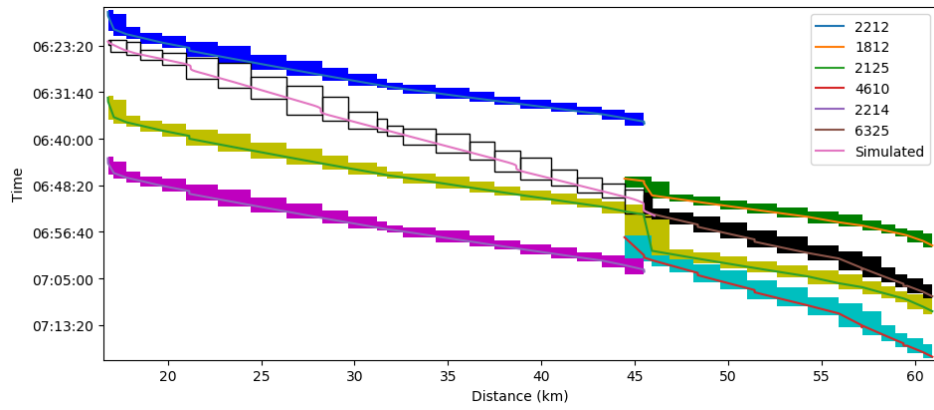


Figure F.13: Scenario 3 - Baseline - Compressed

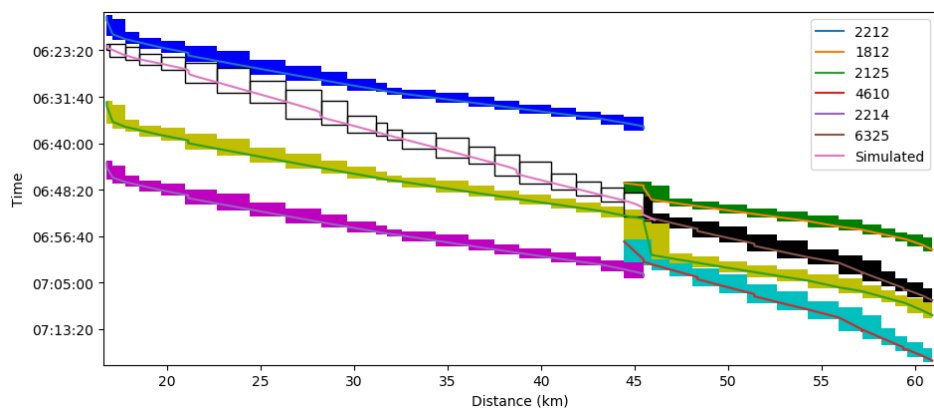


Figure F.14: Scenario 3 - Infill - Compressed

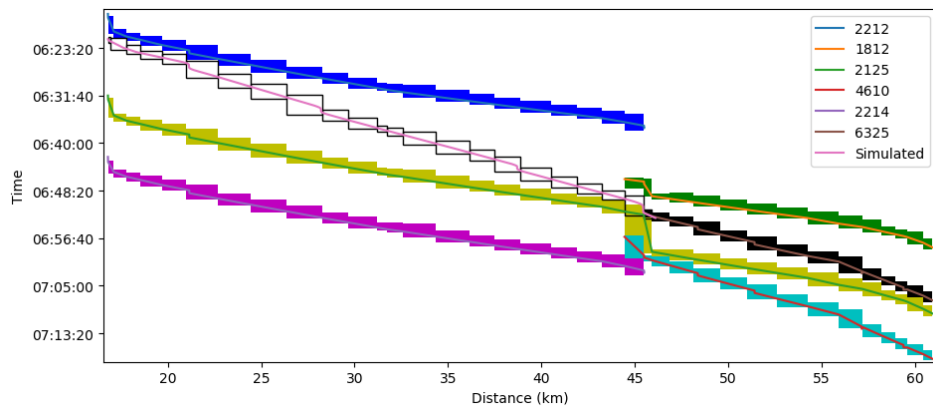


Figure F.15: Scenario 3 - ETCS L2 - Compressed